

Small disulfide loops in peptide hormones mediate self-aggregation in secretory granule biogenesis

Inauguraldissertation
zur
Erlangung der Würde eines Doktors der Philosophie
vorgelegt der
Philosophisch-Naturwissenschaftlichen Fakultät
der Universität Basel

von

Jennifer RECK

2021

Genehmigt von der Philosophisch-Naturwissenschaftlichen Fakultät

auf Antrag von

Prof. Dr. Martin Spiess

Prof. Dr. Jean Pieters

Dr. Stéphane Gasman

Basel, 30.03.21

Prof. Dr. Marcel Mayor

*may the flowers remind us
why the rain was so necessary*

XAN OKU

Acknowledgements

First of all, I would like to express my deep gratitude to the “dream team” of Spiess lab. Especially Prof. Dr. Martin Spiess, without whom nothing would have been possible, and Nicole Beuret. Both of you have been like “chaperones” helping me to take the good path in my thesis, so one-thousand thanks to you. Also many thanks to all the other current and former members of the lab, Cristina Baschong, Tina Junne Bieri, Mirjam Pennauer, Valentina Millarte, Marco Janoschke, Daniela Stadel, Dominik Buser, Simon Schlienger and Gaetan Bader to have been such a support through scientist talks and more importantly many non-scientist “Friday talks”. I could never ask for a better atmosphere in a team. Thank you so much.

I also want to thank the other members of my committee, Pr. Dr. Jean Pieters, Dr. Friant for their helpful advices and their time. Also Pr. Dr. Stéphane Gasman to have nicely accepted to be my external member and Prof. Dr. Marcus Rüegg for being the chairperson of my committee.

Also many thanks to Dr. Alexander Schmidt and the Image Core Facility, especially Dr. Laurent Guerard for their help in my project and all the members of the 5th floor who helped me through the departmental seminars

Last but clearly not least, thanks to my family, my mom, Corinne Reck, my Dad, Jean-Christophe Reck, my brother, Jonathan Reck and my boyfriend, Amaury Paris, for their unconditional support, and love. This thesis is for you...

Table of contents

ACKNOWLEDGEMENTS	1
TABLE OF CONTENTS	3
SUMMARY	5
PART I	7
SMALL DISULFIDE LOOPS IN PEPTIDE HORMONES MEDIATE SELF-AGGREGATION IN SECRETORY GRANULE BIOGENESIS	7
I. INTRODUCTION.....	8
1. <i>The endocrine system produces and secretes hormones</i>	8
1.1 Different types of hormones	8
1.2 The endocrine system.....	8
1.3 Hormone receptors	12
1.4 Peptide hormones	13
2. <i>Transport through the secretory pathway</i>	13
2.1 Endoplasmic reticulum (ER) entry	13
2.2 The correct folding of proteins is ensured by ER quality control.....	14
2.3 The trans-Golgi network (TGN) is a sorting platform	17
2.4 Constitutive vs. regulated secretion	18
3. <i>Regulated secretory pathway</i>	19
3.1 Composition of secretory granules and prohormone processing	19
3.2 Generation and maturation of secretory granules.....	20
3.3 Fusion of MSGs with the plasma membrane and release of hormones.....	23
4. <i>What controls secretory granule biogenesis and cargo sorting?</i>	25
4.1 The interaction of regulated secretory cargos with membrane proteins/lipids.....	25
4.2 Granins are essential for granule biogenesis.....	26
4.3 Actomyosin complex controls secretory granule biogenesis and sorting	26
4.4 Regulated cargos contain sorting motifs	27
5. <i>The starting point of this thesis project</i>	28
5.1 Bad and good amyloid aggregation	28
5.2 The nonapeptide vasopressin is responsible for bad and good amyloids formation of its precursor.....	30
5.3 Small disulfide loops in vasopressin and other hormones	30
II. RESULTS.....	32
1. <i>CC loops mediate ER aggregation of a non-folded reporter</i>	32
1.1 CC loops mediate aggregation to different extents.....	33
1.2 The aggregates colocalize with PDI in the ER	36
1.3 Ultrastructure of CC loop constructs	39
2. <i>CC loops mediate sorting of a constitutive reporter into secretory granules</i>	41
2.1 α -1 protease inhibitor (A1Pi) as a reporter for CC loop-mediated granule sorting.....	41
2.2 The CC loop disulfide bonds are formed efficiently.....	43
2.3 CC loops are mediating sorting into secretory granules.....	46
2.4 CC loop constructs are located in functional secretory granules	53
2.5 CC loops mediate Lubrol insolubility	58
2.6 Mutation of the cysteines in a CC loop abolishes granule sorting.....	61
III. DISCUSSION	64

PART II.	71
HOW DOES MUTANT GROWTH HORMONE BLOCK THE SECRETION OF THE WILD-TYPE IN THE DOMINANT GROWTH HORMONE DEFICIENCY TYPE II DISEASE?	71
I. INTRODUCTION.....	72
1. <i>Growth hormone (GH)</i>	72
2. <i>Autosomal dominant growth hormone type II</i>	73
II. RESULTS.....	75
III. DISCUSSION	80
MATERIALS AND METHODS	82
SUPPLEMENTARY MATERIALS	88
REFERENCES	93
CURRICULUM VITAE	103

Summary

Unlike constitutively secreted proteins, peptide hormones are first stored in densely packed secretory granules, before regulated release from the cell upon stimulation. Secretory granules are formed at the trans-Golgi network by self-aggregation of the prohormones as functional amyloids. The nonapeptide hormone vasopressin, which forms a small disulfide (CC) loop, was shown to be responsible for granule formation of its precursor in the TGN as well as for toxic fibrillar aggregation of misfolding mutants in the endoplasmic reticulum (ER), proposing ER aggregates to be mis-localized amyloid aggregates that evolved to mediate sorting into granules. Several other hormone precursors also contain similar small CC loops suggesting their function as a general device to mediate aggregation for granule biogenesis. To test this hypothesis, we studied the CC loops of various peptide hormones, vasopressin, amylin, calcitonin, prorenin, and prolactin, in order to determine their capacity *(i)* to induce ER aggregation of a misfolded reporter; *(ii)* to mediate aggregation of a constitutive protein into secretory granules.

For ER aggregation, CC loops were fused to a misfolded and truncated version of the neurophysin II portion of provasopressin, NPΔ, as a reporter, transiently expressed in COS-1 and Neuro-2a cells, and analyzed by immunofluorescence microscopy as well as by immunogold electron microscopy. We found that all CC loops induce ER aggregation although to different extents and with different morphologies, some only detectable by electron microscopy.

To study granule sorting, either one or two CC loops were fused to the constitutively secreted protein α -1 proteinase inhibitor (A1Pi), used as a reporter. Stably expressing AtT20 cell lines were generated and analyzed by immunofluorescence microscopy for accumulation in secretory granules, by stimulated secretion, and for insolubility to Lubrol extraction. All assays showed that the CC loops are able to reroute A1Pi into the regulated secretory pathway, thus supporting our hypothesis.

Altogether, the results show that CC loops mediate both the aggregation of a misfolded reporter in the ER as well as sorting of a constitutive protein into secretory granules, indicating that CC loops act as general secretory granule signals by mediating self-aggregation, advancing our mechanistic understanding of regulated secretion.

Part I.

Small disulfide loops in peptide hormones
mediate self-aggregation in secretory granule
biogenesis

I. Introduction

1. The endocrine system produces and secretes hormones

1.1 Different types of hormones

Hormones are chemical messengers in higher multicellular organisms which are transported mainly via the bloodstream to target and stimulate specific tissues and organs. Hormones can be divided in different types: *(i)* steroids like oestrogen and testosterone, derived from cholesterol; *(ii)* soluble small organic molecules such as epinephrine and norepinephrine, and *(iii)* peptide and protein hormones, for instance oxytocin and growth hormone (GH). These molecules are essential for the regulation of physiology and behavior, and allow the long-distance communication between organs and tissues.

1.2 The endocrine system

Hormones are produced mainly by specific endocrine tissues/glands belonging to the so-called endocrine system. This system results in the communication between glands producing and releasing different types of messengers (hormones) into interstitial spaces, which then reach the bloodstream and the different targeted organs or tissues. This system is responsible for the functions of almost all cells, organs, and tissues throughout the body, among them growth and development, regulation of metabolism, sleep, and sexual behavior. The human body is composed of eight endocrine tissues/glands: the pituitary glands (anterior and posterior), the hypothalamus, the pineal gland, the thyroid gland, the parathyroid gland, the adrenal gland, the pancreas, and ovaries or testes (Hiller-Sturmhofel and Bartke, 1998).

- **The pituitary** is the main gland of the body. It receives information from the brain and the hypothalamus to control all the other glands. This gland is composed of two lobes, the posterior and the anterior pituitary (Perez-Castro et al., 2012; Figure 1).

The anterior pituitary is made of different types of neuroendocrine cells producing and secreting different hormones. The somatotroph cells secrete the growth hormone

whose principal function is to stimulate growth and development of all tissues of the body. The corticotroph cells are implicated in the secretion of adrenocorticotropin (ACTH); its main role is to increase the release of cortisol from the adrenal gland. The thyrotroph cells secrete the thyroid stimulating hormone (TSH) that stimulates the thyroid to produce its hormones. The gonadotroph cells secrete gonadotropic hormones; luteinizing hormone (LH) and follicle-stimulating hormone (FSH), essential for reproduction by targeting the gonads. Finally, the lactotroph cells secrete prolactin, well known to induce the production of milk in females.

The posterior pituitary does not produce hormones, but serves as a storage and release center for hormones. Those hormones are synthesized by the magnocellular neurosecretory cells of the supraoptic and paraventricular nuclei located in the hypothalamus and extend their axons to the posterior lobe. Indeed, this lobe secretes the oxytocin and vasopressin hormones. Even if the structure of those two hormones is very similar, they are different by their roles. Oxytocin is known to play a role in childbirth, female reproduction, social bonding and breast-feeding, whereas, the role of vasopressin is to maintain the water homeostasis of the body.

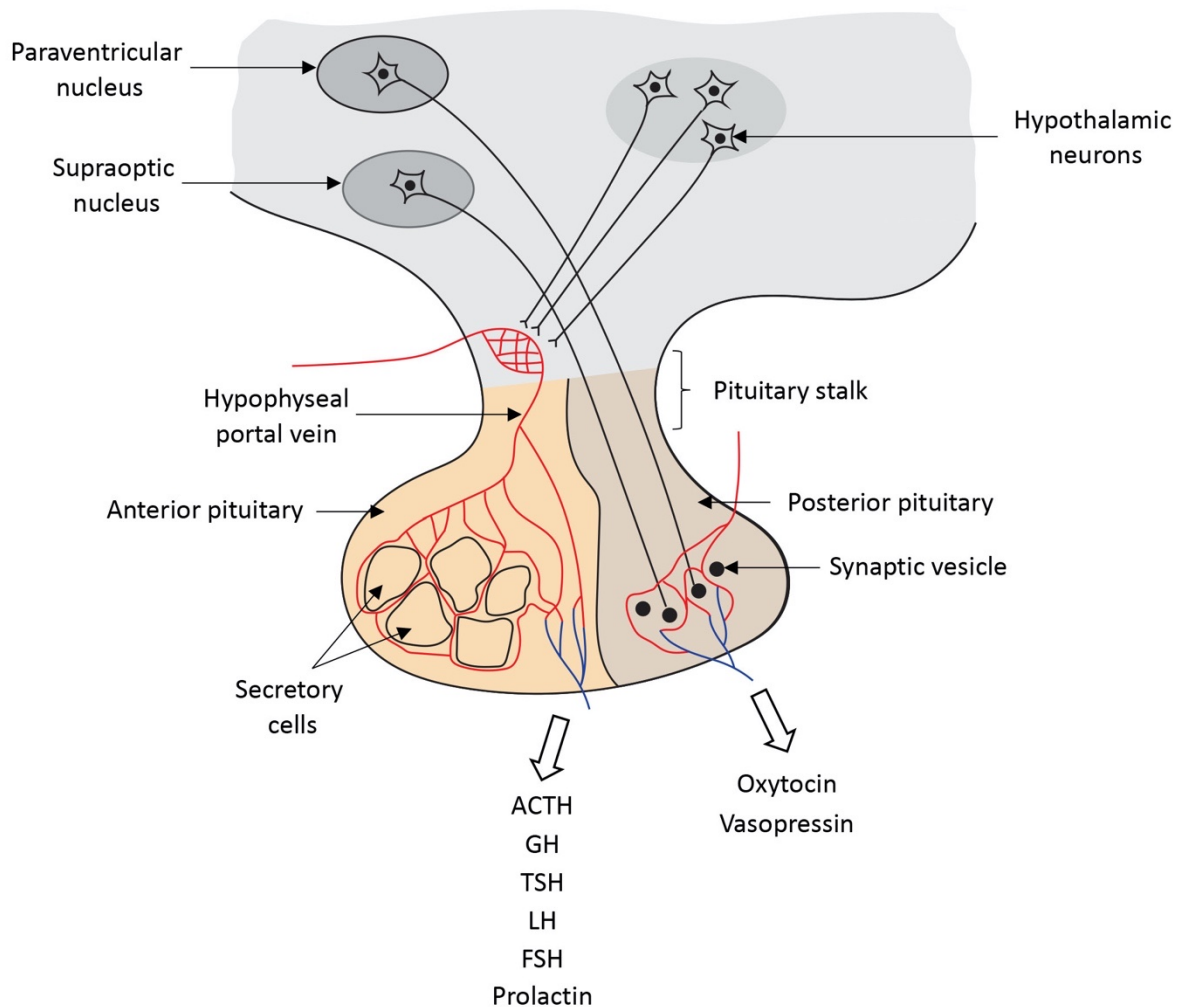


Figure 1. The pituitary gland

The pituitary gland is composed of two lobes, the anterior and posterior. The anterior lobe is composed of various secretory cells that produce and secrete ACTH, GH, TSH, LH, FSH and prolactin. The posterior lobe contains the axon terminals of cells in the hypothalamus to secrete oxytocin and vasopressin.

- The hypothalamus** is a portion of the brain that allows the connection between the endocrine system and the nervous system. It does it by controlling the hormone secretion *via* the anterior pituitary gland through the capillaries of the hypophyseal portal system (HPS). The hypothalamus secretes hormones to the HPS to signal the pituitary gland to stimulate or inhibit the release of specific hormones (Hiller-Sturmhofel and Bartke, 1998). Firstly, the hypothalamus secretes stimulating hormones: the gonadotropin-releasing hormone (GnRH); the corticotropin-releasing hormone (CRH); the thyrotrophin-releasing hormone and the growth hormone-releasing hormone (GHRH) which stimulate the anterior pituitary gland to secrete FSH

and LH; ATCH; TSH and GH respectively. Secondly, the hypothalamus secretes inhibiting hormones: somatostatin and dopamine which inhibit the release of GH and prolactin, respectively. Finally, as mentioned before, oxytocin and vasopressin, produced by the hypothalamus, are transported to the posterior pituitary by neural connections allowing the storage until release. The hypothalamus in addition, has many different functions such as maintaining a constant temperature of the body, controlling appetite, and sleep cycles.

- **The pineal gland** is located in the brain and is responsible for the secretion of melatonin and serotonin that regulate the circadian rhythm.
- **The thyroid gland** is located in the neck and secretes hormones that control the metabolism. The two main hormones are triiodothyronine (T3) and thyroxine (T4). Those hormones play many roles, among them, regulation of body weight, energy consumption, and internal temperature. This gland communicates with the hypothalamus and the pituitary which maintain the balance of these hormones. It also secretes calcitonin, which reduces blood calcium level.
- **The parathyroid gland** is located behind the thyroid gland and secretes the parathyroid hormone which, in opposition to calcitonin, increases blood calcium level.
- **The adrenal glands** are located on top of both kidneys and secrete catecholamines (epinephrine and norepinephrine) known to induce the fight-or-flight response, and steroid hormones such as aldosterone and cortisol in response to ACTH, regulating some essential functions such as metabolism and blood pressure.
- **The pancreas** is located in the abdomen and contains islets of Langerhans that release insulin, glucagon and amylin to maintain blood glucose balance.
- **The ovaries**, the female reproductive system, secrete mainly oestrogen and progesterone hormones regulating menstrual cycle, fertility, and the development of secondary sexual characteristics.

- **The testes**, the male reproduction system, produce testosterone which regulates fertility and secondary sexual characteristics development.

Other endocrine tissues/organs

The kidney is not considered part of the endocrine system, even though it secretes hormones like prorenin that regulates blood pressure or erythropoietin that helps to produce red blood cells by stimulating the bone marrow. Besides, other organs can be considered as endocrine glands but only at certain periods of time. This is the case for the placenta during pregnancy and the thymus until puberty. The placenta is formed during pregnancy in the uterus and produces hormones needed for a healthy pregnancy and for preparation to labour (oestrogen, progesterone and placenta lactogen). However, the thymus, located behind the sternum is active only until puberty. This organ secretes thymosin, the essential hormone for the production and the development of T-cells which have a central role in immunity.

Additionally, when the molecule is not secreted into the bloodstream but in a duct or outside of the body, the organ is described as exocrine. That includes salivary glands, sweat glands, mammary glands, lacrimal glands, sebaceous glands and mucus glands. Furthermore, a gland can even be both, endocrine and exocrine, at the same time. For instance, the pancreas whose cells secrete insulin into the bloodstream, but also digestive fluid into the pancreatic duct, helping digestion of the food (Perez-Castro et al., 2012). Finally, more and more tissues are found to produce messenger molecules to “talk back” to the brain or to communicate with other tissues, for instance leptin from adipocytes.

1.3 Hormone receptors

Hormones are tightly regulated since they are targeted to specific organs and/or tissues by binding to specific receptors on the target cell. These receptors can be divided into two types (Baxter and Funder, 1979): (i) trans-membrane receptors used by water soluble hormones, including peptide/protein hormones (except thyroid hormone). They are tyrosine kinase receptors or G protein-coupled receptors triggering intracellular signaling cascades. (ii) intracellular receptors used by lipid-soluble hormones, such steroids and thyroid hormone that pass the plasma membrane. The binding between hormones and intracellular receptors

triggers conformational change of the receptor, nuclear import, and binding of the hormone-receptor complex to promoter elements allowing the specific regulation of gene expression.

1.4 Peptide hormones

Peptide hormones are produced by professional endocrine cells and secreted in a regulated manner in concentrated form *via* so-called secretory granules. These secretory granules are stored close to the plasma membrane until a stimulus triggers fusion and release, allowing a rapid response when required. Prototypes of such professional endocrine cells are the β cells of the pancreas producing insulin and α cells producing glucagon allowing the regulation of blood glucose.

For a peptide hormone to be synthesized and secreted in order to fulfill its function, it has to traffic through different organelles and undergo several modifications explained in detail in the following chapter.

2. Transport through the secretory pathway

2.1 Endoplasmic reticulum (ER) entry

In eukaryotic cells, secretion of proteins involves the passage through several organelles constituting the secretory pathway. Secretory proteins are synthesized on cytosolic ribosomes that are targeted to the ER typically by an N-terminal signal sequence composed of a bench of hydrophobic amino acids. During protein synthesis by the ribosome, the emerging signal sequence is recognized by the signal recognition particle that slows down protein synthesis and mediates the targeting of the nascent polypeptide on the ribosome to the ER membrane *via* the interaction with the signal recognition particle receptor (Keenan et al., 2001; Lutcke, 1995). After this interaction, protein synthesis continues and the secreted protein is translocated into the ER lumen *via* the Sec61 translocon (Park and Rapoport, 2012). Finally, on the luminal side, the signal sequence is cleaved off by signal peptidase.

2.2 The correct folding of proteins is ensured by ER quality control

In order to be functional and to fulfill its role within the cell, a protein has to be correctly folded by acquiring its native conformation. As the polypeptide is translocated into the ER lumen, it may be co-translationally N-glycosylated by oligosaccharyl transferase. The ER lumen maintains oxidizing conditions allowing the formation of disulfide bonds catalyzed by Hsp100 family of oxidoreductases, primarily protein disulfide isomerase (PDI). PDI oxidizes cysteines for disulfide bond formation and is also able to shuffle incorrect bonds that remain exposed on the surface. However, folding may not be perfect and physiological problems like ER stress can lead to an accumulation of non-native proteins. This ER stress is caused by different disturbances including environmental changes, as well as genetic or oxidative changes. To ensure the correct folding of proteins in absence but also in presence of ER stress, the ER is using different proteins and mechanisms for their recognition. First of all, misfolded proteins are recognized by chaperone proteins. Indeed, non-native proteins contain biophysical features, such as unpaired cysteines or exposed hydrophobic regions, which could lead to aggregation, that are recognized by several chaperones that help the non-native protein to fold and to be modified properly. The most known and abundant ones are the heat shock proteins Hsp40, Hsp70 (BiP), Hsp90, and Hsp100 family oxidoreductases such as PDI, and the lectins calnexin and calreticulin (Ellgaard and Helenius, 2003).

Environmental stress or mutations in secretory proteins may lead to accumulation of misfolded and non-native proteins, causing ER stress and potentially disease, such as antitrypsin deficiency or cystic fibrosis (Rutishauser and Spiess, 2002). Accumulation of misfolded proteins triggers the unfolded protein response (UPR) to maintain a balance between the load of ER proteins and the folding and degradation capacity.

UPR:

To maintain protein homeostasis, the UPR uses two different strategies: the upregulation of ER chaperone expression and/or the decrease of translation rate. These pathways require the use of three molecular ER stress sensors: dsRNA-activated protein kinase-like ER kinase (PERK), inositol-requiring enzyme 1 (IRE1,) and activating transcription factor 6 (ATF6) (Tirasophon et al., 1998; Walter and Ron, 2011; Figure 2). In the absence of misfolded

proteins, the Hsp70 chaperone BiP, is bound to these three sensors, blocking their activity. However, when the amount of non-native proteins is too high, BiP is recruited for their folding and is therefore released from these receptors (Lee, 2005). This dissociation leads to the activation of those three sensors. Indeed, PERK and IRE1 are activated and these type 1 transmembrane proteins homodimerize and auto-phosphorylate their own kinase domains. PERK, also phosphorylates the translation factor eIF2 α , inducing inactivation of translation initiation and leading to a general reduction of protein synthesis (Kebache et al., 2004; Raven et al., 2008). In parallel, the phosphorylated domain of IRE1 activates the transcription factor Xbp1 binding protein (XBP1) via mRNA processing to upregulate chaperones and expression of ER associated degradation (ERAD) genes (Hetz and Glimcher, 2009; Yang et al., 2020). The third sensor is ATF6 and when activated, is transported to the Golgi and cleaved by proteases to release a cytosolic domain that is imported into the nucleus and acts as a transcription factor to stimulate the expression of chaperone's genes (Chen et al., 2002; Shen et al., 2002; Yoshida et al., 2001).

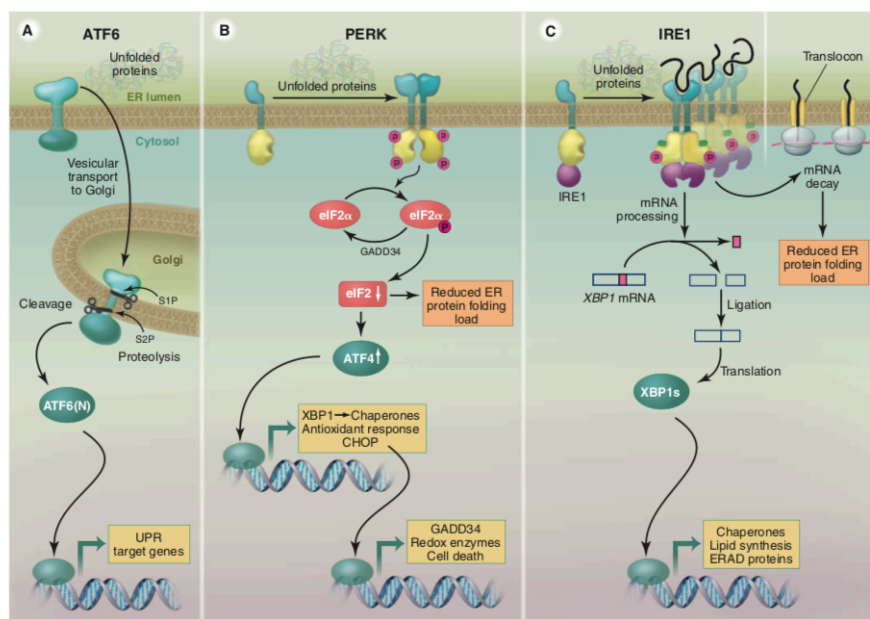


Figure 2. The unfolded protein response (UPR)

The UPR is composed of three different signals that sense the misfolded proteins in the ER. Each signal deals with unfolded proteins by different mechanisms. Once activated, IRE1 and PERK activate their own kinase domains. After this, IRE1 activates the transcription factor XBP1 that upregulates chaperones and ERAD gene expression. In parallel, PERK phosphorylates the translation factor eIF2 α that inhibits the translation initiation and then reduces general protein synthesis. In addition, ATF6 is translocated to the Golgi, cleaved by proteases into domains which are imported to the nucleus and act as transcription factors to upregulate chaperone gene expression. (From Walter and Ron, 2011).

ERAD:

Proteins that are unable to fold are eliminated by ERAD. It involves a protein complex in the ER membrane of several proteins whose individual functions are not fully understood yet. It mediates recognition of ERAD substrates, retrotranslocation through the ER membrane into the cytosol, and ubiquitination for degradation by the proteasome. The core component is HRD1 (HMG-CoA reductase degradation protein 1), a multispanning protein that acts as an E3 ubiquitin ligase (together with ubiquitin activating enzyme E1, and conjugating enzymes E2 in the cytosol) and most likely as the retrotranslocation pore. ERAD is composed of different steps: *(i)* the recognition of the misfolded protein with luminal chaperones, mainly BiP (Hsp 70) by the HRD1 partner protein Sel1L (Suppressor/enhancer of Lin-12-like); *(ii)* the retrotranslocation of the substrates coupled to ubiquitination; *(iii)* extraction of the substrate into the cytosol by the ATPase p97/CDC48 and *(iv)* the hydrolysis of the poly-ubiquitinated proteins by the proteasome (Hebert and Molinari, 2007; Nakatsukasa and Brodsky, 2008; Spiess et al., 2020; Figure 3).

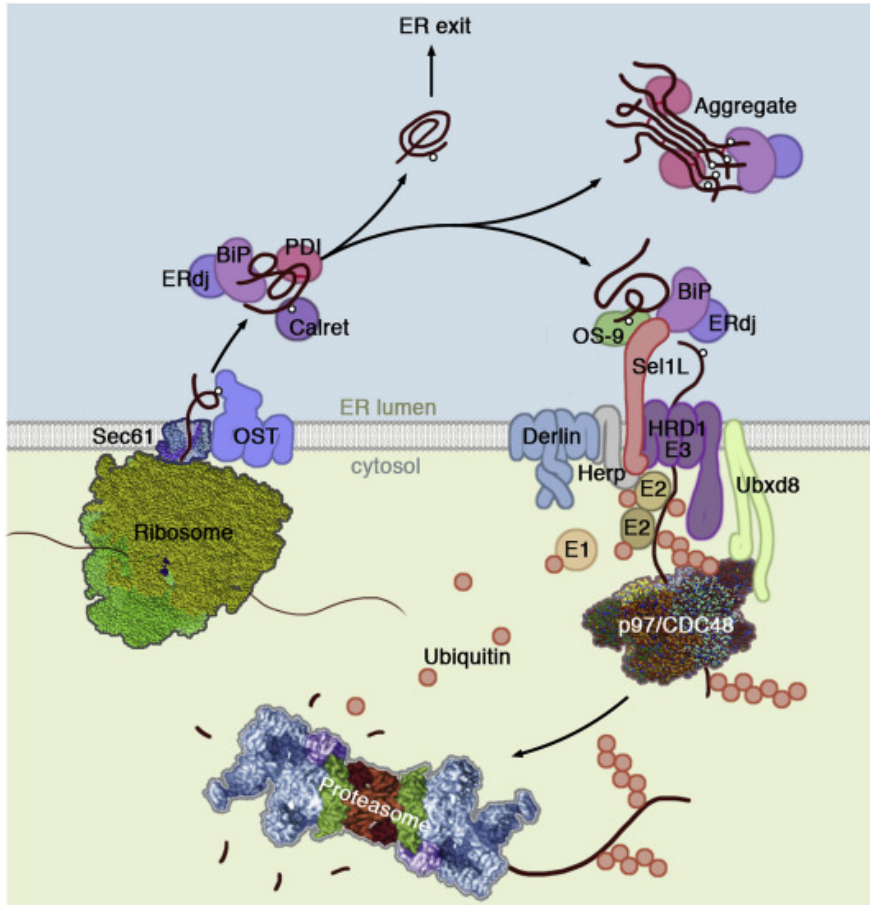


Figure 3. ER associated degradation (ERAD)

Secreted proteins are targeted to the ER, translocated to the ER lumen by the Sec61 translocon and may be N-glycosylated by oligosaccharyl transferase (OST). Chaperones (PDI, calreticulin and BiP-ERdj) bind to the proteins to help their proper folding and to prevent the formation of aggregates. Well-folded proteins leave the ER, whereas misfolded proteins are retrieved back to the cytosol *via* the retrotranslocation complex composed of HRD1 (E3 ubiquitin ligase), Sel1L (adaptor subunit of HRD1), Derlin and Herp (scaffold proteins). The protein is pulled out of the ER by the ATPase p97/CDC48 and is then ubiquitinated by the collaboration of E1 ubiquitin activating enzyme, E2 conjugating enzymes and E3 ubiquitin ligase to be finally recognized by the proteasome and hydrolysed. (From Spiess et al., 2020).

2.3 The trans-Golgi network (TGN) is a sorting platform

When proteins are correctly folded, they are transported to the Golgi by COPII-coated vesicles. The Golgi apparatus forms stacks of typically 3–8 cisternae through which cargo flows from the cis to the trans side. The cisternae contain specific enzymes such as glycosidases and glycosyltransferases for modification of N-glycans, for O-glycosylation and glycosaminoglycan synthesis. Proteins are transported through Golgi stacks to finally reach the trans-Golgi network (TGN) which is a platform for the sorting of cargo proteins to different

destinations (Pakdel and von Blume, 2018). Indeed, secreted proteins will be delivered to the plasma membrane (constitutive secretion) and lysosomal proteins to endosomes (Kornfeld and Mellman, 1989). In specialized endocrine or exocrine cells, specific secretory proteins will be incorporated in secretory granules for transport to the cell periphery (regulated secretion).

How proteins are sorted from the TGN is poorly understood. In order to be targeted to the correct compartment, it is believed that proteins contain signals or motifs that are recognized by specific receptors. A relatively well understood example is the modification of lysosomal proteins with a mannose 6-phosphate group on N-linked glycans that is recognized by mannose 6-phosphate receptors for transport to endosomes (Braulke and Bonifacino, 2009; Puertollano et al., 2001). The receptors interact with the AP-1 adaptor complex of clathrin coats to be incorporated into specific transport vesicles. However, for both constitutive and regulated secretion, putative signals and their receptors have so far remained elusive.

2.4 Constitutive vs. regulated secretion

Secreted proteins can follow two types of pathways (Kim et al., 2006): *(i)* the constitutive one where proteins are continuously secreted and regulation occurs at the level of gene expression and *(ii)* the regulated pathway where proteins are packaged into secretory granules for storage and secreted upon stimulation.

- (i)* The constitutive secretory pathway is found in all cell types to deliver newly synthesized proteins to the plasma membrane and to the extracellular matrix. Despite its importance, this pathway is still poorly understood. It is also called “the default pathway” because no signals in the secreted proteins have been discovered so far.
- (ii)* The other way for proteins to be exocytosed is the regulated secretory pathway present in endocrine, some exocrine, and other specialized cells. This pathway is based on the storage of the secretory proteins including peptide hormones, in densely packed secretory granules before regulated release from the cell upon stimulation. This regulated pathway will be explained in more detail in the following part.

3. Regulated secretory pathway

For a protein to be secreted on demand, it requires an organelle able to store and exocytose it upon a specific stimulus. It is exactly the role of secretory granules, also called dense-core secretory vesicles. Secretory granules are able to store a large amount of secretory material consisting of packed protein aggregates which give rise to the dense core appearance in electron microscopy. Secretory granules have generally a diameter of 80-120 nm and an estimated number of 10 000-30 000 in endocrine and chromaffin cells (Bartolomucci et al., 2011). The generation of secretory granules takes place at the TGN and involves various steps of maturation. Furthermore, secretory granules contain specific regulated cargo proteins described below.

3.1 Composition of secretory granules and prohormone processing

The composition of regulated proteins in secretory granules depends on the cell type. The granules are generally composed of *(i)* prohormones, *(ii)* members of the granin family, and *(iii)* processing enzymes.

- (i)* Before being functional, hormones are frequently produced and incorporated into granules as prohormones (hormone precursors) that undergo proteolytic processing in order to give rise to active peptides. As an example, proopiomelanocortin (POMC), secreted from the anterior pituitary, is a polypeptide precursor whose processing generates three main active peptides, α -melanocyte-stimulating hormone that regulates appetite and sexual behavior, ACTH that regulates the secretion of glucocorticoids, and β -endorphin which is an opioid peptide.

- (ii)* In addition to prohormones, specific other proteins are incorporated into secretory granules, among them the granin family members. The granin family is composed of eight members; the most known and studied ones are chromogranin A (CgA), chromogranin B (CgB), secretogranin II (SgII), and secretogranin III (SgIII). There are also other related proteins, 7B2 (SgV), NESP55 (SgVI), VGF (SgVII) and

proSAAS (SgVIII). Granins are characterized by their tendency to aggregate at acidic pH. Since they are found widespread in secretory granules of different endocrine tissues, they have been considered to be helper proteins for secretory granules formation and several studies have implicated CgA, CgB, SgII and SgIII in the biogenesis of secretory granules (Courel et al., 2010; Hosaka and Watanabe, 2010; Huh et al., 2003; Kim et al., 2001). In addition, they also contain dibasic cleavage sites which are potential sites for proteolysis. Indeed, as for prohormones, granins may be processed in a tissue-specific manner to biologically active peptides. Another property of granins is their ability to bind calcium (Ca^{2+}). As a matter of fact, their Ca^{2+} -binding capacity has been shown to help the regulation of cytosolic Ca^{2+} concentration (Yoo, 2010).

- (iii) Prohormone processing requires the activity of different prohormone convertases (PCs) and carboxypeptidases, endo- and exopeptidases, respectively. During the maturation of the secretory granules and in parallel to the decrease of the pH that activates processing enzymes, the prohormones undergo proteolytic cleavage by specific enzymes. PCs generally cleave after a dibasic amino acid motif such as Lys-Lys or Lys-Arg. Nine different PCs have been characterized: PC1/3, PC2, furin, PC4, PC5/6, PACE4, PC7, SKI-1 and PCSK9 (Seidah et al., 2008). In addition, the carboxypeptidases remove the basic residues from the carboxyl terminus. These two coordinated cleavages are required for the maturation of the prohormones and typically followed by the resulting peptide's amidation. This modification is catalyzed by an enzyme called peptidylglycine α -amidating monooxygenase (PAM) which has two catalytic units: a peptidylglycine α -hydroxylating monooxygenase (PHM) and a peptidyl α -hydroxyglycine α -amidating lyase (PAL) domain which act sequentially to produce an α -amidated peptide.

3.2 Generation and maturation of secretory granules

As already mentioned, the regulated secretion pathway is employed for secretion of a protein only when it is required and upon a stimulus. The mechanism of sorting into the regulated pathway is not entirely understood. Two hypotheses were proposed (Arvan and Castle, 1998;

Borgonovo et al., 2006). The first one, “sorting for entry”, is based on the presence of receptors at the TGN for inclusion into secretory granules. The second hypothesis, “sorting by retention”, is the one agreed by the field and suggests that the formation of regulated secretory granules is mediated by aggregation of the proteins. Beuret et al (2004), has reported that regulated secreted proteins were stored and secreted *via* granule-like structures in non-regulated cells that do not contain any receptor for the foreign protein. Unfortunately, these two models are not mutually exclusive. Indeed, receptors might connect aggregates with the budding membrane. In that manner, receptors would be strongly substoichiometric to cargo, which might explain that they are not easy to identify.

However, at the TGN, the secretory granules pinch off as immature secretory granules (ISGs) and undergo several steps in order to become mature (MSGs; Figure 4) which include:

- (i) **Removal of incorrectly sorted proteins.** During the budding at the TGN, some constitutive and lysosomal proteins are missorted into secretory granules such as lysosomal enzymes and constitutive secretory proteins and need to be removed. This removal is performed by the budding off of so-called constitutive-like vesicles from ISGs and requires AP-1/clathrin coats (Dittie et al., 1996; Kim et al., 2006) where most of the missorted protein are rerouted back to the constitutive pathway.
- (ii) **Acidification of the ISGs** induced by V-ATPases pumping protons into secretory granules. It has been shown that the pH from the TGN to the MSGs decreases from 6.2-6.5 at the TGN to 5.7-6.3 in ISGs and to 5.0-5.5 in MSGs (Hutton, 1982; Orci et al., 1986; Urbe et al., 1997). Inhibition of V-ATPase activity, with the V-ATPase inhibitor bafilomycin, generates a lower number of dense-core secretory granules in PC12 and AtT20 cells (Taupenot et al., 2005). Furthermore, acidification is necessary for the activation of the proteolytic enzymes such as prohormone convertases and carboxypeptidases (Steiner et al., 1992). As an example, in AtT20 cells, blocking V-ATPase induces the inhibition of POMC prohormone processing which leads to its secretion *via* the constitutive pathway (Tanaka et al., 1997).

- (iii) **Membrane remodeling** such as homotypic fusion (fusion of two ISGs). These fusions are responsible for the generation of big-sized ISGs and require the SNARE (soluble N-ethylmaleimide-sensitive factor attachment protein receptors) protein syntaxin 6 (Wendler et al., 2001).
- (iv) **Granule condensation** by acidification and removal of water. It induces a dense-core morphology of the granule and completes the maturation of the secretory granules (Kim et al., 2006).

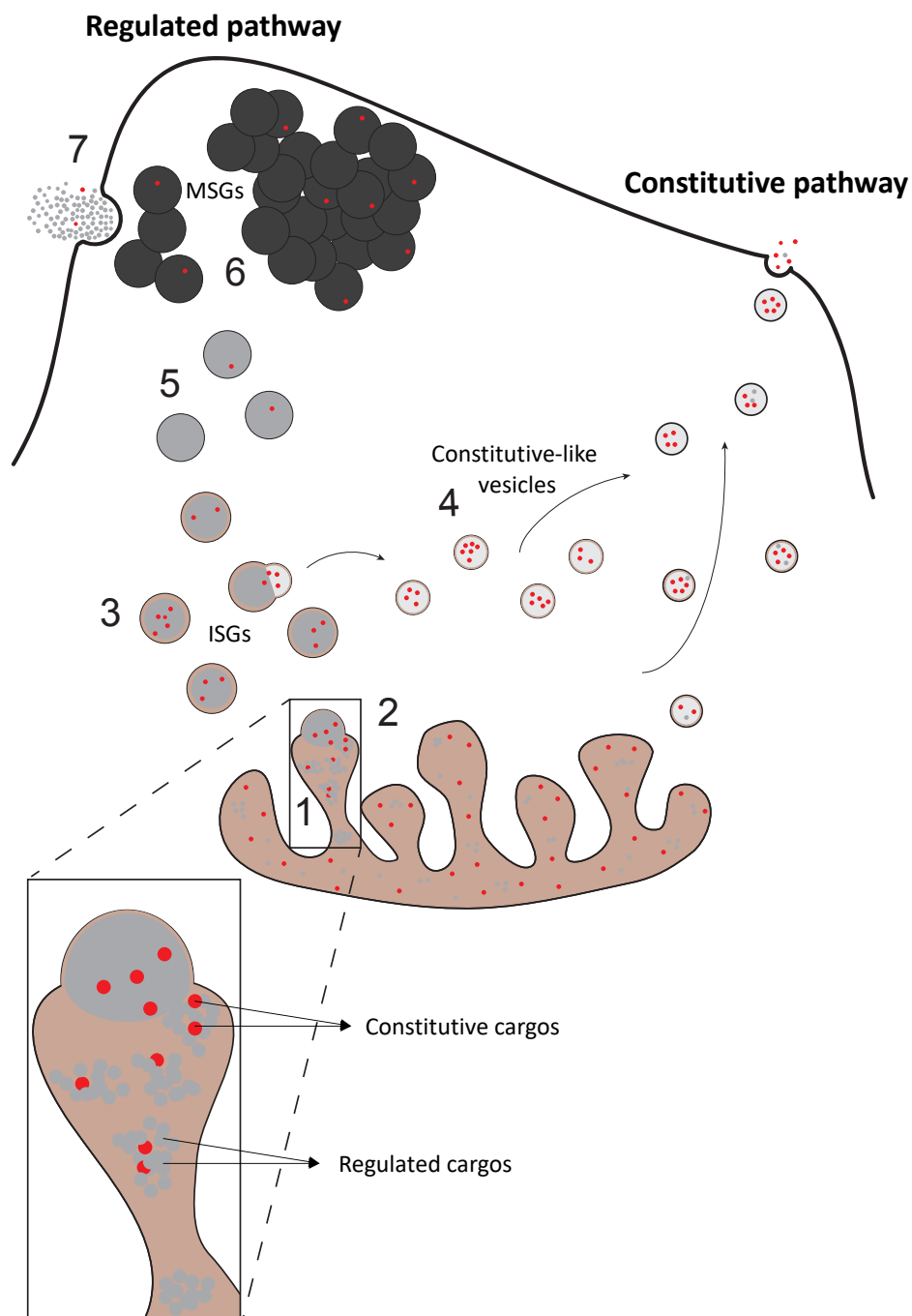


Figure 4. Secretory granules biogenesis and maturation vs. constitutive pathway

Constitutive vesicles are budding from the TGN and fusing with the plasma membrane upon arrival. The mechanism(s) of vesicle formation is poorly understood. The secretory granule biogenesis and maturation have been more extensively studied:

(1) Regulated cargos are aggregating at the TGN, trapping with them some constitutive proteins. (2) The aggregates allow the budding of the TGN membrane and (3) the pinching off of ISGs. (4) The majority of missorted proteins are removed *via* constitutive-like vesicles. (5) ISGs undergo acidification and membrane remodeling (not shown). (6) The final maturation step is the condensation of granule cargos and removal of water. The MSGs are forming two different pools of granules with high or low sensitivity to Ca^{2+} representing 1% and 99% of the total granules, respectively (Burgoyne and Morgan, 2003; Heinemann et al., 1993). (7) After a stimulus, granules fuse with the plasma membrane allowing the release of their content.

3.3 Fusion of MSGs with the plasma membrane and release of hormones

MSGs are transported and stored in a F-actin rich cortex (the cortical area) close to the plasma membrane, waiting for a stimulus mediating the fusion with the plasma membrane and the release of their content by exocytosis. Exocytosis is the final step of the regulated secretion pathway. It is triggered by an increase of Ca^{2+} and is composed of several steps including (i) tethering, (ii) docking and priming, and (iii) fusion of the MSGs to the plasma membrane involving various factors (Messenger et al., 2014; Figure 5).

- (i) The tethering of secretory granules is the initial attachment of the granules to the plasma membrane mediated by the tethering factors such as Rab3D, Rab27B and synaptogagmin-like proteins (Slps).
- (ii) Exocytosis requires the formation of a SNARE complex generated by the interplay between proteins located on the granules, V-SNAREs (V for vesicle), vesicle-associated membrane proteins called VAMP proteins and at the plasma membrane, T-SNARE (T for target), syntaxins and SNAP25 proteins. Indeed, in close proximity, V-SNAREs and T-SNAREs are interacting and leading to the formation of SNAREpin complex, involved in docking and priming. The protein Munc18-1 plays a role in the formation and the stability of SNARE complexes. Indeed, Munc18-1 interacts first with syntaxin which prevent the formation of the complex, but when SNAP25 and VAMP2 are in closed configuration, Munc18-1 switches to its role of facilitating the formation of SNAREpin.

- (iii) Finally, in response to Ca^{2+} , the last step is the fusion of the secretory granules with the plasma membrane. This is driven by synaptotagmin that contains two domains (C2 domains) which are Ca^{2+} binding sites and by this, Ca^{2+} sensors. Synaptotagmin triggers VAMP2-mediated membrane fusion where the complex SNAREpin provides the driving force for the fusion.

The example of secretory granule's exocytosis in acinar cells of the pancreas is shown in the Figure 5.

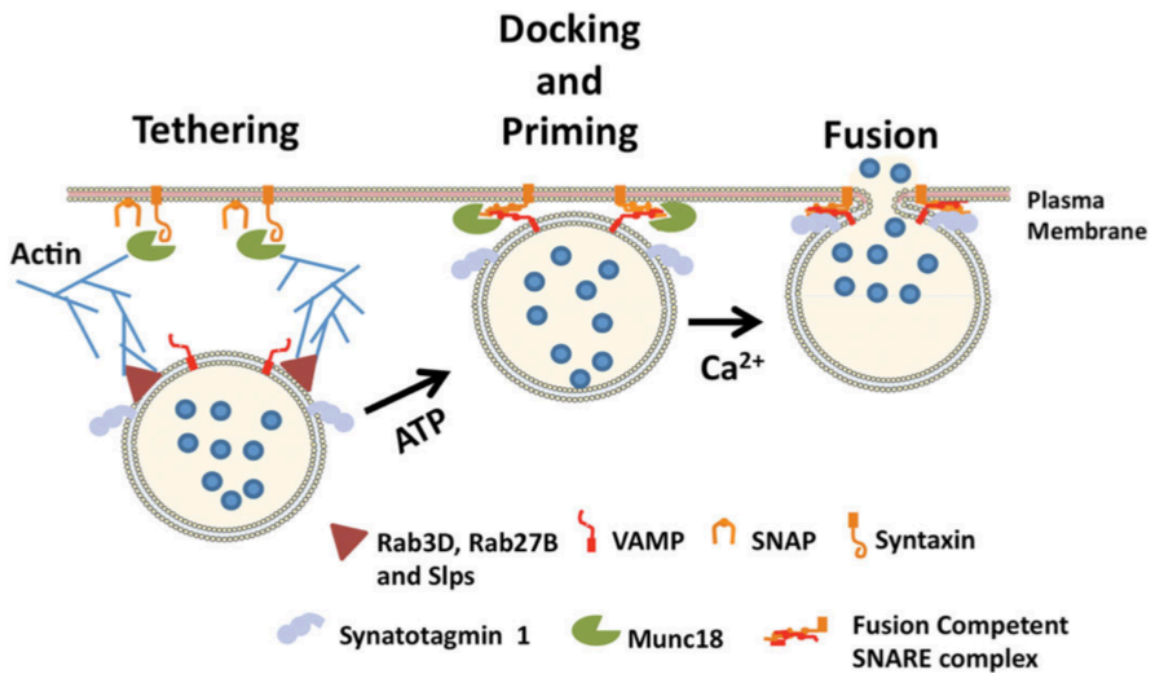


Figure 5. Exocytosis of acinar secretory granules

Exocytosis of secretory granules consists of several steps: tethering, docking, priming, and fusion involving proteins and factors. Rab3D, Rab27B, and Slps play a role in tethering while the formation of the SNAREpin (T-SNARE and V-SNARE interaction) is stabilized by Munc18 responsible for docking and priming. Finally, in response to elevated Ca^{2+} level, synaptotagmin 1 triggers VAMP2-mediated granule fusion. (From Messenger et al., 2014).

Depending on the cell type, the release of hormones into the bloodstream is stimulated either by membrane depolarization or by the binding of a chemical messenger to a specific receptor. Both kinds of stimuli lead to an increase of Ca^{2+} concentration in the cytosol *via* the opening of Ca^{2+} channels at the plasma membrane or of the ER (Meldolesi, 2002). There are different pools of secretory granules which differ in their ability to respond to Ca^{2+} and are classified as high-sensitive and low-sensitive to Ca^{2+} representing 1% and 99% of the total secretory

granules, respectively (Burgoyne and Morgan, 2003; Heinemann et al., 1993). Furthermore, it has been shown by pulse-chase experiments using multiple probes that newly synthesized insulin is released first in human pancreatic- β cells (Hou et al., 2012).

4. What controls secretory granule biogenesis and cargo sorting?

What are the molecular mechanisms controlling protein aggregation allowing secretory granules biogenesis? What are the determinants involved in the sorting of secretory granule cargos? Here, I describe the last advances in this topic.

Four mechanisms involved in the sorting of secretory granule cargos have been proposed: 1. the interaction of regulated secretory cargos with granule membrane proteins or lipids, 2. the involvement of granins, 3. the implication of actomyosin complex, and 4. the presence of sorting motifs in regulated cargos

4.1 The interaction of regulated secretory cargos with membrane proteins/lipids

- Interaction of granule proteins with lipids:
Lipids seem to be implicated in the process of granule formation. Indeed, cholesterol-rich membrane was shown to play a role in the targeting of regulated proteins into secretory granules and formation of them (Wang et al., 2000). Hosaka et al. (2004) suggested that SgIII binds cholesterol on the membrane of secretory granules and induces the retention of CgA in the secretory granules. In addition, it was also shown that some proteolytic enzymes such as PC2 (Blazquez et al., 2000), CPE (Dhanvantari and Loh, 2000) and PC3 (Arnaoutova et al., 2003) bind to cholesterol-rich membrane patches.
- Interaction of granule proteins with membrane-associated proteins:
Evidence of the interaction between granule proteins and proteins associated with the granule membrane has been found. Indeed, proenkephalin, proinsulin, POMC and brain-derived neurotrophic factor precursor were suggested to interact with CPE

allowing their incorporation into secretory granules (Cool and Loh, 1998; Lou et al., 2005). It was also shown that SCLIP and SCG10, two trans-Golgi proteins, interact with CgA and regulate protein secretion in chromaffin cells (Mahapatra et al., 2008). Indeed, the downregulation of either SCLIP or SCG10 led to a decreased secretion level of CgA and CgB respectively, as well as a general decrease in chromaffin granule density, suggesting a role of these proteins in granule formation and maturation. Furthermore, HID-1, a peripheral membrane protein, was shown to be implicated in neuropeptide sorting and insulin secretion (Hummer et al., 2017). The depletion of HID-1 led to a decrease in granule number, a defect in cargo sorting and an impairment of TGN acidification.

4.2 Granins are essential for granule biogenesis

It appears that CgA and also granins in general, are essential for granules biogenesis. Indeed, in PC12 cells, downregulation of CgA expression led to a decrease of granule number, while the expression of CgA in fibroblast mediated the formation of granule-like structures (Kim et al., 2001; Loh et al., 2004). Furthermore, it was shown that deficient-CgA mice undergo reduction in adrenal chromaffin cells (Kim et al., 2005). In addition, in PC12 cells, the depletion of CgB or SgII expression also reduced granule number and size (Courel et al., 2010; Huh et al., 2003). SgIII has also been implicated in secretory granules sorting by interacting with CPE, cholesterol-rich membrane, and CgA (Hosaka and Watanabe, 2010).

4.3 Actomyosin complex controls secretory granule biogenesis and sorting

It has been shown in PC12 and COS-7 cell lines, that F-actin and myosin 1b control secretory granules biogenesis and sorting (Delestre-Delacour et al., 2017). Indeed, the knockdown of myosin 1b led to a strong reduction of the number of secretory granules. Furthermore, F-actin mediated secretory granule biogenesis through the actin-related-protein 2/3 (Arp2/3) activation.

4.4 Regulated cargos contain sorting motifs

Different types of motifs/domains have been reported to be important for granule sorting:

- Paired basic amino acids:

Paired basic amino acids are present in proneurotensin (Felicangeli et al., 2001), prorenin (Brechler et al., 1996), and progastrin (Bundgaard et al., 2004) and were shown to direct these proteins into secretory granules.

- α -helix domain:

A common domain, forming a α -helix, present in PCs was shown to be responsible for granules sorting. Indeed, such a helix is present in PC1/3; PC2 and PC5/6A and was reported to reroute a constitutively secreted protein into secretory granules (Dikeakos et al., 2007a; Dikeakos et al., 2007b). Such a domain is also present in carboxypeptidase E (Dikeakos et al., 2007b), prosomatostatin (Mouchantaf et al., 2001), CgA (Taupenot et al., 2002) and in the neuropeptide precursor VGF (Garcia et al., 2005) and was shown to be necessary and sufficient to target these cargos to secretory granules.

- Disulfide loop domain:

The presence of a disulfide loop has already been shown to mediate secretory granules incorporation in the 90ies. Indeed, the N-terminal disulfide loop of CgB was reported to be sufficient to target cargos to secretory granules (Chanat et al., 1993; Glombik et al., 1999; Kromer et al., 1998) and the fusion of a related N-terminal loop, presents in POMC, with a reporter protein, was mediated its incorporation into granules (Cool and Loh, 1994; Tam et al., 1993). More recently, it has also been shown that the N-terminal domain of CgA containing a disulfide bond from C17–C38 (22 residues) was important for granule sorting (Taupenot et al., 2002). Furthermore, this same domain induced granule-like structures in COS-1 cells (Stettler et al., 2009).

To summarize, despite extensive studies trying to clarify the mechanisms mediating secretory granule formation and regulated protein secretion in the past decades, they are still poorly understood and need to be overcome. Furthermore, prohormones have a tendency to aggregate and understanding the mechanism underlying regulated cargo sorting is crucial

because a disturbance in their sorting can lead to different diseases, especially *via* amyloid formation which is shown in the following part.

5. The starting point of this thesis project

5.1 Bad and good amyloid aggregation

Amyloids are a type of aggregates forming cross β -sheets where β -strands are perpendicular to the fiber axis. They have two features of diffraction, 4.7 Å which is the space between strands and ~ 10 Å which corresponds to the distance of side chains packing between β -sheets. The assembly in amyloid fibrils is nucleation dependent (Figure 6). Indeed, *in vitro*, there is first a lag phase which allows the formation of a fibril nucleus followed by an exponential phase where the fibrils grow until they reach an equilibrium phase (Chiti and Dobson, 2017; Jackson and Hewitt, 2017; Knowles et al., 2014).

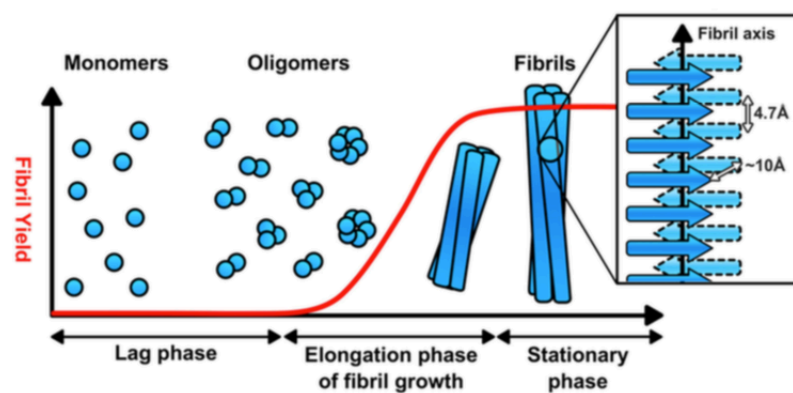


Figure 6. Amyloid fibril formation

The formation of amyloids starts by a lag phase in which monomers form oligomers that serve as nuclei for rapid fibril assembly called the elongation phase. Fibrils assemble and grow until reaching stationary phase. The inset shows the cross β -structure with the relevant repeat distances. (From Jackson and Hewitt, 2017).

- Protein misfolding and (bad) amyloid formation in human diseases

Protein misfolding disorders (PMDs) is a class of diseases associated with the presence of misfolded or aggregated proteins. In those PMDs, there is a class of amyloidosis diseases where the aggregation is mediated by amyloids, among them, Alzheimer,

induced by amyloid- β -peptide accumulation, or Parkinson caused by α -synuclein amyloid plaques (Chiti and Dobson, 2017; Westermarck, 2005). Among these proteins and peptides known to form amyloid fibers in human diseases, polypeptide hormones are over-represented; for instance, amylin (islet amyloid polypeptide) in diabetes mellitus type 2, calcitonin in medullary carcinoma of the thyroid, or prolactin in pituitary prolactinoma.

- Functional (good) amyloids mediate secretory granule sorting

Amyloids were first identified as toxic aggregates which cause various amyloidosis diseases. However, some amyloids were also recognized as having physiological functions, so-called functional amyloids. For instance, curli fibrils, appendages found in many Gram negative and Gram positive bacteria in biofilms, are described as amyloids. In addition, the melanocyte proteins PMEL17 expressed in pigment cells of the skin and the eye are forming amyloids allowing the polymerization of melanin, a natural pigment (Jackson and Hewitt, 2017). Interestingly, Maji et al (2009) showed *in vitro*, that peptide and proteins hormones form amyloid aggregates and *in vivo*, using mouse pituitary tissue, that pituitary hormones such as prolactin and growth hormones, colocalized with amyloid-specific dyes. These findings indicate a biological function of amyloids, suggesting prohormones to be stored as functional amyloids into secretory granules.

The correlation of Maji et al (2009) evidences that prohormones are concentrated in secretory granules as functional amyloids and that several mutated prohormones give rise to severe amyloidosis diseases, suggests that sequences evolved to form functional amyloid aggregation in granules may also be responsible for pathological amyloid aggregation. However, the mechanisms controlling amyloid formation are still poorly understood and it is challenging, but also essential, to have a better understanding of these mechanisms, that would be useful to develop strategies fighting against amyloidosis.

5.2 The nonapeptide vasopressin is responsible for bad and good amyloids formation of its precursor

Vasopressin is synthesized as a precursor, pre-provasopressin, composed of a signal sequence for ER targeting, the nonapeptide vasopressin, neurophysin II (NPII) as a protein carrier, and a glycopeptide. The structure of the precursor is stabilized by seven disulfide bonds in NPII and one in vasopressin. More than seventy different mutations throughout the precursor were shown to cause autosomal dominant neurohypophyseal diabetes insipidus characterized by an abnormal increase of thirst and of dilute urine. Except one, all mutations are dominant. These mutations were shown to disrupt the proper folding of the precursor leading to the formation of toxic fibrillar and amyloid-like aggregates in the ER (Beuret et al., 2017; Birk et al., 2009). Furthermore, Beuret et al. (2017) studied the sequences responsible for amyloid-aggregation of the mutants and identified the glycopeptide and the nonapeptide of vasopressin as amyloidogenic sequences. Interestingly, in AtT20 cells, the same sequences causing pathogenic ER aggregation were responsible for regulated granule sorting, supporting the proposal of Maji et al. (2009) that peptide hormones form functional amyloids in order to be secreted *via* granules. It was concluded that ER aggregates of mutant provasopressin are mis-localized amyloid aggregates that evolved to mediate sorting into granules and are induced by the same sequences, the glycopeptide and the nonapeptide vasopressin.

5.3 Small disulfide loops in vasopressin and other hormones

The nonapeptide vasopressin shown to mediate either pathogenic or functional amyloids aggregation in the ER and in secretory granules respectively, contains a small disulfide bond from Cysteine-1 to Cysteine-6, which we called a CC loop. Similar CC loops with 6–12 residues are present in several other peptide prohormones (Table 1). Of the 12 (pro)hormones listed in Table 1, four were also found by Maji et al. (2009) to aggregate as amyloids (vasopressin, oxytocin, prolactin and growth hormone), which was the basis for the proposal that granule aggregation is actually based on a functional amyloid.

prohormones containing CC loop(s)	length of the CC loops (amino acids)	N-ter	C-ter
Vasopressin	6	CYFQNCPRG...	
Oxytocin	6	CYIQNCPLG...	
Prolactin	8 and 9	...LPICPGGAARCQVT...	...LLKCRIIHNNNC•
Growth hormone	9		...MKCRRFAESSCAF•
Somatostatin	12		...AGCKNFFWKTFTSC•
Cortistatin	12		...PCRNFVKTFSSCK•
Prorenin	8	...SSKCSRLYTACVYH...	
Amylin	6	...KCNATCATQ...	
Calcitonin	7	...RCGNLSTCMLG...	
Osteocalcin	7		...REVCELNPDCDEL...
Urotensin 2	6		...TPDCFWKYCV•
Urotensin 2B	6		...KRACFWKYCV•

Table 1. List and sequences of prohormones containing a CC loop

Taking all together, it brought us to the question:

Do small disulfide (CC) loops in peptide hormones mediate self-aggregation in secretory granule biogenesis?

To answer this question, we tested the impact of different CC loops from several prohormones – vasopressin, amylin, calcitonin, prorenin, and prolactin – on the aggregation of a misfolded reporter in the ER and on the sorting of a constitutive protein into secretory granules.

II. Results

The starting point of our analysis of CC loops as potential aggregation motifs were studies on provasopressin (Beuret et al., 2017; Birk et al., 2009; Shi et al., 2017; Spiess et al., 2020). This prohormone was shown to contain two aggregating elements, CCv (the CC loop of vasopressin), and the glycopeptide (Figure **7A**). Both induce aggregation of folding-deficient mutants in the ER and of a folded precursor at the TGN into secretory granules. We hypothesized that these two motifs are naturally inducing aggregation and evolved to mediate sorting into and biogenesis of secretory granules as functional amyloids (Maji et al., 2009). The CC loop caught particularly our attention after the observation that similar CC loops are present in several peptide hormones or precursors and we decided to first test the CC loops' ability to aggregate in the ER in comparison to CCv.

1. CC loops mediate ER aggregation of a non-folded reporter

It has previously been shown that a truncated version of pre-provasopressin, CCv-NPΔ (called 1–75 in Beuret et al., 2017), cannot fold and is retained in the ER forming fibrillar aggregates. It is composed of a signal sequence, the vasopressin hormone CCv, and a C-terminally truncated form of neurophysin II (NPΔ) fused to a hexahistidine (His₆) tag. When the CCv segment was replaced by a sequence composed of prolines and glycines (Pro1) to eliminate the ring and disrupt secondary structures, ER aggregation was essentially abolished (Beuret et al., 2017; Birk et al., 2009). To test whether CC loops of other prohormones are also able to cause aggregation, we replaced the CCv sequence by other CC loops (CCx, where x indicates the origin of the different CC loops) from various hormones: CCa from amylin, CCc from calcitonin, CCr from prorenin, and CCpN from the N-terminus of prolactin (Figure **7B**, left). CCpC, the C-terminal CC loop of prolactin, was fused C-terminally to NPΔ (as illustrated in Figure **7B**, right).

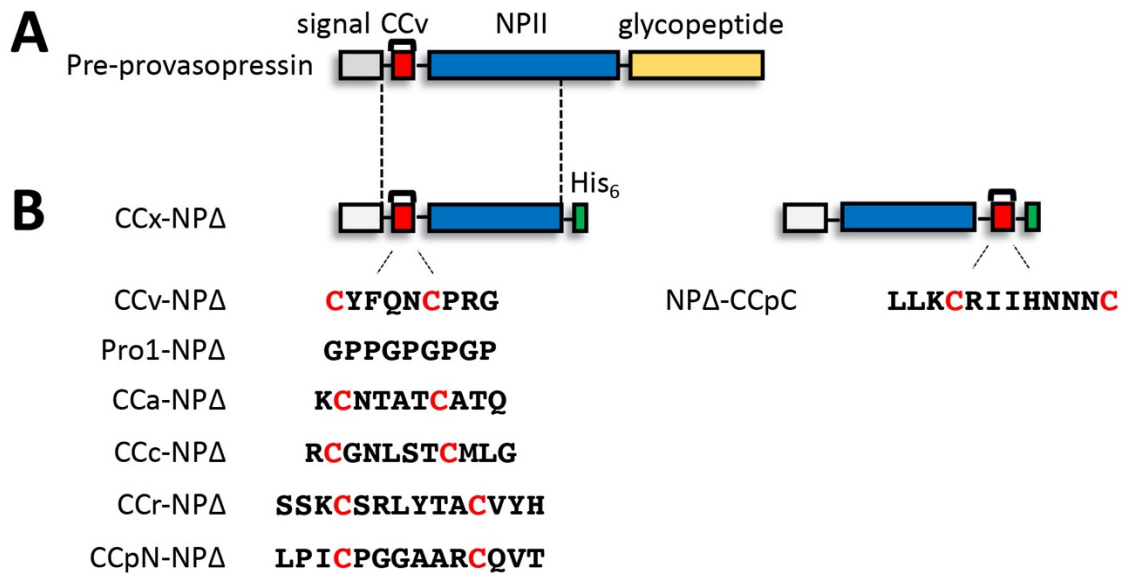


Figure 7. Schematic representation of CC loop constructs

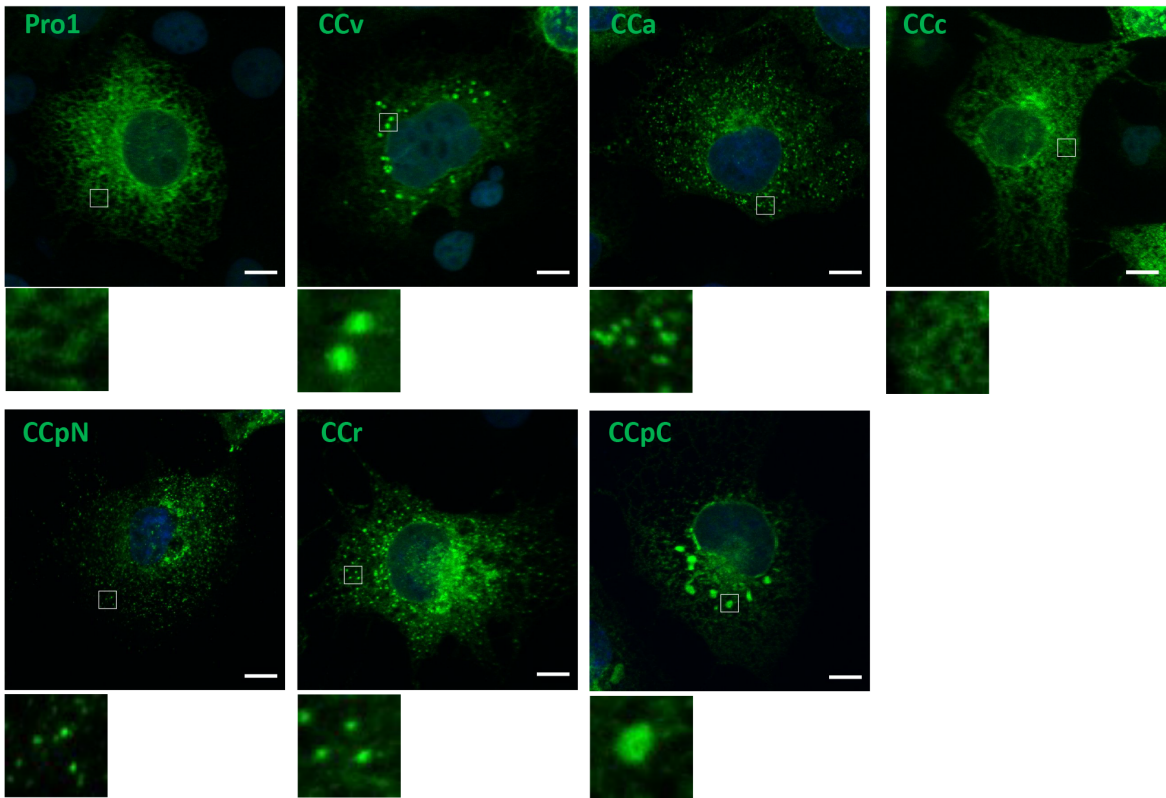
Schematic representation of pre-provasopressin (**A**) and CCx-NPΔ constructs (**B**) to study aggregation in the ER. Pre-provasopressin is composed of its signal sequence, CCv (the nonapeptide vasopressin with its disulfide bond), neurophysin II (NPII), and the glycopeptide. The constructs CCx-NPΔ are based on a truncated version of pre-provasopressin composed of the signal sequence of pre-proenkephalin, vasopressin (CCv), the 65 first amino acids of NPII, and a His₆ tag. The vasopressin sequence, CCv, was replaced by the indicated sequences composed of a proline/glycine-rich peptide Pro1 as a negative control, and the different CC loops of amylin (CCa), calcitonin (CCc), prorenin (CCr), or the N-terminal one of prolactin (CCpN). In construct NPΔ-CCpC, the C-terminal CC loop of prolactin was inserted C-terminally between NPΔ and the His₆ tag.

1.1 CC loops mediate aggregation to different extents

To analyze the aggregation propensity, we transiently transfected our CCx-NPΔ constructs and Pro1-NPΔ as a negative control in either COS-1 fibroblast cells or in the neuroblastoma cell line Neuro-2a, and analyzed their localization by immunofluorescence microscopy (Figure **8**). Transfected cells containing discernible fluorescence aggregations were quantified as a percentage of total expressing cells. In COS-1 cells, Pro1-NPΔ was found evenly distributed in the ER network in the majority of expressing cells. In contrast, CCv-NPΔ produced clear accumulations in most cells, confirming CCv's capacity to mediate ER aggregation as previously observed (Beuret et al., 2017; Birk et al., 2009). Similarly, CCa, CCr and CCpN make rather fine aggregates, which are rarely produced for CCc, whereas CCpC, frequently produced rather large accumulations (Figure **8A**). In comparison, Neuro-2a cells seem to only produce aggregates when CCv, CCa and CCpN are expressed (Figure **8B**).

A

COS-1

**B**

Neuro-2a

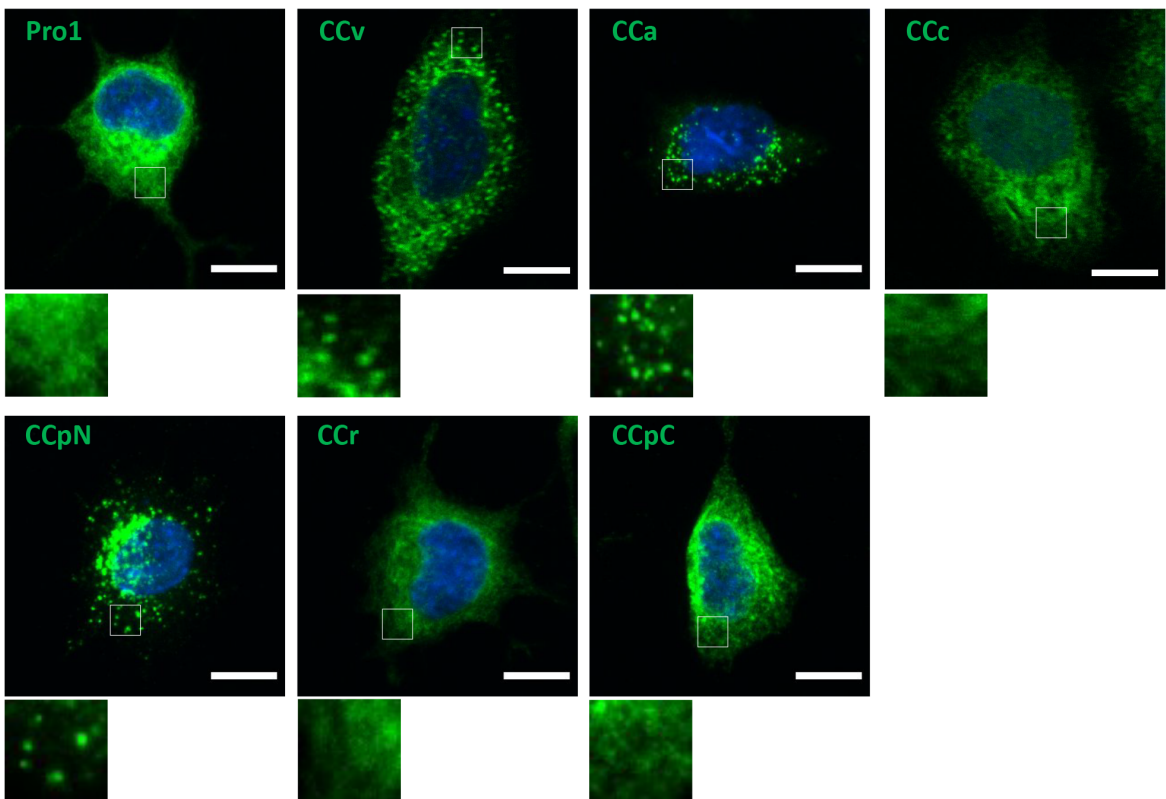


Figure 8. ER aggregation of CCx–NPA constructs in COS-1 and Neuro-2a cells

COS-1 (A) and Neuro-2a cells (B) were transiently transfected with the NPA constructs listed in Figure 7B, stained with anti-His₆ antibodies, and analyzed by immunofluorescence microscopy. Below each image, enlargements of the regions indicated by white squares are shown. Scale bars, 10 μm.

Quantitation confirmed in COS-1 cells, the ability of all constructs, except CCc, to produce a statistically significant increase of cells with aggregation above background (Figure 9A). The highest aggregation propensity was found for CCpN, CCv and CCa. In Neuro-2a, aggregation of CCpN and CCv was equally high, while it was reduced for CCa and even not significant for CCr and CCpC, as well as again for CCc (Figure 9B).

The analysis thus shows differences in aggregation between the different CC loops and between the expressing cell lines. The latter might be due to expression levels, which are likely to be higher in COS-1 cells where plasmids with SV40 origins – as it is the case for the expression plasmid pcDNA3 we used – are amplified. Alternative explanations are differences in chaperone levels and/or ERAD capacities of the cell lines. Overall, it appears that the Neuro-2a expression system is less permissive of aggregation of our constructs and thus more clearly displays the differences in aggregation efficiency of the different CC loops tested.

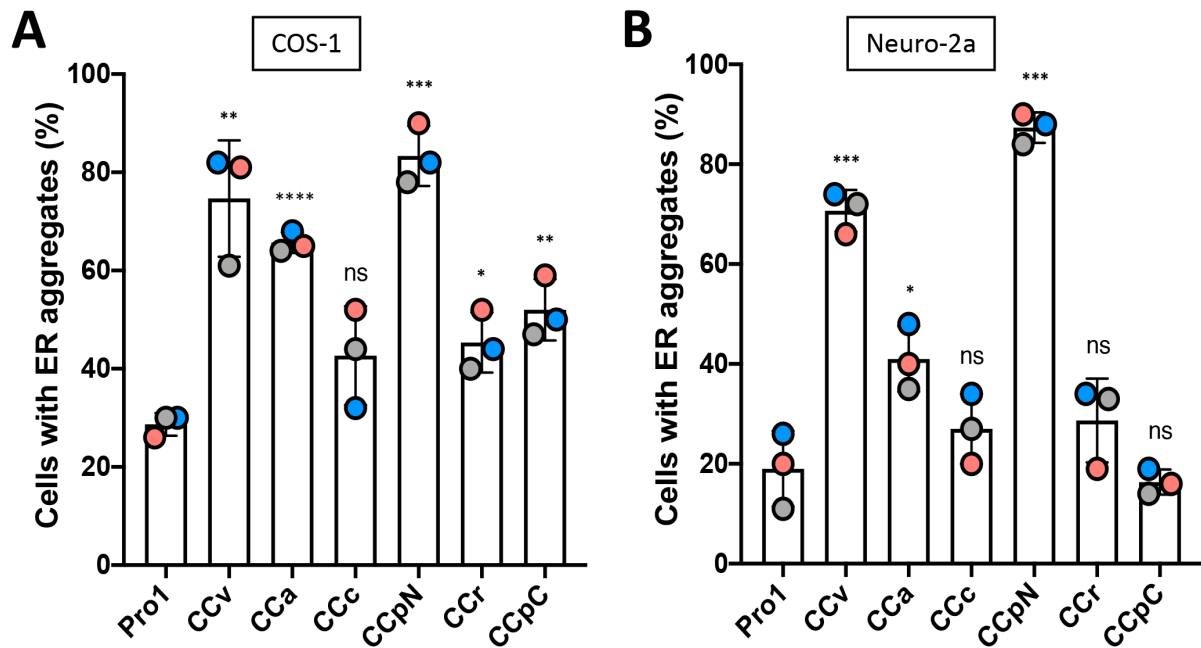
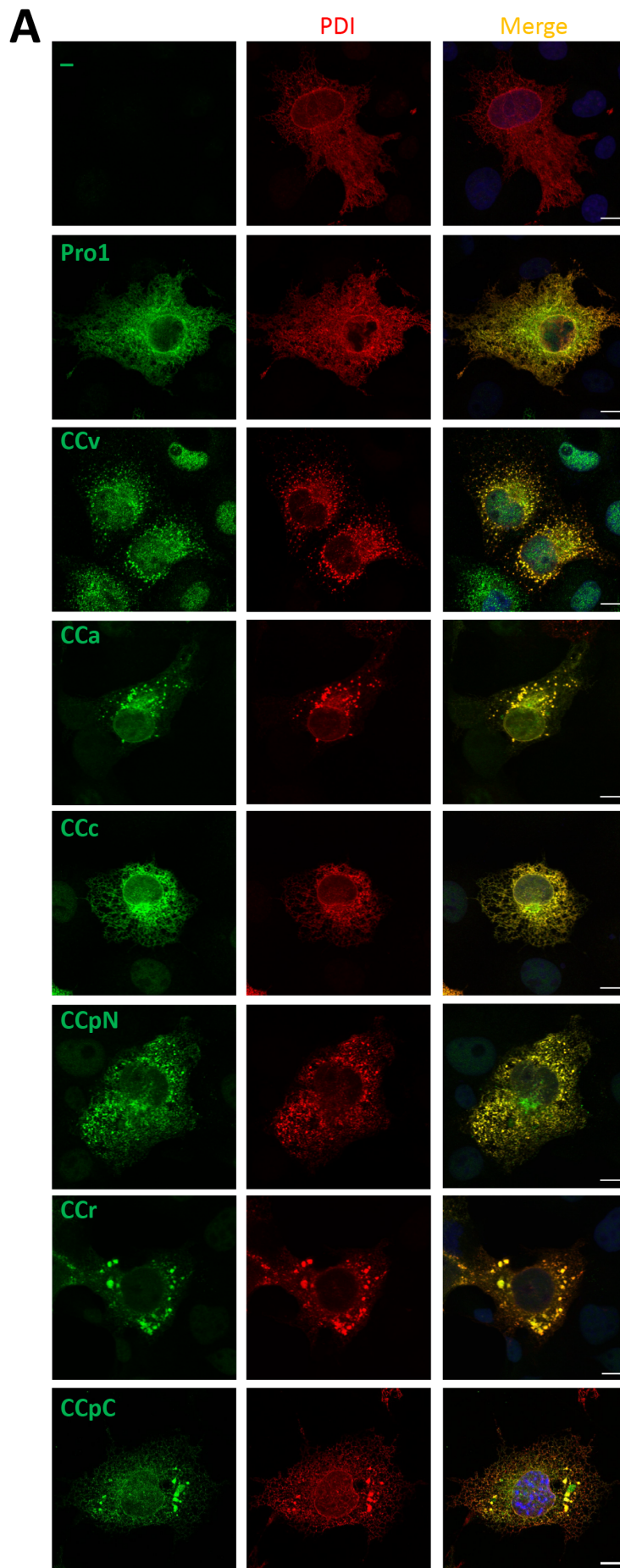


Figure 9. Quantitation of CC loop-mediated ER aggregation

COS-1 (A) and Neuro-2a (B) cells were transiently transfected with the NPA constructs listed in figure 7B and imaged by immunofluorescence microscopy as in Figure 8. The number of cells with aggregates were quantified from 100–150 expressing cells for each construct in three independent experiments. Statistical significance was calculated using the unpaired Student's t-test. ns, non-significant; * $p \leq 0.05$; ** $p \leq 0.01$; *** $p \leq 0.001$; **** $p \leq 0.0001$.

1.2 The aggregates colocalize with PDI in the ER

To confirm the localisation of the CCx-NPA aggregates in the ER, we transiently co-transfected, in both cell types, the NPA constructs with a N-terminal tagged version of PDI (myc-PDI), an ER chaperone introducing and shuffling disulfide bonds. We then performed immunofluorescence staining and imaged the cells by confocal microscopy (Figure 10A and 10B). Myc-PDI expressed alone in either COS-1 or Neuro-2a cells was visualized in the typical network pattern of the ER, as expected. When co-expressed with Pro1-NPA or the CCx-NPA constructs, myc-PDI clearly colocalized with each of them confirming the localisation of the proteins in the ER. Myc-PDI not only colocalized with the NPA fusion proteins in the normal ER, but also concentrated in the aggregates. This result was not surprising, since the neurophysin II fragment in the constructs, is unable to fold and is, with nine cysteines, a substrate of PDI. It should also be pointed out that the fraction of cells with visible aggregates was reduced upon co-expression with myc-PDI. Indeed, PDI overexpression is likely to increase the capacity of the cell to keep NPA constructs in solution and competent for degradation by ERAD.



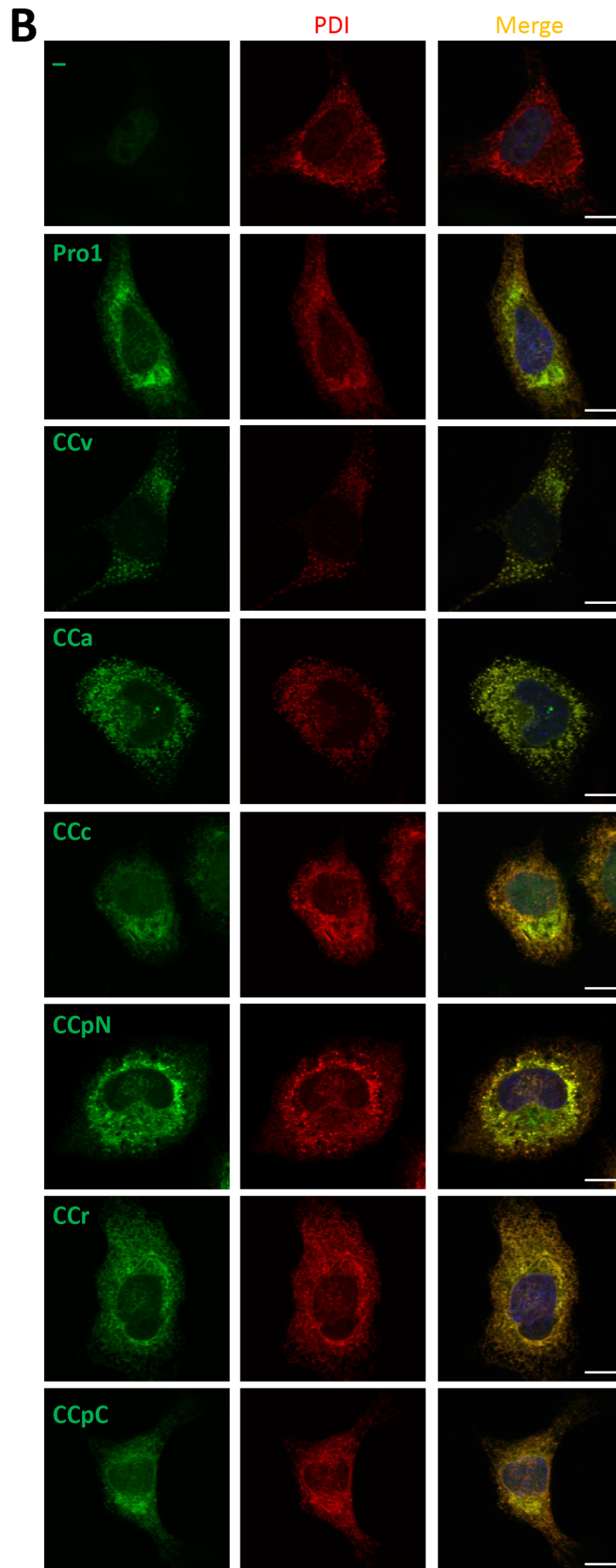


Figure 10. CC loop aggregates colocalize with an ER marker

Immunofluorescence micrographs of COS-1 (A) or Neuro-2a (B) cell lines co-transfected with the N Δ constructs listed in Figure 7B and with myc-tagged PDI are shown. Cells were stained for the indicated N Δ constructs with anti-His₆ antibodies and for PDI with anti-myc antibodies. Scale bars, 10 μ m.

1.3 Ultrastructure of CC loop constructs

Previously, it has been observed that folding-deficient mutants of pre-provasopressin aggregating in the ER form amyloid-like fibrils (Birk et al., 2009). For this reason, we studied the ultrastructure of our protein aggregates by electron microscopy. To unambiguously identify structures containing CCx-N Δ proteins, we applied immunogold detection using anti-His₆ antibodies and 10-nm colloidal gold conjugated secondary antibodies (Figure 11). We performed the experiments only in Neuro-2a cells, the more relevant model cell line for our study.

The anti-His₆ antibodies allowed us to detect signals in aggregates, but hardly at all in the ER. When the proteins were not aggregated, their concentrations were below the threshold of detection. Indeed, the gold staining is specific for concentrated proteins, and no gold on mitochondria, nuclei, or in mock-transfected cells was observed. As expected, we identified dense structures with different sizes and shapes, depending of the CC loop tested, that were decorated with gold. We observed gold-positive very round aggregates for CCv with a size between 180 to 420 nm, similar size roundish aggregates for CCpN and bigger roundish or more elongated structures for CCa, between 1200 nm to 2400 nm. Surprisingly, even CCc, CCr, and CCpC, unconvincing by immunofluorescence, showed immunogold-positive dense structures. CCc aggregates did not show specific shapes and sizes, while for CCr and CCpC, we clearly observed smaller concentrated structures, between 60 and 80 nm and 30–150 nm in size respectively. The discrepancy to the light microscopy experiments could be explained by the small sizes of the dense-structure, which certainly cannot be resolved by immunofluorescence and even in clusters might not be detectable. As to their internal morphology, the aggregates were always very compact and no evidence of fibrillar substructure could be detected.

We conclude that besides vasopressin, CC loops of several other prohormones also have the capacity to mediate ER aggregation in different cell lines and to different extents. The aggregates have different shapes and sizes showing specificity of the CC loops tested.

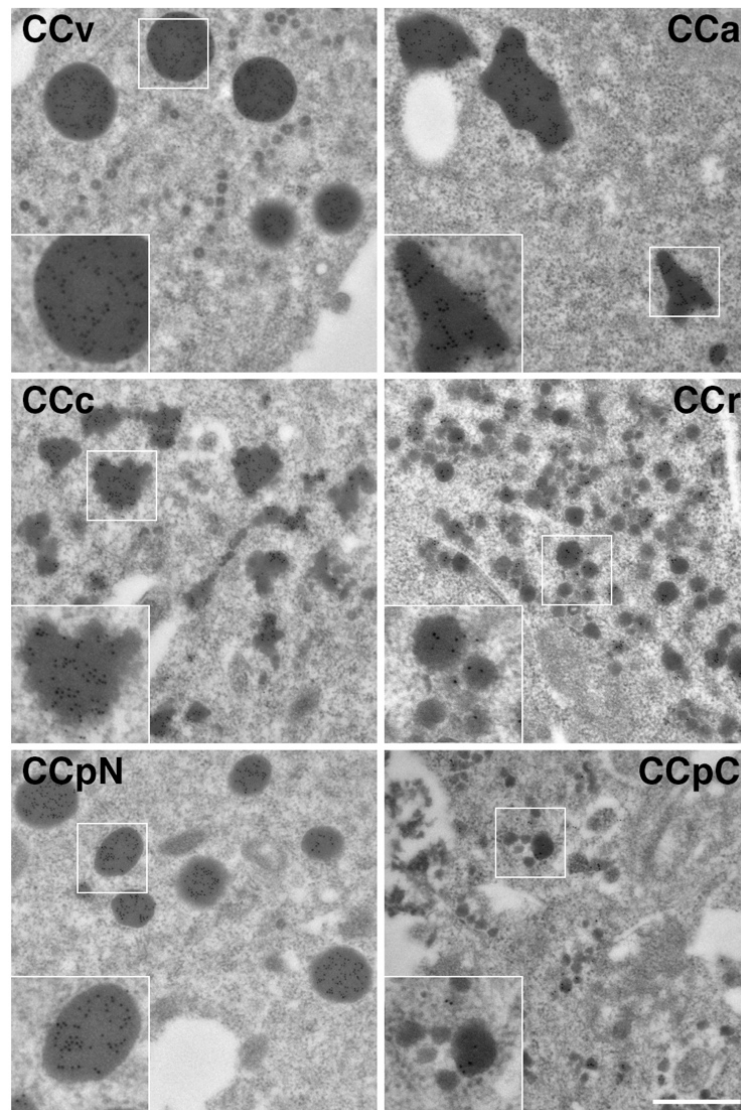


Figure 11. CC loop aggregates show different EM morphologies

Electron microscopy images of the NP Δ constructs in transfected Neuro-2a cells immunogold-stained using anti-His₆ antibodies are shown. No gold-stained structures were detected for Pro1-NP Δ . Onsets show enlargements of the corresponding boxed areas. Scale bar, 500 nm.

2. CC loops mediate sorting of a constitutive reporter into secretory granules

ER aggregation of provasopressin mutants is believed to be the inadvertent result of sequences that evolved to mediate self-aggregation in the TGN for sorting into secretory granules. Our finding that CC loops of different prohormones mediate aggregation of a misfolded reporter in the ER, just like vasopressin, supports the hypothesis that CC loops might act as general aggregation motifs in granule biogenesis.

2.1 α -1 protease inhibitor (A1Pi) as a reporter for CC loop-mediated granule sorting

To directly investigate the role of CC loops in the granule biogenesis process, we looked for a reporter that is constitutively secreted and does not aggregate on its own. We considered different artificial reporters (secretory forms of GFP, mCherry, or the Fc fragment of IgG), but we decided to use a known and natural constitutive protein, A1Pi as a reporter. A1Pi has previously been used as a constitutively secreted protein for comparison with regulated cargo such as the granins (Beuret et al., 2017; Glombik et al., 1999; Kromer et al., 1998). It was also successfully used as a fusion protein with CgB to identify its N-terminal domain of 31 residues with a single disulfide bond to contribute to granule sorting.

We fused A1Pi to our CC loops at the N-terminus and to a His₆ and a myc tag at the C-terminus (generating A1Pimyc and CCx-A1Pimyc; Figure **12A**). To enhance a potential effect of CC loops in secretory granule sorting, we designed additional constructs where we fused a second copy of the CC loop at the C-terminus in front of the tags (2xCCx-A1Pimyc; Figure **12A**). Indeed, hormone precursors may be dimeric (provasopressin) or have more than one aggregating motif (CCv and glycopeptide; Beuret et al., 2017).

All A1Pimyc constructs were transfected into AtT20 cells, stably expressing cells were selected, and clonal cell lines isolated. To be sure that the expression level of our constructs in each cell line cannot affect our results, we selected clones with very similar expression levels. Therefore, to determine the expression levels of the constructs, cell lines were metabolically labelled with [³⁵S]methionine for 30 min, immunoprecipitated with anti-myc

antibodies, and analyzed by SDS-gel electrophoresis and autoradiography (Figure **12B**). As a loading control, actin expression was analyzed simultaneously. However, since actin was not consistently discernible on the autoradiographs, we normalized the expression level of the A1Pimyc constructs to a background band of ~130 kDa (ns for non-specific band), whose intensity closely paralleled that of actin (Supplementary Figure **S1**). Cell lines of each constructs were chosen for further analysis with very similar rates of synthesis mostly within $\pm 20\%$ (Figure **12B**).

As expected, two forms of labelled A1Pimyc or CCx-A1Pimyc constructs were produced, corresponding to the high-mannose ER form (lower band) and the complex glycosylated form (higher band). The presence of the complex glycoform indicates that already within 30 min, significant amounts of A1Pi with and without CC loops had left the ER and reached the medial Golgi compartments, where glycan remodelling to the complex structures takes place. The presence of CC loops in the constructs thus did not interfere with A1Pi folding and did not cause ER retention themselves, a prerequisite to study sorting at the TGN.

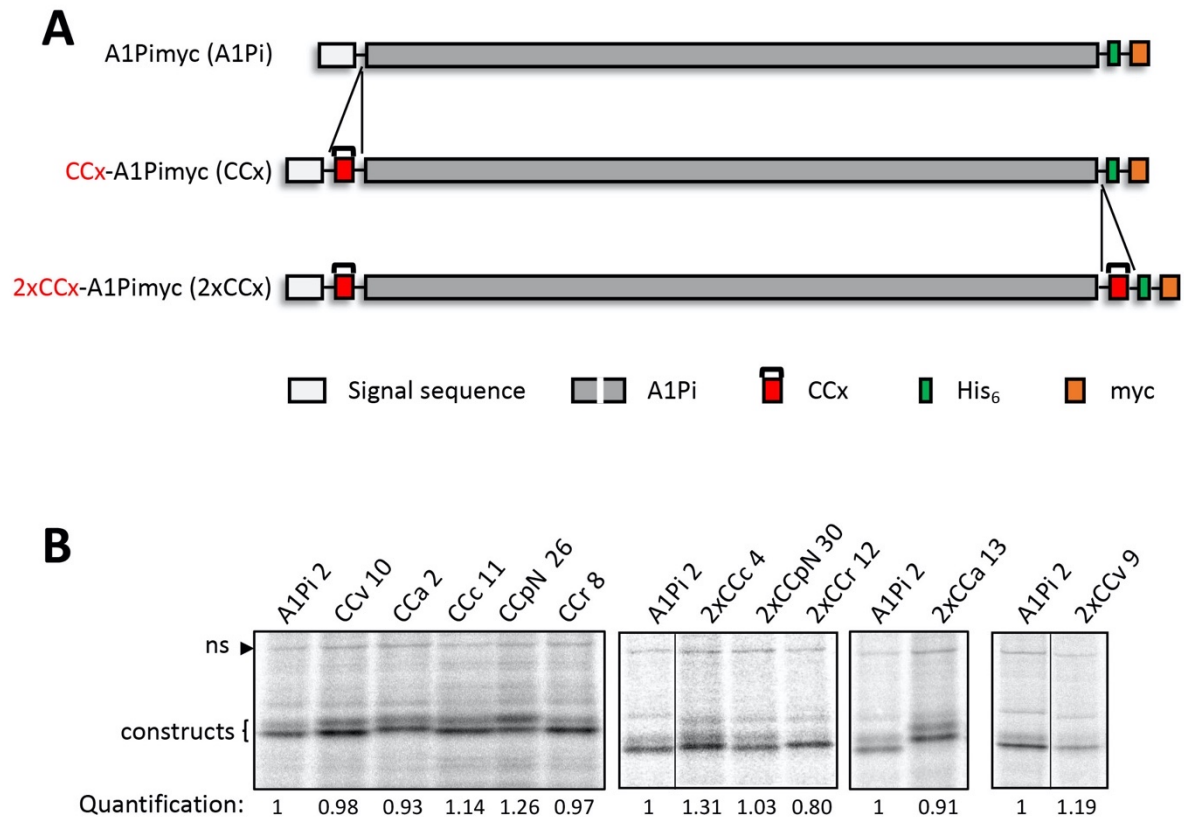


Figure 12. Model proteins to determine granule sorting in stable AtT20 cell lines

(A) Schematic representation of the parental reporter protein, composed of the signal sequence of pre-proenkephalin, A1Pi, a His₆ and a myc tag. The CC loop sequences listed in Figure 7B were inserted between signal sequence and A1Pi to produce the constructs CCx-A1Pimyc. For constructs 2xCCx-A1Pimyc, a second copy of the same CC loop sequence was inserted at the C-terminus of A1Pi. (B) AtT20 cell lines stably expressing A1Pimyc, CCx-A1Pimyc, or 2xCCx-A1Pimyc were generated and cloned. To identify clonal lines with similar expression levels, they were labeled with [³⁵S]methionine for 30 min. The constructs were immunoprecipitated with anti-myc antibodies and analyzed by SDS-gel electrophoresis and autoradiography. The lines matching best are shown, analyzed together with the control cell line expressing A1Pimyc. The number designates the respective clonal cell line. The expression level of each clone normalized to the non-specific band (ns) as a loading control and to A1Pimyc is indicated below each lane. A1Pi constructs appear as high-mannose and complex glycosylated forms, demonstrating efficient ER exit. Every panel corresponds to a single gel with identical exposure. Black lines indicate deleted lanes.

2.2 The CC loop disulfide bonds are formed efficiently

In provasopressin, CCv is part of a folded structure with a binding pocket in the neurophysin II fold (Chen et al., 1991; Wu et al., 2001). In our A1Pi fusion constructs, CCv and all other CC loops are attached externally to the globular reporter. It is thus an important question, whether the disulfide bond in the added sequence is fully, partially, or not at all oxidized to a

disulfide loop, when the protein exits the ER, reaches the TGN, and eventually is secreted. To determine the oxidation state of the CC loops' disulfide bonds, we collected media from our cell lines and immunoprecipitated the proteins for subsequent mass spectrometry analysis (Figure **13**). Two samples were prepared for each construct, with or without reduction by tris(2-carboxyethyl)phosphine (TCEP). Subsequently, all samples were incubated with iodoacetamide to alkylate the thiol groups of free cysteines. After either trypsin or Lys-C digestion, the resulting peptides that cover both cysteines in the disulfide-bonded or the twice carbamidomethylated states were analyzed by mass spectrometry. Suitable peptides for this approach were present in the A1Pimyc construct with CCa, CCc, CCr and CCv (illustrated in Figure **13A**), but not with CCpN (either with trypsin or Lys-C digestion).

For all four peptides, the nonreduced sample contained the unmodified, disulfide-bonded version indicating that all secreted proteins contained the disulfide bond in their CC loop (Figure **13B**). After reduction, the cysteines, were efficiently modified by carbamidomethylation, a post-translational modification induced by the reaction between cysteines and iodoacetamide, and detected by mass spectrometry. The reduction was very efficient except for CCv and CCr, where residual disulfide bonded peptide was observed (CCv red-V peptide SS and CCr red-R peptide SS, figure **13B**). In addition, no modifications were detected in nonreduced samples suggesting that no free cysteines were present. The peptides were exclusively detected in the material of the cell lines expressing the corresponding construct, demonstrating specificity.

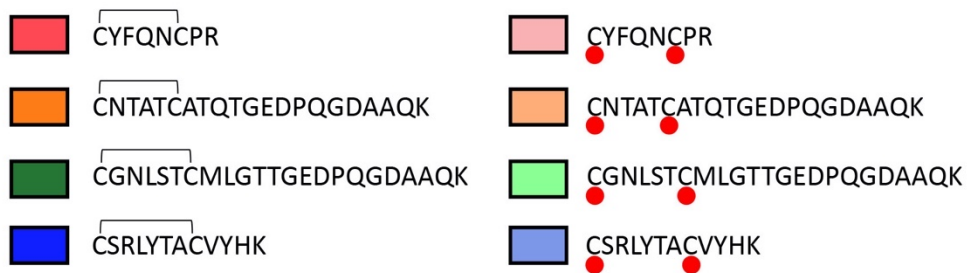
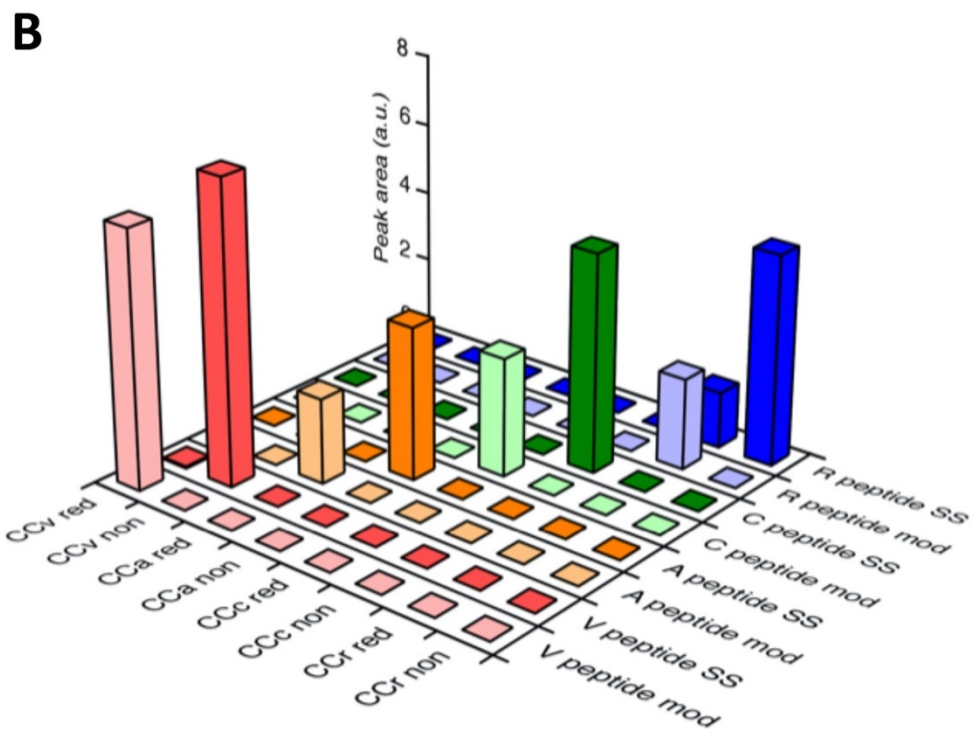
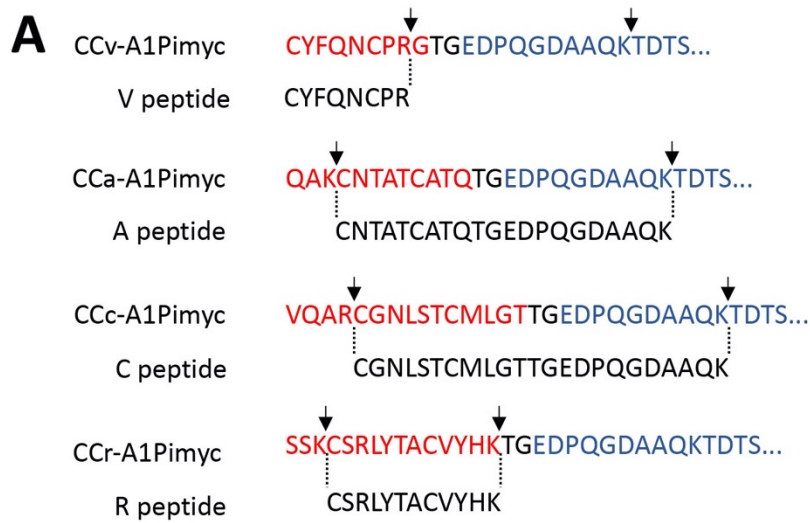


Figure 13. Mass spectrometry shows that the disulfide bonds are made

CCv-A1Pimyc, CCa-A1Pimyc, CCc-A1Pimyc, or CCr-A1Pimyc were immunoprecipitated from media of the expressing cell lines using anti-myc antibodies. One half of each sample was reduced with TCEP (red) while the other was not (non), before they were reacted with iodoacetamide to modify free cysteine thiols. Samples were fragmented either with trypsin (CCv-A1Pimyc, CCa-A1Pimyc, CCc-A1Pimyc) or Lys-C (CCr-A1Pimyc) and analyzed by mass spectrometry for the specific peptides covering the two cysteines of the four CC loops (A), either in the disulfide-bonded or the doubly carbamidomethylated forms (shown by red dots). The signal intensities of all peptide masses in all samples are plotted in (B). Signals (peak areas) for each peptide were normalized to the control A1Pi peptide as loading control. Resulting values for each peptide were further adjusted to fit into the same plot. The reduction was very efficient except in samples CCv red and CCr red, where residual disulfide bonded peptide was observed (CCv red-V peptide SS and CCr red-R peptide SS). No modified peptides were detected in nonreduced samples indicating that no free cysteines were present. a.u.: arbitrary unit.

2.3 CC loops are mediating sorting into secretory granules

At first, we studied the localisation of A1Pimyc and CCv-A1Pimyc, our negative and positive controls, respectively, for granules accumulation. We performed confocal immunofluorescence microscopy staining anti-myc antibodies for our protein of interest and anti-CgA antibodies as an endogenous granule marker. In the first place, cell lines were grown on different coverslips and analyzed in parallel. Unfortunately, staining was variable between experiments and between coverslips. In particular, staining was very sensitive to the time of fixation with paraformaldehyde. Considering this technical problem and to perform this experiment in the best condition possible, we decided to always grow our cell lines together with a A1Pimyc cell line as a standard for direct comparison on the same coverslips and for the cells to be treated equally. To distinguish the two cell lines when cultured together, we prepared an A1Pimyc cell line that stably expressed cytosolic EBFP (enhanced blue fluorescent protein; A1Pimyc+EBFP) detectable by a third fluorescence channel (Figure 14). As expected, neither the expression level of A1Pimyc, as assessed by radioactive labelling, was altered by EBFP production (Figure 14A), nor was the localisation of A1Pimyc upon fluorescence microscopy changed (Figure 14B).

Equally for the two cell lines with or without EBFP expression, A1Pimyc was located mainly in the ER and Golgi, but was also detected to some extent in the tips of the spindle-shaped cells where secretory granules containing the endogenous marker CgA accumulate. To detect constitutive cargos in granules was not surprising, since they are known to be missorted into

immature secretory granules, before being mostly removed to the constitutive pathway *via* constitutive-like vesicles (Kim et al., 2006). However, a stronger signal in the tips was observed for cells expressing CCv-A1Pimyc (Figure **14B**), thus confirming the ability of CCv to mediate granule sorting.

To quantify granule sorting, the mean intensity of the anti-myc signal in the tips defined by CgA staining was determined and normalized for that in co-cultured A1Pimyc+EBFP cells (Figure **14C**). Normalization of myc-positive granules by CgA could not be achieved because of an unexplained variation in CgA intensity in the tips depending of the protein expressed. Quantitation confirmed that CCv increased storage of the reporter A1Pi in secretory granules by ~70%, while there was no difference in A1Pimyc localisation between the A1Pimyc expressing cell lines with and without EBFP expression.

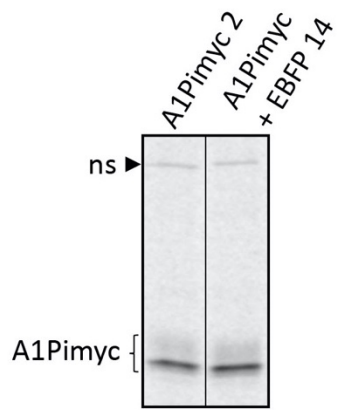
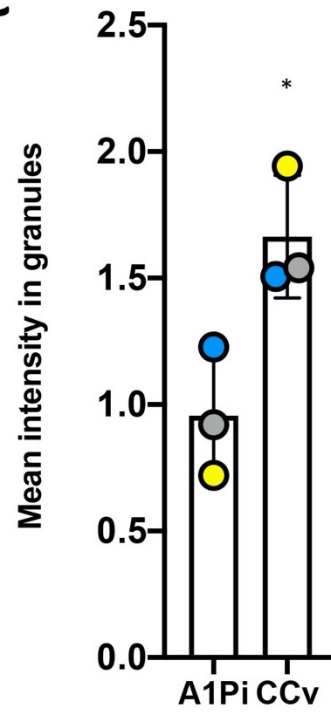
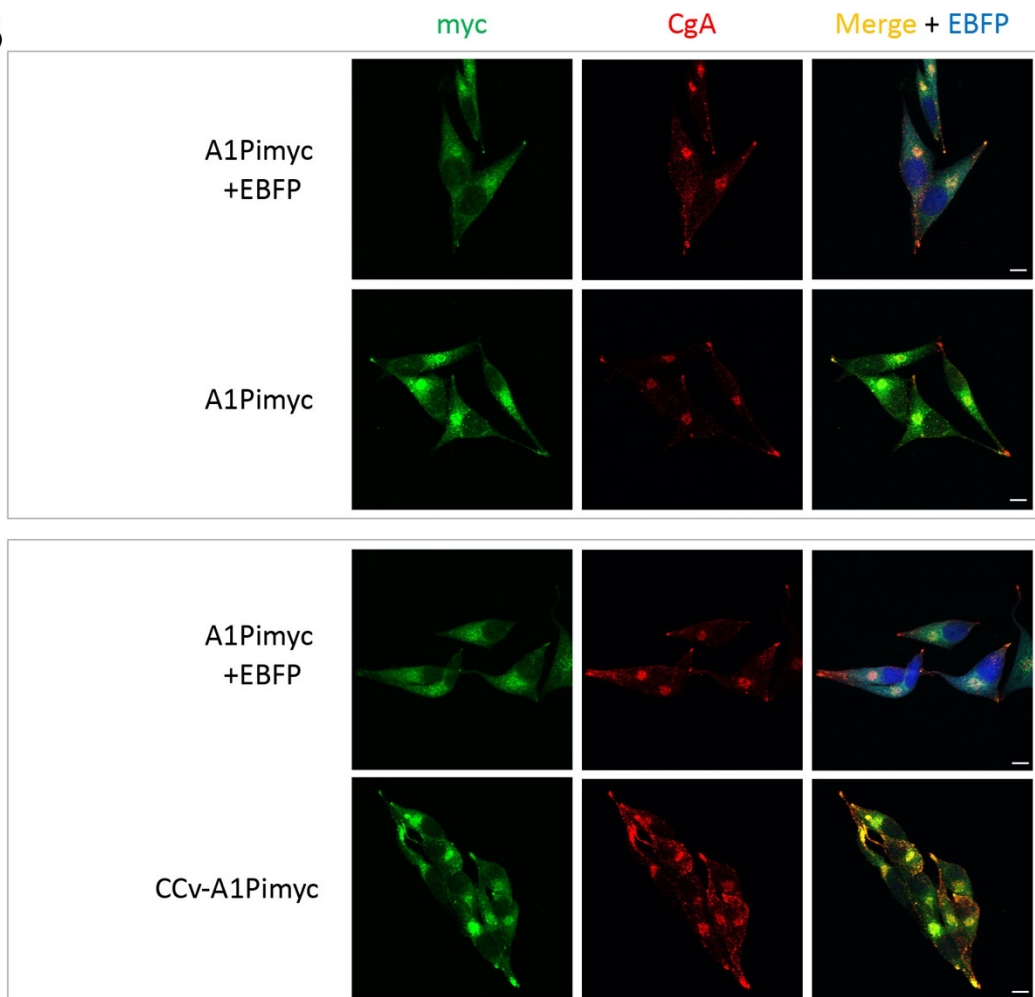
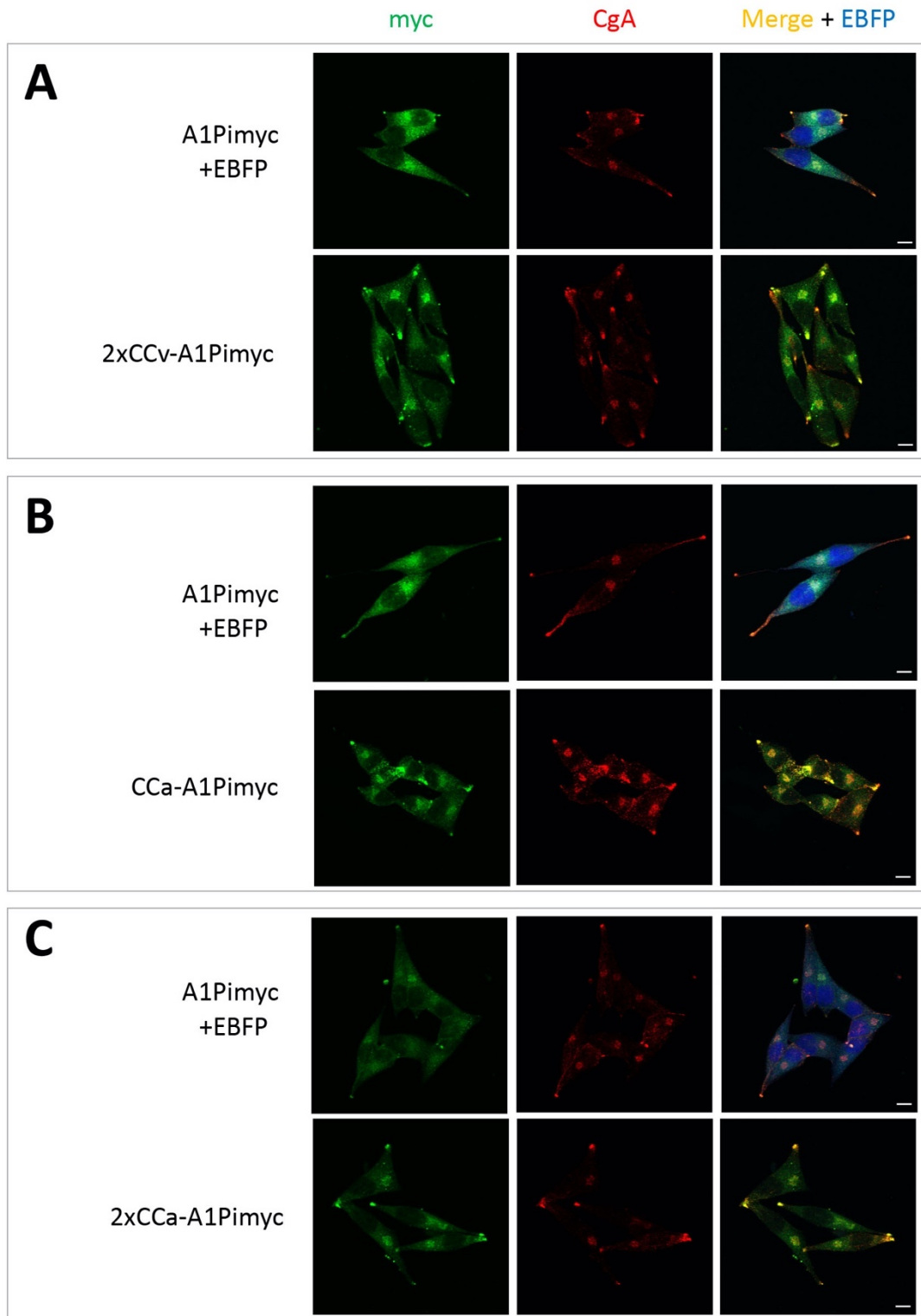
A**C****B**

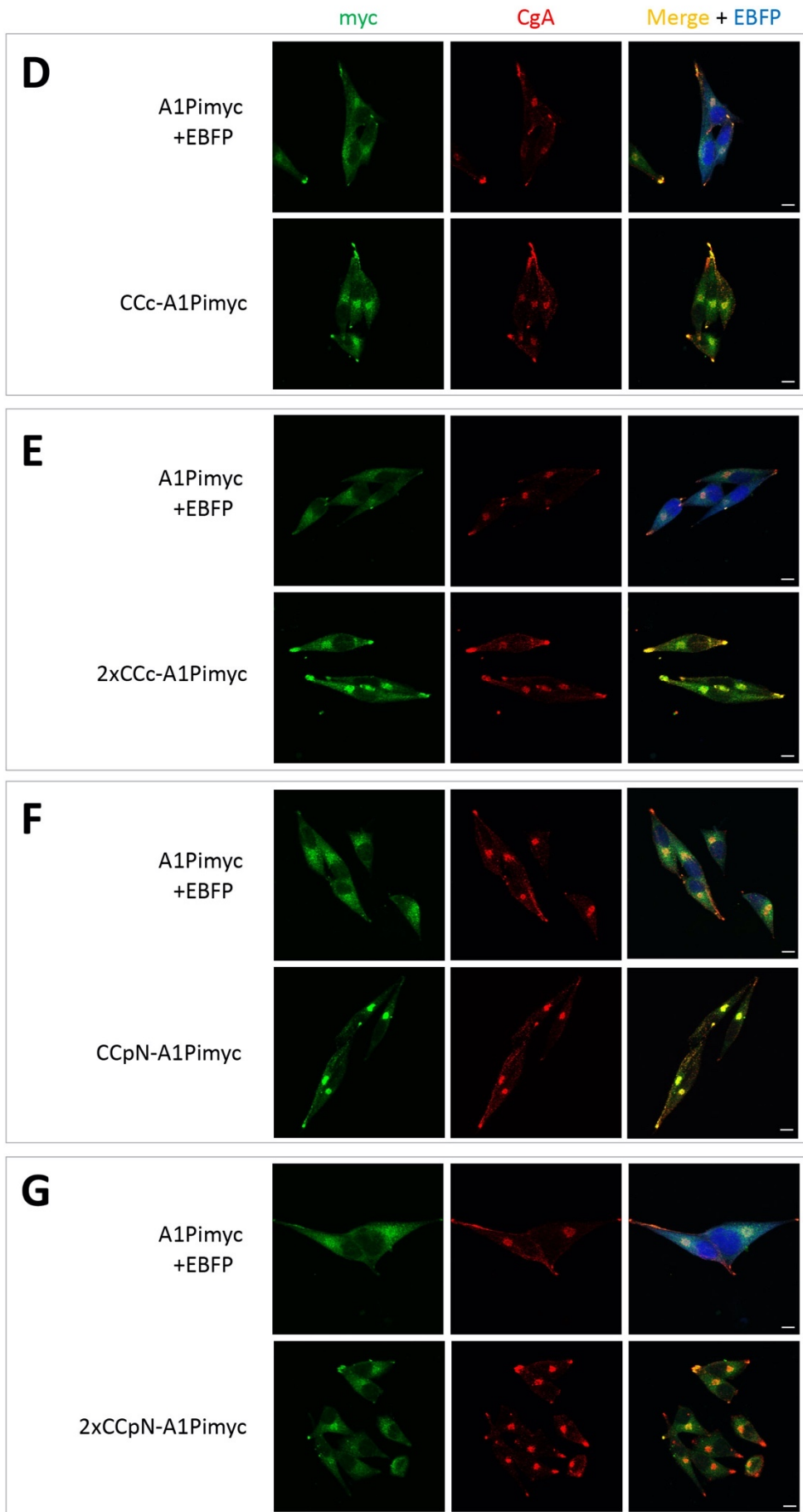
Figure 14. Generation of an EBFP expressing A1Pimyc cell line

To be able to compare CCx-A1Pimyc localization with that of control A1Pimyc on the same coverslip, the A1Pimyc expressing cell line was transfected with a EBFP plasmid and a stable cell line was selected. **(A)** To confirm unaltered expression of A1Pimyc, the original cell line and the EBFP-expressing one (A1Pimyc+EBFP) were labelled for 30 min with [³⁵S]methionine, immunoprecipitated with anti-myc antibodies, analyzed by SDS-gel electrophoresis and autoradiography. ns, non-specific band. **(B)** A1Pimyc+EBFP cells were co-seeded on the same coverslip with the cell lines expressing A1Pimyc or CCv-A1Pimyc, stained for anti-myc and anti-CgA antibodies, and imaged by confocal microscopy. Scale bars, 10 μm. **(C)** Granule quantitation of mean intensity of myc in A1Pimyc and CCv-A1Pimyc normalized to A1Pimyc+EBFP cell line are shown. Twenty images with two to eight cells in each of them were analyzed by coverslip in three independent experiments. Statistical significance was calculated using the unpaired Student's t test. *p ≤ 0.05.

Using this approach, we also analyzed the localisation and accumulation in granule tips of the different CCx-A1Pimyc and 2xCCx-A1Pimyc proteins (Figure 15). The different constructs were accumulated with different intensities in CgA-positive granules. Obviously, some CC loops, as CCc and CCr seem to have a huge impact on A1Pimyc sorting while CCpN do not seem to have any effect. The granules were quantified (Figure 16) and except CCpN-A1Pimyc and 2xCCpN-A1Pimyc, which were not significantly increased in granules compared to the reporter alone, all other CC constructs were accumulated into granules. While CCc produced the highest accumulation of ~three-fold of the control, CCa and CCr showed approximately the same effect as CCv. The increase by CCpN appeared similar, but was not quite significant (p = 0.062). The constructs with two copies of CC loops did not generally improve granule accumulation, but showed a positive effect in the cases of CCv and CCr.

This result shows that four out of five CC loops (except CCpN) have the ability to direct A1Pimyc into secretory granules.





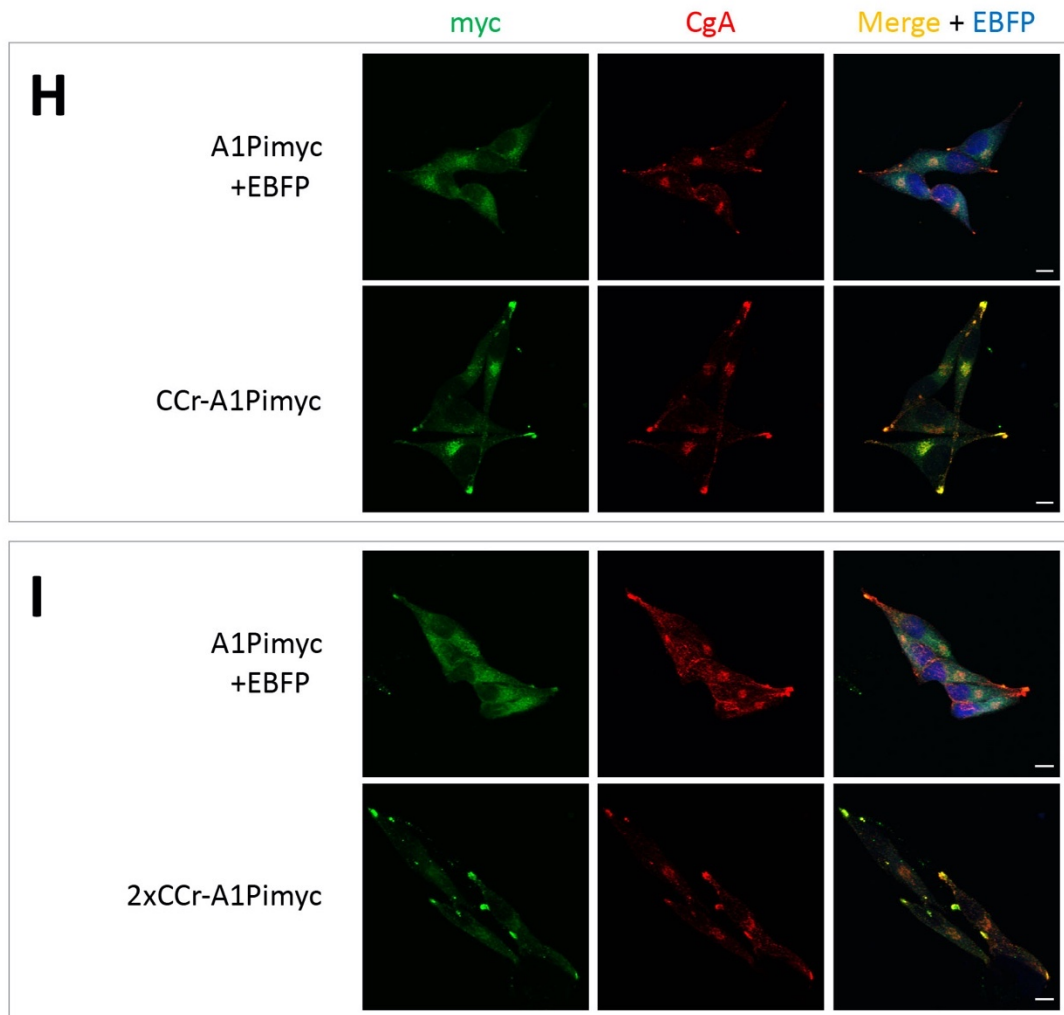


Figure 15. Immunofluorescence localization of CCx-A1Pimyc and 2xCCx-A1Pimyc in comparison to A1Pimyc

Immunofluorescence micrographs of cell lines expressing 2xCCv-A1Pimyc (A), CCa-A1Pimyc (B), 2xCCa-A1Pimyc (C), CCc-A1Pimyc (D), 2xCCc-A1Pimyc (E), CCpN-A1Pimyc (F), 2xCCpN-A1Pimyc (G), CCr-A1Pimyc (H), or 2xCCr-A1Pimyc (I) grown on the same coverslip with A1Pimyc+EBFP cells are shown, stained for anti-myc and anti-CgA antibodies, and imaged as in Figure 14. Scale bars, 10 μ m.

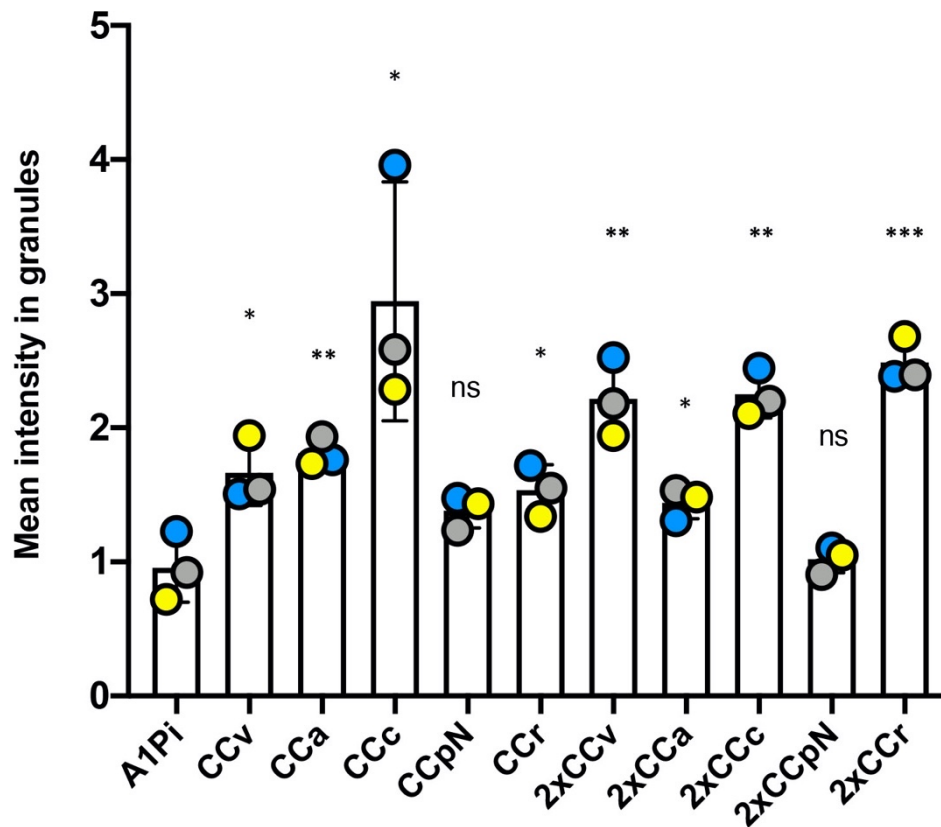


Figure 16. CC loops sort A1Pi into secretory granules

The indicated cell lines were grown together with A1Pimyc+EBFP cells on the same coverslips, stained, and imaged as in Figure 14. The granules in tips as defined by CgA staining, were quantified for A1Pimyc, CCx-A1Pimyc and 2xCCx-A1Pimyc and normalized to that of A1Pimyc in A1Pimyc+EBFP cells on the same coverslip. Twenty images with two to eight cells in each of them were analyzed by coverslip in three independent experiments. Statistical significance was calculated using the unpaired Student's t-test. ns, non-significant; * $p \leq 0.05$; ** $p \leq 0.01$; *** $p \leq 0.001$.

2.4 CC loop constructs are located in functional secretory granules

We showed that CC loops allowed the sorting of A1Pimyc into secretory granules by immunofluorescence microscopy. To test whether these granules are functional, we analyzed the stimulated secretion of the different A1Pi constructs. For this experiment, we compared the release of proteins from cells incubated in secretion medium lacking Ca^{2+} divalent cations to detect secretion *via* the constitutive pathway, with that from cells in stimulation medium that was supplemented with barium chloride (BaCl_2) to induce the release of granule contents. Barium ions trigger an intracellular increase of calcium that activates fusion of secretory granules with the plasma membrane and by this the secretion of their contents.

As a positive control, we first analyzed stimulated secretion of the endogenous granin CgA from parental AtT20 cells. Secretion and stimulation media were collected after 1 h incubation and the aliquots analyzed by quantitative near-infrared fluorescent immunoblotting (Figure **17A**). Four forms of CgA were detected: unprocessed full-length CgA, as well as two large and one small processed fragments. Proteolytic processing is a sure indication of granule sorting. Accordingly, the processed bands were strongly increased in the medium upon stimulation, whereas the full-size protein remained the same (or was even slightly reduced), indicating constitutive secretion. The intensities of the processed bands in the non-stimulated sample were too low to reliably quantify a stimulation factor (the fold-increase of release into media with BaCl₂ vs. without). Since our A1Pimyc constructs are not processed in secretory granules and we rely on quantifying total protein with and without stimulation, we quantified the change in total secreted protein upon stimulation also for CgA for comparison. For this, the signals of all CgA forms were quantified and normalized to VHH_{mCherry} nanobodies added to the media as a loading control and to the cell number in the corresponding well (Figure **17B**). CgA was three-fold stimulated. This result provides a background on the sorting efficiency of a professional granule cargo in AtT20 cells, indicating that a substantial fraction of the protein is released constitutively in unprocessed form. Similar stimulation experiments performed in PC12 cells (derived from pheochromocytoma of the rat adrenal medulla), another cell line frequently used to study the regulated pathway, using the same reagent, even showed less than two-fold stimulation of CgA secretion (Delestre-Delacour et al., 2017).

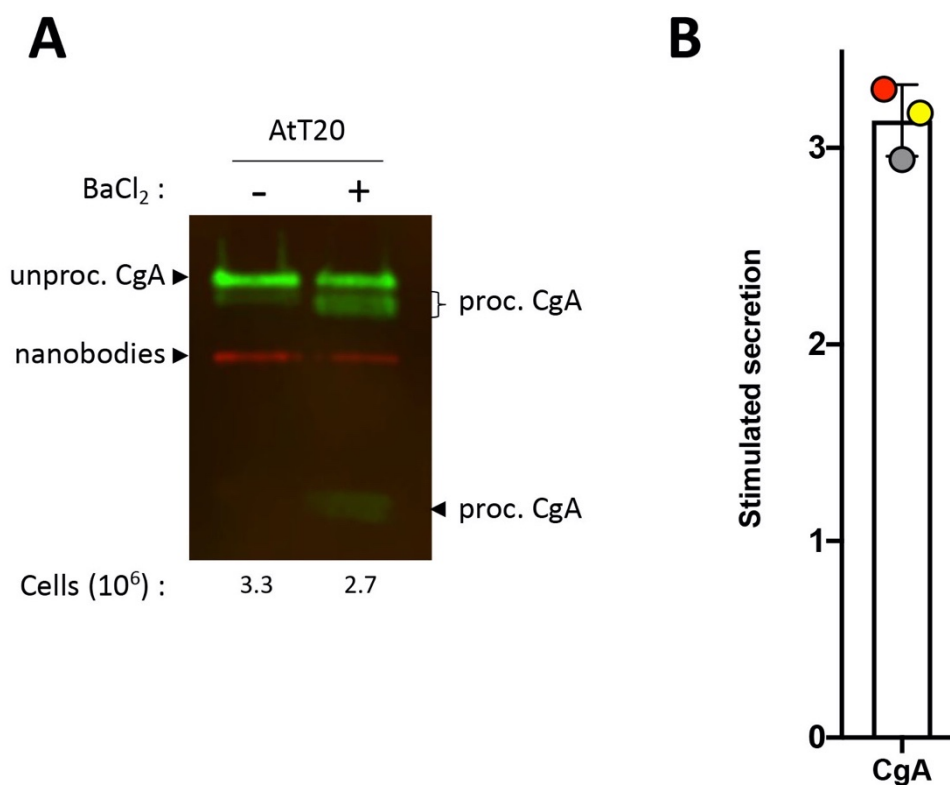


Figure 17. Stimulated secretion of the endogenous regulated cargo CgA

(A) Parental AtT20 cells were grown in two separate wells each, of which one was incubated with secretion medium (–) and the other with stimulation medium (+) containing BaCl₂; both containing VHH_{mCherry} nanobodies as a subsequent loading control. After 1 h, the media were collected and subjected to quantitative near-infrared immunoblot analysis for endogenously expressed CgA. The cells used for the experiment were counted in each well to compensate for potential differences in cell number and shown below each lane. The bands in green and red represent the CgA forms and the VHH_{mCherry} nanobodies, respectively. The immunoblot analysis revealed the unprocessed full-length protein (unproc.), as well as processed forms (proc.). (B) Stimulated secretion was determined by quantifying the constructs' intensities of all CgA's forms normalized to nanobodies signal and cell number, and expressed as the ratio of stimulated to non-stimulated secretion. The average and standard deviation correspond to three independent experiments, with individual values indicated.

Stimulated secretion experiments were performed with our cell lines expressing the A1Pimyc constructs and quantified (Figure 18). Secretion of the reporter, A1Pimyc, alone was not stimulated by BaCl₂ incubation. In contrast, all CC fusion proteins except CCpN-A1Pimyc, were stimulated significantly by 50–90%. Again, the presence of two copies of a CC loop in the construct did not generally increase the effect. The only exception was CCpN for which two copies, but not one, resulted in significant stimulation. With this one exception, the results with the estimated secretion assay are consistent with the immunofluorescence assay,

indicating that increased concentration in the granule tips is due to sorting into functional secretory granules. Why 2xCCpN was not detected to be concentrated in tips by immunofluorescence is not clear. Compared to the stimulation of CgA, the CC loops proteins were less efficient than an endogenous and professional regulated protein.

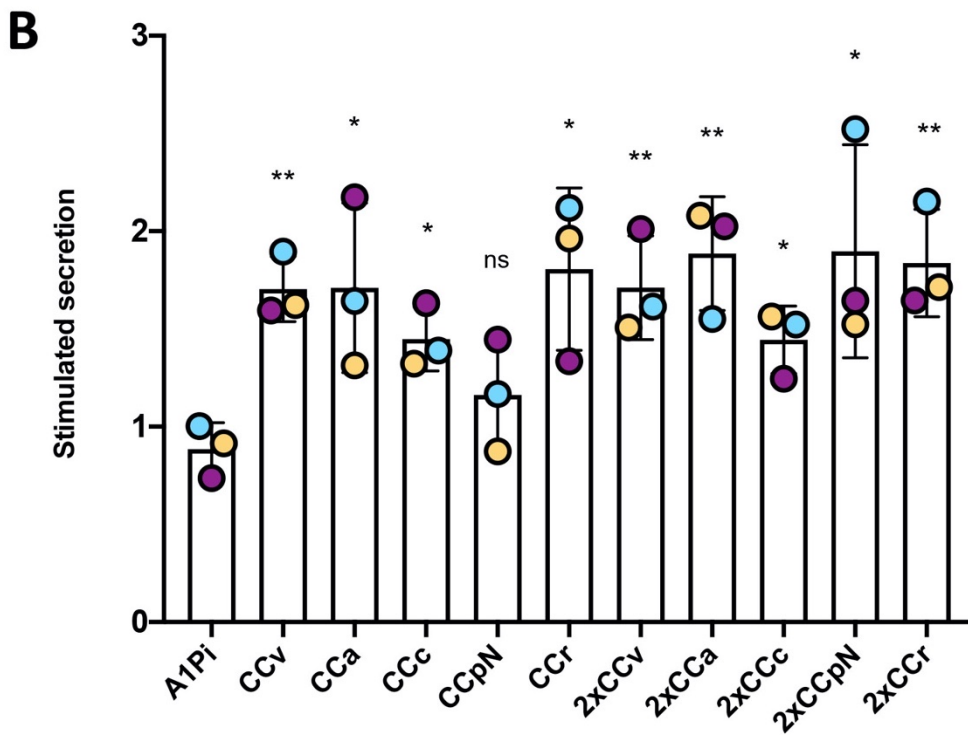
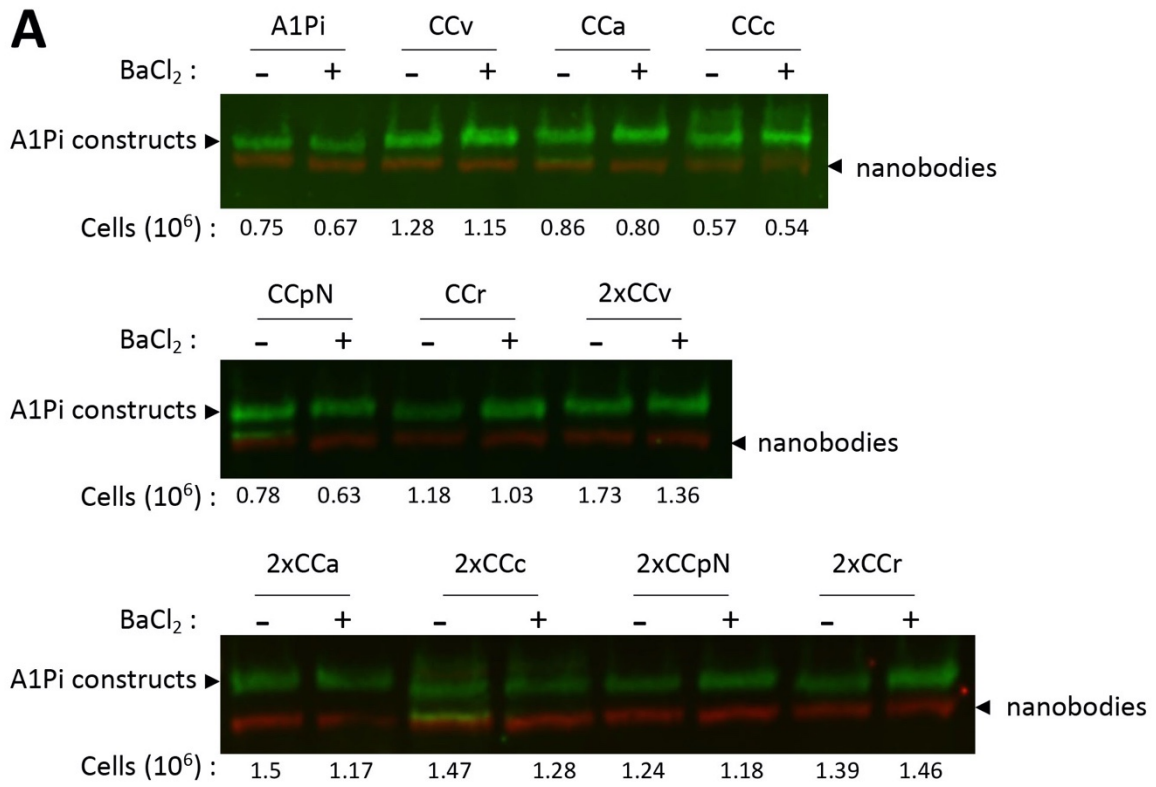


Figure 18. CC loops mediate secretion *via* functional secretory granules

(A) Stimulated secretion experiments as described in Figure 17 were performed with the indicated cell lines and 30 min media incubation. The bands in green and red represent the A1Pi constructs and the VHH_{mCherry} nanobodies, respectively. The cells used for the experiment were counted in each well to compensate for potential differences in cell number and shown below each lane. (B) Stimulated secretion was quantified as for CgA in Figure 17B. Average and standard deviation of three independent experiments are shown, with individual values colored by experiment. Statistical significance was calculated using the unpaired Student's t test. ns, non-significant; * $p \leq 0.05$; ** $p \leq 0.01$.

2.5 CC loops mediate Lubrol insolubility

Aggregation of hormones into secretory granules must be transient to allow rapid dissolution upon release into the extracellular medium. Dannies and colleagues empirically found conditions that solubilized most cellular proteins, but retained the condensed granule cargo largely in an insoluble, pelletable state using Lubrol as the detergent (Lee et al., 2001; Zhu et al., 2002). As a positive control for Lubrol insolubility experiments, we first tested POMC, an endogenous professional regulated cargo (Figure 19). AtT20 cells were incubated in 1.5% Lubrol for 1 h at 4°C. After a low-speed centrifugation, the post-nuclear supernatant was ultracentrifuged for 1 h at high speed. Equal fractions of pellet and supernatant were analyzed by immunoblotting for POMC (Figure 19A). We can observe three forms of POMC, two high-molecular weight forms corresponding to two full-size forms of POMC and a smaller processed form of POMC corresponding to the N-terminal peptide/fragment of proopiomelanocortin (NPP). Processing indicates sorting into secretory granules. The high-molecular weight forms were recovered mostly in the supernatant, whereas the processed form was to a similar extent found in the insoluble pellet fraction. This selectivity for processed POMC in the pellet thus confirms specificity of the assay. Quantitation indicated ~40% of processed POMC to be insoluble to Lubrol (Figure 19B), which is similar to ~50% insolubility previously reported for the growth hormone (Lee et al., 2001).

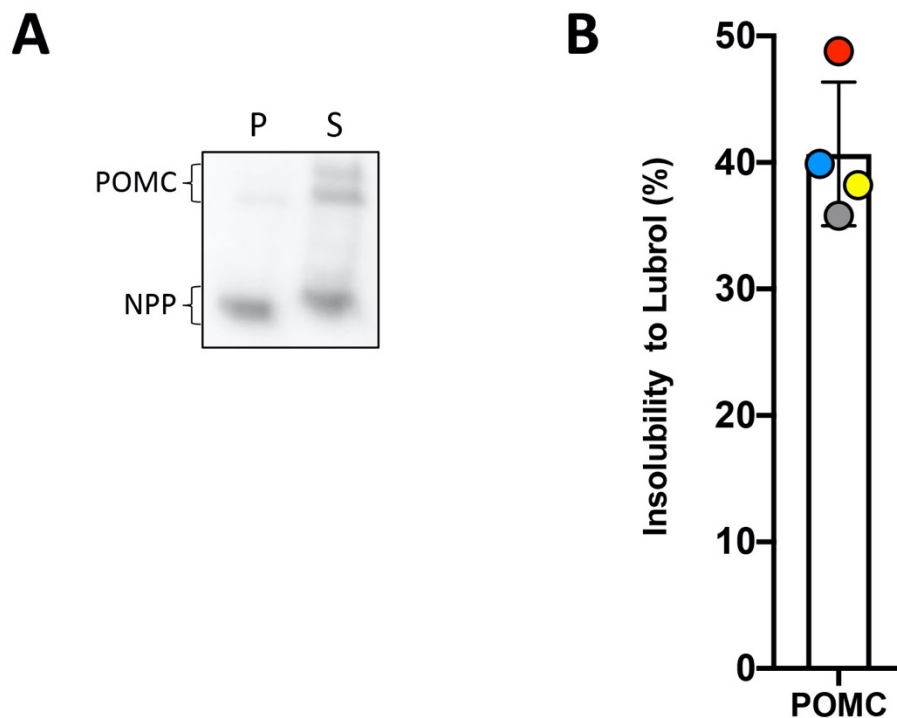


Figure 19. Insolubility of endogenous POMC to Lubrol

(A) AtT20 cells were incubated with 1.5% Lubrol at 4°C. The post-nuclear supernatant was centrifuged at 50'000xg for 1 h. Equal fractions of supernatant (S) and pellet (P) were analyzed by immunoblotting for endogenous POMC. While full-length POMC was mostly detected in the supernatant, a large fraction of processed (NPP) POMC was pelleted. (B) The percentage of Lubrol insoluble processed POMC was quantified. The average and standard deviation of four independent experiments are shown.

We then performed this experiment with all our A1Pimyc constructs (Figure 20). A1Pimyc proteins are not processed in secretory granules. However, since they are N-glycosylated and converted from an EndoH-sensitive high-mannose-type glycan in the ER to an EndoH-resistant complex form in the Golgi, we can at least distinguish the protein in the ER and cis-Golgi from that in the late Golgi, TGN, and secretory granules. Then, to better separate the two glycoforms of A1Pimyc and derivatives, the soluble and insoluble fractions were incubated with EndoH for 1 h before immunoblot analysis (Figure 20A). While the ER forms of all constructs were completely soluble, specifically the complex forms were recovered in the insoluble fraction to variable extents (Figure 20B). For A1Pimyc, which is our negative control, between 12 and 27% of the complex form was insoluble, likely corresponding to the background of the constitutive secretory protein trapped in the granule aggregates. A1Pimyc

fused to one or two CC loops increased insolubility of 30–50%, again with the exception of CCpN-A1Pimyc (and the increase of CCa-A1Pimyc was not significant)

These experiments demonstrate once again that CC loops have the ability to reroute A1Pimyc into secretory granules.

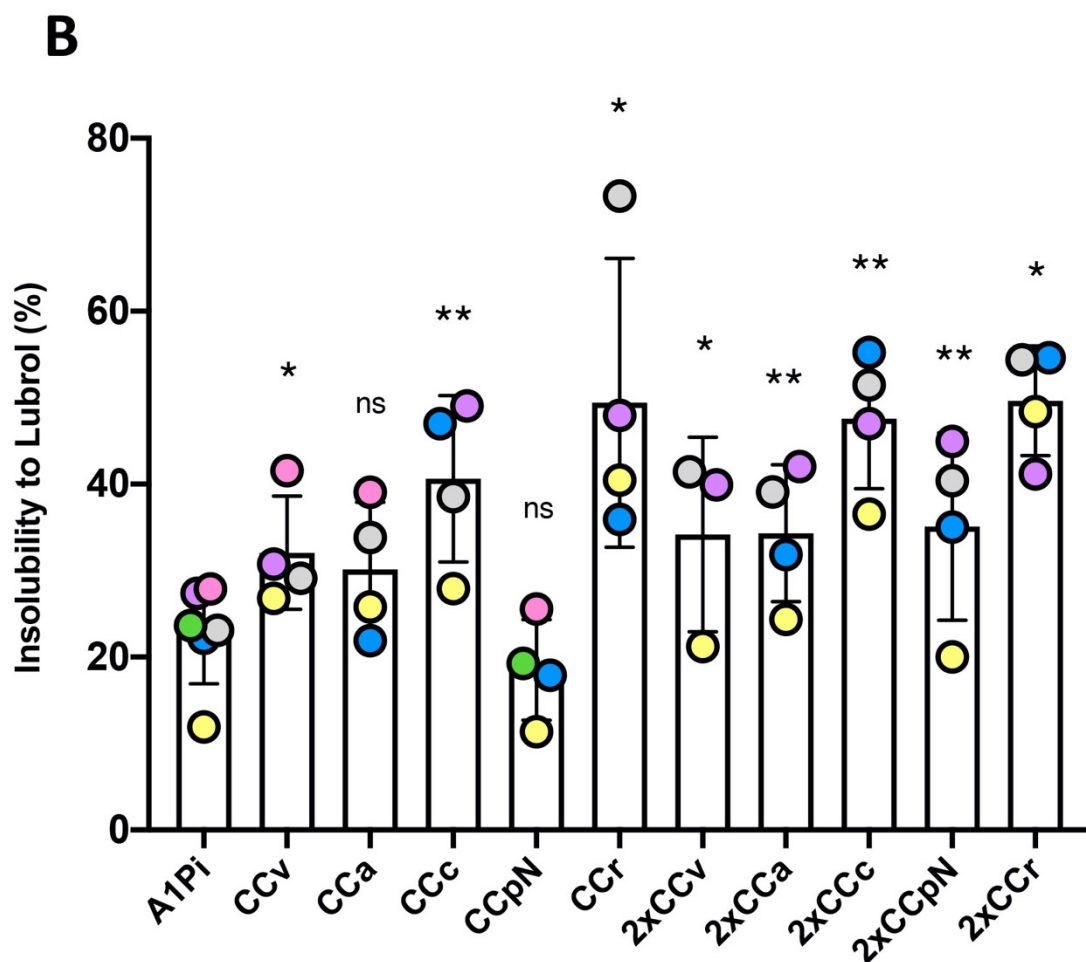
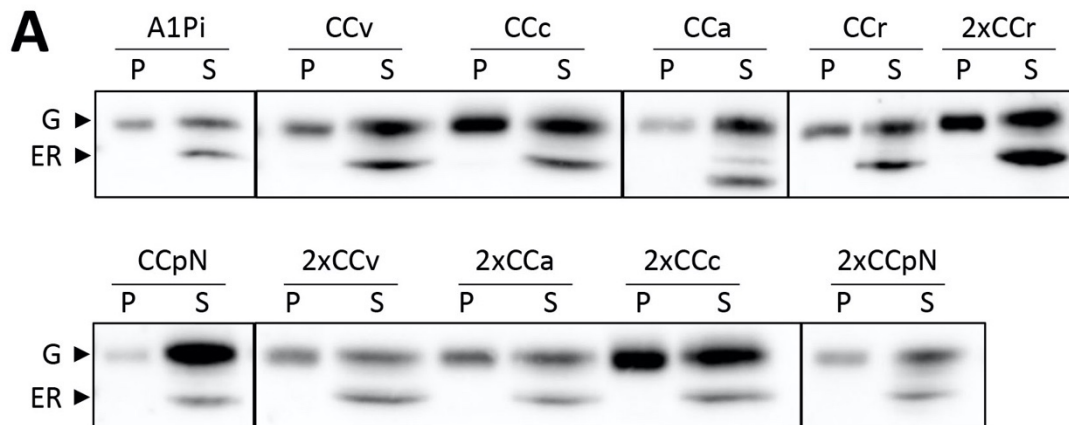


Figure 20. Some CC loops enhance Lubrol insolubility

(A) Lubrol experiments were performed as in figure 19, using anti-myc antibodies. To better separate ER and Golgi/post-Golgi (G) forms of the A1Pimyc constructs on the gel, the samples were incubated with EndoH, thus deglycosylating the high-mannose ER form. (B) The percentage of Lubrol-insoluble Golgi/post-Golgi (G) forms of the proteins was quantified. The average and standard deviation correspond to four independent experiments, with individual values colored by experiment. Statistical significance was calculated using the paired Student's t-test. ns, non-significant; * $p \leq 0.05$; ** $p \leq 0.01$.

2.6 Mutation of the cysteines in a CC loop abolishes granule sorting

The three different assays used above to test granule sorting strongly suggest that different CC loops mediate sorting into the regulated pathway to different extents, the weakest being CCpN. To test specificity for disulfide bond and sequence, we mutated both cysteines of the generally most active CC loop, CCc (Figure 21A). Both cysteines were exchanged by two prolines in construct PPc-A1Pimyc. A stable AtT20 cell line, expressing PPc-A1Pimyc was isolated with similar expression level, determined by metabolic labelling, as the A1Pimyc expressing cell line (Figure 21B). The localization of PPc-A1Pimyc was analyzed by immunofluorescence microscopy (Figure 21C). PPc-A1Pimyc was poorly detected in secretory granules, as was confirmed by quantitation (Figure 21D). Indeed, PPc-A1Pimyc showed the same low signal in granule tips as A1Pimyc, demonstrating that the cysteine mutation completely inactivated granules sorting.

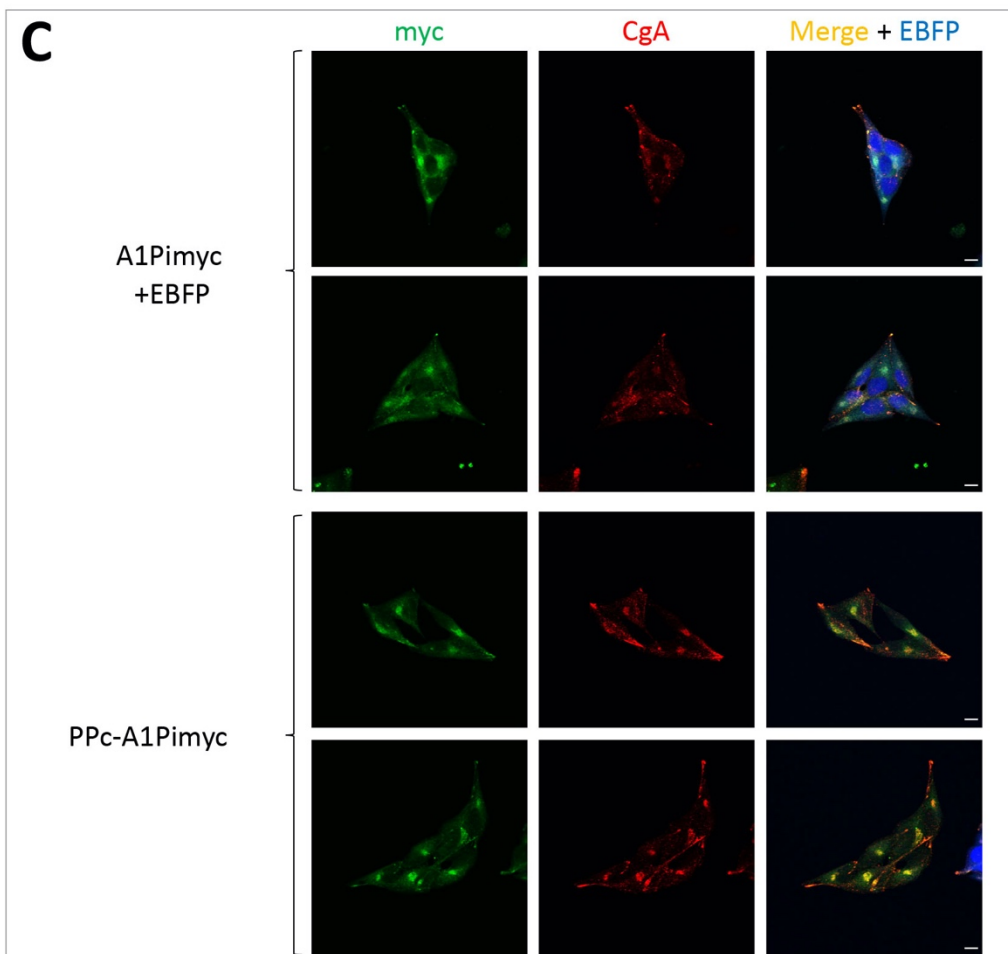
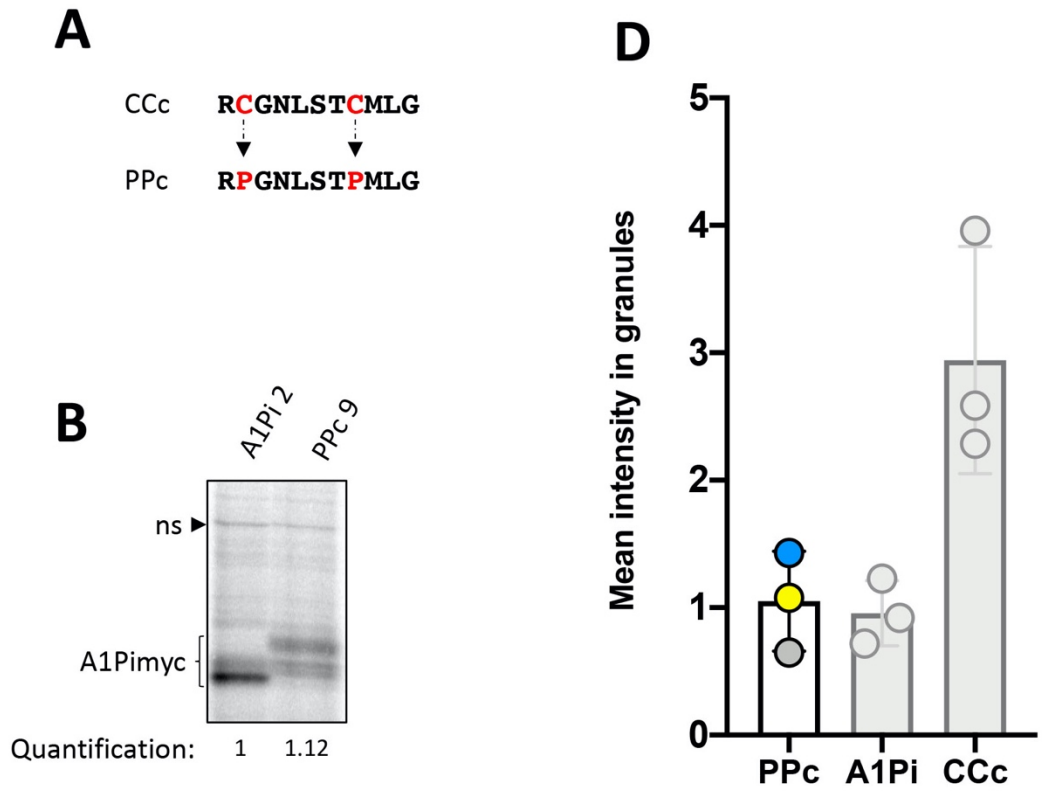


Figure 21. The cysteines are necessary for CCc-A1Pimyc to be sorted into secretory granules
(A) The cysteines of CCc were mutated with prolines as indicated and called PPc. (B) PPc-A1Pimyc and A1Pimyc were labeled with [³⁵S]methionine for 30 min, the constructs were immunoprecipitated with anti-myc antibodies and the expression levels were compared by SDS-gel electrophoresis and autoradiography. The expression level of PPc-A1Pimyc clone normalized to the non-specific band (ns) as a loading control and to A1Pimyc is indicated below the lane. (C) PPc-A1Pimyc was grown together with A1Pimyc+EBFP cells on the same coverslips, stained, and imaged as in Figure 14C. Scale bars, 10 μm. (D) The granules in tips as defined by CgA staining were quantified for PPc-A1Pimyc and normalized to that of A1Pimyc in A1Pimyc+EBFP cells on the same coverslip. Twenty images with two to eight cells in each of them were analyzed by coverslip in three independent experiments. On the graph in grey, is reported previous data from figure 16.

Taken altogether, CC loops were found to be able to direct A1Pimyc, a constitutive reporter, into the regulated pathway and thus to constitute a general type of signal for granules sorting, most likely by aggregation.

III. Discussion

In the case of provasopressin, granule sorting by self-aggregation and ER aggregation of mutant proteins causing diabetes insipidus, were brought together by the amyloid hypothesis of secretory granule biogenesis proposed by Riek and colleagues (Maji et al., 2009). It suggests that motifs evolved for functional aggregation in the TGN cause pathological aggregation of mutant proteins in the ER. Accordingly, to test a potential general role of CC loops in aggregation, we tested their role in both systems.

CC loops mediate ER aggregation

We have studied the ER aggregation potential of CC loops by fusing them to a misfolded reporter, NPA, using two different techniques: (i) immunofluorescence confocal microscopy, with two different cell lines, COS-1 fibroblast and Neuro-2a neuroblastoma cells; (ii) electron microscopy by immunogold-staining in Neuro-2a cells.

Immunofluorescence microscopy

Immunofluorescence microscopy revealed visible accumulations that appeared to different extents depending on the CC loops expressed and the cell lines used. In COS-1 cells, five CC loops out of six produced significant accumulations in the ER above the background of the Pro1 construct that served as the negative control, compared to three out of six in Neuro-2a cells. This difference of CC loops' aggregation capacity in the two cell lines is probably due to a variable chaperone and/or ERAD capacity as well as a higher expression level in COS-1 cells where expression plasmids with an SV40 origin of replication are amplified (like pcDNA3 that we used). However, some CC loops have a higher impact in inducing aggregation than others in both cell lines. Indeed, CCv, CCa and CCpN seem the most potent causing ER aggregation, whereas CCc, CCr, and CCpC, have rather less effect. With immunofluorescence microscopy, accidental accumulations of the antigen and artefacts lead to background puncta. In addition, there is an unknown propensity of the NPA reporter to aggregate on its own that might contribute to the percentage of cells expressing Pro1-NPA that scored positive (~20-30%). Another consideration is that accumulations or aggregates need to have a minimal size to appear as discernable puncta. Smaller ones may be undetected.

Electron microscopy

In contrast, our electron microscopy analysis was not quantitative, but allowed to detect aggregates specifically by gold staining irrespective of their size. In addition, it also provides morphological information and, at least potentially, information on density and substructure of the aggregates. All CCx-NPΔ constructs, but not the control Pro1, were found to produce structures morphologically identifiable as aggregates containing the expressed proteins as demonstrated by immunogold staining. This suggests on the one hand, that our negative control Pro1-NPΔ and thus the fusion partner NPΔ alone, do not aggregate substantially on their own. On the other hand, it indicates that the aggregation propensity of CCc, CCr, and CCpC were likely underestimated in the fluorescence microscopy assay. The sizes and forms of the aggregates varied widely. Some CC loops, CCv, CCpN, and CCa typically produced large aggregates with diameters of 180–2400 nm with very round structures for CCv and CCpN. In contrast, CCc, CCr, and CCpC showed irregular shapes or very small structures between 30 and 150 nm in diameter. These are exactly the CC loops that did not score significantly positive in the light microscopy assay used above. It is thus likely that they have been missed in the first assay. While we cannot make quantitative statements on these CC loop constructs, we nevertheless conclude that all of them have the ability to cause substantial aggregation in the ER.

As to the internal morphology of the aggregates, all constructs were found to be very dense and did not allow to positively demonstrate a fibrillar substructure. Diabetes insipidus mutant ΔE47 of full-length provasopressin expressed in Neuro-2a cells previously showed a loosely packed tangle of fibrils (Birk et al., 2009), supporting the notion of amyloid-like aggregation. In COS-1 cells, the aggregates appeared denser and fibrils were hardly detectable (Birk et al., 2009). Similarly, the provasopressin disease mutation C61X (stop codon at residue 61 of NPII), fused to a myc tag (thus corresponding to 1–72myc) and expressed in neuroblastoma HN10 cells, revealed relatively dense aggregates in which fibrillar substructure was still discernable (Beuret et al., 2017). Our CCv-NPΔ (i.e. 1–75His₆) and all other CCx-NPΔ constructs in Neuro-2a produced aggregates that were too dense to reveal any fibrillar structure. It should, however, be pointed out that fibrillarity is also not detectable in secretory granules for which an underlying amyloid structure was postulated (Maji et al., 2009).

In summary, we found that all CC loops are able in the ER to produce aggregates with similar dense appearance, but different sizes and shapes. The result thus supports the hypothesis that CC loops are a general motif able to mediate aggregation, similar to provasopressin in the ER.

CC loops reroute a constitutive protein into secretory granules

To test the CC loops for their capacity to aggregate into secretory granules, we fused them to a folded and known constitutive secretory protein, A1Pi. Three different methods have been performed to analyze their rerouting into secretory granules: *(i)* localization to CgA-positive secretory granules by immunofluorescence microscopy, *(ii)* stimulated secretion, and *(iii)* insolubility to Lubrol.

Immunofluorescence microscopy

By immunofluorescence, we measured the accumulation of the protein of interest in secretory granules collected in the tips of cellular extensions of AtT20 cells. Even the negative control A1Pimyc was detected to some extent in CgA-positive secretory granules. This was not surprising, since it has previously been observed that constitutive proteins are not efficiently excluded from immature secretory granules and only subsequently removed to some degree by constitutive-like secretion (Dittie et al., 1996; Kim et al., 2006). In addition, some constitutive proteins may also be trapped in the aggregates made by regulated cargo proteins.

Importantly, most CC loop fusion constructs produced significantly increased accumulation in granules compared to the reporter A1Pimyc alone. Indeed, CCc, CCa, 2xCCv, 2xCCc, and 2xCCr proved to be the most effective in mediating localization in granules, up to three-fold in the case of CCc, followed by CCv, CCr, and 2xCCa with smaller effects. In contrast, CCpN, one and even two copies, did not improve the rerouting of A1Pi into the granules. In other cases, like CCv and CCr, two copies fused to the reporter improved granule localization to some extent.

Stimulated secretion

To study the functionality of secretory granules containing A1Pimyc and the CC loop constructs, we performed a stimulated secretion assay. Endogenous regulated cargos are frequently processed in secretory granules which allows to distinguish between the fractions

of the proteins that take the regulated or the constitutive routes. This experiment was performed first with the regulated cargo CgA. The majority of CgA is secreted constitutively as the full-length protein, whereas the processed forms are well regulated and hardly secreted into the medium without stimulation. Unfortunately, for our A1Pimyc constructs, we cannot distinguish the population that was sorted into granules from that released constitutively, because they are not processed. Nevertheless, we observed significant stimulated secretion for all CC loops, except CCpN, in the range of 1.5–2-fold confirming the functionality of the granules. This effect is substantial, considering that it is "diluted" by the constitutive fraction. If stimulated secretion of CgA is quantified in the same manner (i.e. comparing all forms, processed and unprocessed), only three-fold stimulation was observed for this professional regulated cargo protein, indicating the maximal sorting efficiency in AtT20 cells. Interestingly, A1Pimyc secretion was not stimulated at all. This might suggest that indeed, A1Pimyc detected in the tip region by immunofluorescence is only localized in non-stimulatable secretory granules, such as ISGs. Alternatively, it cannot be excluded that the stimulation conditions with BaCl₂ inhibit constitutive secretion to a small amount, approximately compensating for the stimulated release of missorted A1Pimyc. A slight reduction in full-length CgA collected in the media of stimulated vs. non-stimulated cells would be consistent with this interpretation.

Insolubility to Lubrol

Granule cargos have empirically been found to display insolubility to incubation with the detergent Lubrol (Lee et al., 2001; Zhu et al., 2002). Lubrol insolubility experiments with our A1Pimyc fusion proteins further support their inclusion into secretory granules. Indeed, CC loops increase the insolubility of A1Pi to Lubrol, especially CCc, CCr, 2xCCc and 2xCCr have the most effect on A1Pi, while CCv, 2xCCv, 2xCCa and 2xCCpN have a lower one. Around 20% of A1Pimyc is insoluble to Lubrol, showing that A1Pimyc is trapped into insoluble cargos.

The results of all three assays show that CC loops present in prohormones act as novel secretory granule signal supporting the hypothesis that they promote inclusion into secretory granules, most likely by mediating aggregation. The various CC loops displayed different efficiencies in the process. Especially CCc and CCr were the most efficient ones, whereas CCpN was mostly inactive in all the three assays.

General considerations

Interestingly, no amino acid similarities exist between the different CC loops sequences. The only obvious common feature is the disulfide bond forming a small ring structure. Experimentally, we showed, that the disulfide bond is completely formed in the secreted fusion proteins. As a control of specificity, we introduced drastic mutations on CCc by mutating the cysteines to prolines (PPc-A1Pimyc). By immunofluorescence microscopy, PPc did not display any effect on the sorting of A1Pi. However, we cannot exclude that these prolines change the conformation of the peptide entirely. Nevertheless, more experiments have to be performed to identify the important residues within the CC loop sequences.

Riek and colleagues proposed that secretory granules are functional amyloids of regulated cargo proteins (Maji et al., 2009), mainly based on *in vitro* fibrillar aggregation of pituitary hormones including vasopressin and prolactin. Amyloids by strict definition are made of β -sheets packed on top of each other forming long fibers whereby the strands are perpendicular to the fiber axis (cross- β structures). X-Ray analyses reveal characteristic diffraction at 4.7 Å for the distance between hydrogen bonded peptide backbones and ~ 10 Å for sidechain–sidechain packing between sheets (Jackson and Hewitt, 2017).

The small disulfide loops we analyzed here cannot form an amyloid in the strict sense, since they cannot extend to β -strands. They might, however, aggregate in an amyloid-like fashion by forming backbone–backbone hydrogen bonds and sidechain–sidechain packing of fibrous elements. A hallmark of typical amyloids is their stability and insolubility. Amyloid-like aggregation of CC loops are likely to be less stable and thus more soluble under appropriate conditions. Indeed, *in vitro* aggregation studies with somatostatin, a 116-amino acid peptide hormone with a 105–116 disulfide loop, showed that reduction of the disulfide bond even increased aggregation kinetics and reduced re-dissolution kinetics upon dilution (Anoop et al., 2014). This may suggest that CC loops produce imperfect amyloids (only amyloid-like aggregates) to be functional for aggregation, but also for re-dissolution after secretion.

Granule formation at the TGN involves aggregation of natively folded proteins. For an amyloid or amyloid-like fiber to form, a sufficiently long peptide segment has to be exposed or, alternatively, the protein has to unfold first and to refold upon secretion. In the case of vasopressin that contains two aggregating sequences, the glycopeptide is freely exposed, whereas vasopressin folds into a binding pocket in NPII (Chen et al., 1991; Wu et al., 2001). In

the latter case, the changing conditions in the TGN (such as reduced pH, high glycosaminoglycan and Zn^{2+} concentrations) may trigger release to participate in amyloid formation and minimal unfolding would thus be required.

We could postulate that CC loops should generally have a position in its protein that allow it to be exposed easily. The prolactin N-terminal CC loop is naturally exposed and the C-terminal one, that is structurally shared with the growth hormone, also appears to be exposable with minimal conformational changes. In contrast, the CC loop of prorenin is not at the N- or C-terminal end but at the extremity of one of its lobes, suggesting that a small conformational change might expose it sufficiently (Figure 22).

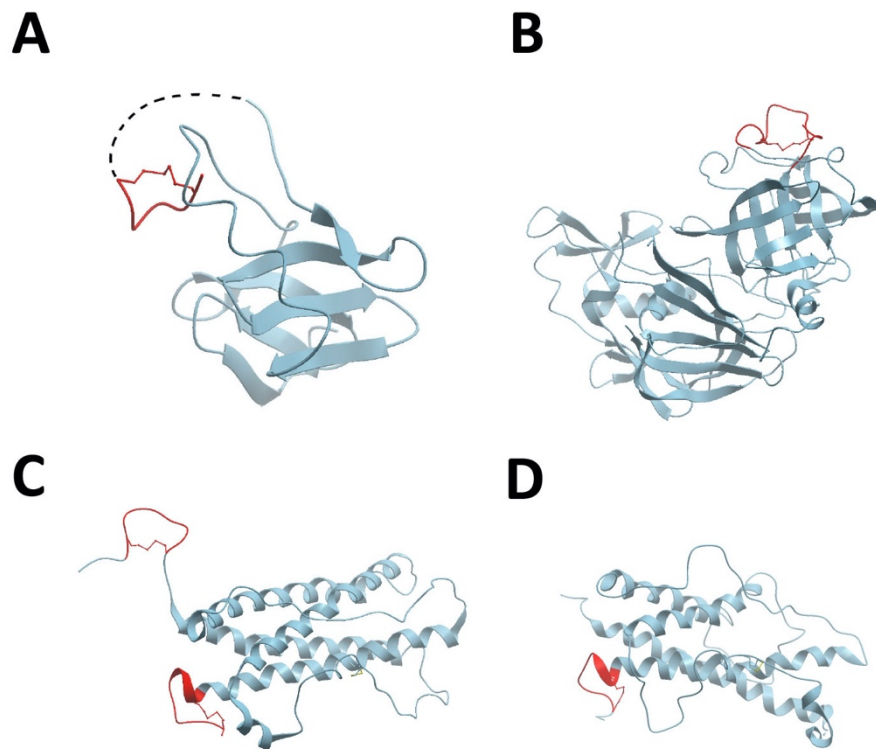


Figure 22. Prohormone structures

Prohormone structures of provasopressin (1JK4; **A**), prolactin (1RW5; **B**), growth hormone (1HGU; **C**) and prorenin (3VCM; **D**) are shown where the CC loops are represented in red. The provasopressin structure is shown without the glycopeptide and the connection between NPII and the CC loop (dashed line).

However, not all prohormones contain a CC loop, meaning that some other determinants and features must be present to mediate granule sorting. This implicates that CC loops are not constituting the only and universal secretory granule signal. Interestingly, CgB contains a

larger disulfide bond of 22 amino acids that have previously been implicated in secretory granule sorting (Glombik et al., 1999; Kromer et al., 1998). This suggests that not only short disulfide bond as CC loops, but also longer ones may display a role in granule sorting.

If CC loops are a general device of functional aggregation, another speculation that emerges from our results is that they may lead to ER aggregation and ERAD overload, when the protein is unable to fold and exit the ER. It is illustrated with the case of diabetes insipidus mutations in provasopressin where CC loops become dangerous for the cell. One might thus speculate that other prohormones with CC loops could behave similarly when mutated, potentially also leading to a dominant phenotype. A candidate in this respect is the growth hormone that contains a CC loop at its C-terminus. Known mutations of growth hormone conduct to the dominant growth hormone deficiency (Binder et al., 2002; Lee et al., 2000; Missarelli et al., 1997) and was also studied during my PhD.

Taken together, our data supports the hypothesis that CC loops of different peptide hormone precursors have the ability to cause aggregation as it is shown when fused to a misfolded reporter in the ER and, when fused to a constitutive secretory protein to reroute it into secretory granules. These findings demonstrate that CC loops act as novel signals for granule sorting, in support of the amyloid hypothesis of granule biogenesis. The work of my thesis constitutes a new advance in the understanding of the regulated secretory pathway, the formation of secretory granules and the aggregation of regulated cargo into granules. Nevertheless, we are still at the beginning of understanding all the mechanisms controlling the regulated secretory pathway.

Part II.

How does mutant growth hormone block the secretion of the wild-type in the dominant growth hormone deficiency type II disease?

I. Introduction

Mutations of the vasopressin precursor lead to dominant neurohypophyseal diabetes insipidus. According to our current understanding, dominance is caused by excessive aggregation in the ER mediated by vasopressin (CCv) and the glycopeptide that have evolved to produce functional amyloids in granule biogenesis at the TGN. Aggregates formed by mutant proteins, if not efficiently removed by ERAD, engage with products of the wild-type allele, interfere with their folding and maturation, and thus cause a dominant phenotype. In parallel to this prohormone, we were wondering whether mutations of other prohormones containing a CC loop and perhaps other aggregating sequences, lead to a dominant disease. Indeed, specific mutations of the human growth hormone (hGH), which contains a CC loop at its C-terminus, are documented to cause dominant growth hormone deficiency type II disease.

1. Growth hormone (GH)

GH, also called somatotropin, is stored and secreted by somatotropic cells from the anterior pituitary gland (Baumann, 1991; Hall et al., 1982). Its main roles are to stimulate growth and increase muscle mass mainly *via* the JAK-STAT signaling pathway. Indeed, this pathway leads to the production of insulin-like growth factor 1 which stimulates growth of bones and of a broad variety of tissues (Kopchick and Andry, 2000; Okada and Kopchick, 2001; Zhu et al., 2001). Wild-type hGH mRNA consists of five exons where its protein is monomeric and composed of 191 amino acids with an N-terminal signal sequence of 26 residues. The mature 22kDa hGH is built of four helices and, interestingly, contains two intramolecular disulfide bonds (de Vos et al., 1992; Wells and de Vos, 1993), including an eight-residues CC loop at its C-terminus (cysteine-182 to cysteine-189), necessary for functional interaction with hGH receptor (Cunningham et al., 1991). The 22 kDa protein represents 75% of the circulating hGH while the remaining 25 % is mainly a bioactive 20 kDa product resulting from mis-splicing deleting amino acids 32 to 46 (Baumann, 1991).

2. Autosomal dominant growth hormone type II

Isolated growth hormone deficiencies (IGHD) are diseases caused by a reduction or total absence of growth hormone secretion and characterized by short stature with a prevalence estimated from 1:4000 to 1:10000 (Lindsay et al., 1994; Rona and Tanner, 1977). Four different types of IGHDs are known (Kamijo et al., 1991; Mullis et al., 1992; Mullis et al., 2002). Type IA IGHD, which is the most severe, is characterized by a total absence of hGH while, type IB is less severe than IA with reduced hGH secretion. Type II and III IGHD are both characterized by a low level of hGH. Type IA and IB have autosomal recessive inheritance, and type III is X-linked. In contrast, type II is an autosomal dominant disease and the one we are interested in this project.

The autosomal dominant growth hormone type II disease (IGHDII) is associated with low levels of hGH and characterized by short stature. It can vary in severity, is generally accompanied by pituitary hypoplasia (smaller pituitary, Hess et al., 2007; McGuinness et al., 2003; Mullis et al., 2005; Ryther et al., 2003), and may develop some additional hormone deficiencies as for ACTH, gonadotropin, and TSH (Alatzoglou et al., 2015). IGHDII is mainly caused by mutations inducing mRNA mis-splicing. It gives rise to deletion of exon 3 (hGH Δ ex3) producing a 17.5 kDa product lacking amino acids 32–71, which corresponds to the loop connecting helix 1 and 2 (Cogan et al., 1995; Cunningham et al., 1991; de Vos et al., 1992). Furthermore, it suppresses the formation of the disulfide bond from cysteines 53 to 165, inducing destabilization of the protein. This exon 3 skipping can be caused by different mutations located in important sites for correct splicing, especially the intervening sequence 3, the exon splice enhancer, and also the intron splice enhancer (Miletta et al., 2016; Mullis et al., 2002). It was shown that this 17.5-kDa product, does not affect the synthesis of the wild-type hGH protein, but rather decreases its stability (Lee et al., 2000). In addition, the mutant protein is retained and aggregates in the ER as well as causes fragmentation of the Golgi apparatus (Graves et al., 2001; McGuinness et al., 2003). Furthermore, transgenic hGH Δ ex3 mice were shown to exhibit mild to severe hypoplasia that would suggest that the severity of the disease depends on the ratio of wild-type to mutant protein leading to an impairment of the maturation of secretory granules containing hGH and loss of somatotroph cells (Lee et al., 2000; McGuinness et al., 2003; Ryther et al., 2003). Moreover, both in tissue

culture and transgenic mice, hGH Δ ex3 mutant exerts a dominant-negative effect on the secretion of wild-type hormone (Ariyasu et al., 2013; Hayashi et al., 1999; Lee et al., 2000; McGuinness et al., 2003).

The mechanism underlying this dominant-negative effect on the secretion of the wild-type is not fully understood yet and is the topic of this project:

How does mutant growth hormone block the secretion of the wild-type in dominant GH deficiency type II disease?

To tackle this question, we studied the localization of the wild-type and the mutant growth hormone by immunofluorescence microscopy, as well as investigated the capacity of the wild-type and mutant to interact with each other by co-immunoprecipitation.

II. Results

Here, we show first experiments to investigate the mechanism by which mutant growth hormone exerts its dominant-negative effect on the secretion of the wild-type protein. We produced two different constructs (Figure **23A**): a wild-type version of the human growth hormone, including its N-terminal signal sequence, fused to an HA tag at its C-terminus (hGH-HA), and a mutated version lacking amino acids 32-71, fused to a myc tag at the C-terminus (hGH Δ ex3myc). At the mRNA level, the hGH is composed of five exons. Deletion of exon 3 results in a mutated protein that causes IGHDII. The wild-type growth hormone contains two disulfide bonds, a CC loop at the C-terminus and a long-range disulfide bond between cysteine 53 and 165. The deletion of the exon 3 removes cysteine 53 and disrupts the native fold and stability of the protein.

The localization of the mutant and the wild-type was studied by immunofluorescence microscopy of transiently transfected Neuro-2a cells, using anti-myc and anti-HA antibodies, respectively. The hGH-HA were concentrated in the tips of the cells as expected for a regulated protein in secretory granules. In contrast, Neuro-2a cells expressing the mutant produced perinuclear aggregates and the mutant did not accumulate into cellular extensions (Figure **23B**), confirming findings by Graves et al. (2001) and McGuinness et al. (2003). Co-staining of wild-type or mutant hGH with CgA, an endogenous granin, confirmed the localization of the wild-type hormone in secretory granules and the absence of the mutant protein in granules (Figure **23C**). We conclude that the folding deficient mutant protein is retained in the ER and forms aggregates, analogously to provasopressin mutants causing diabetes insipidus.

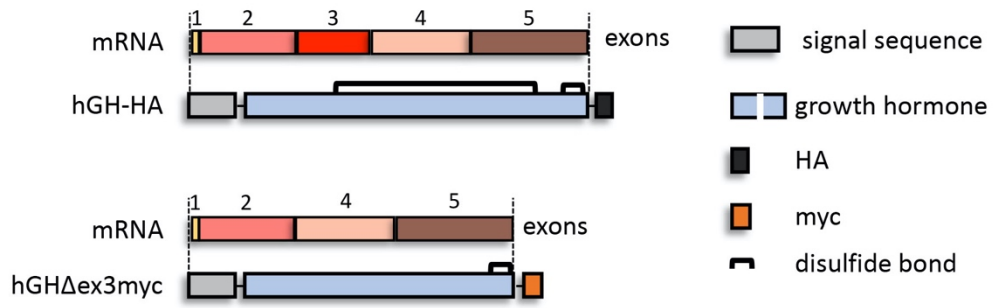
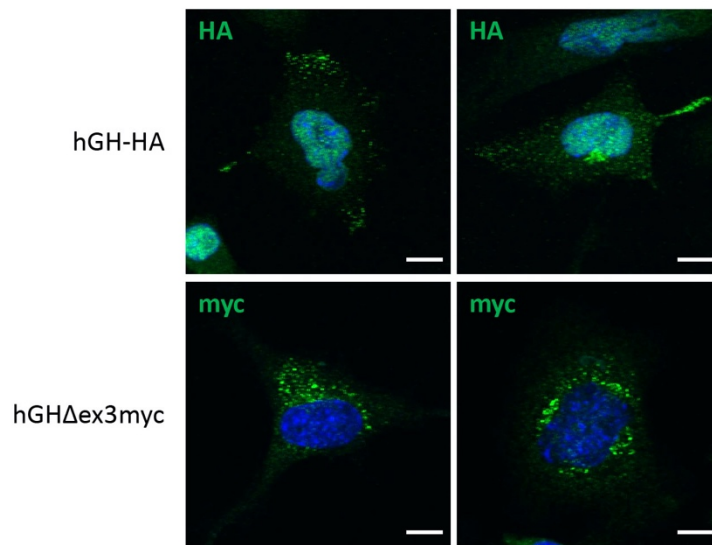
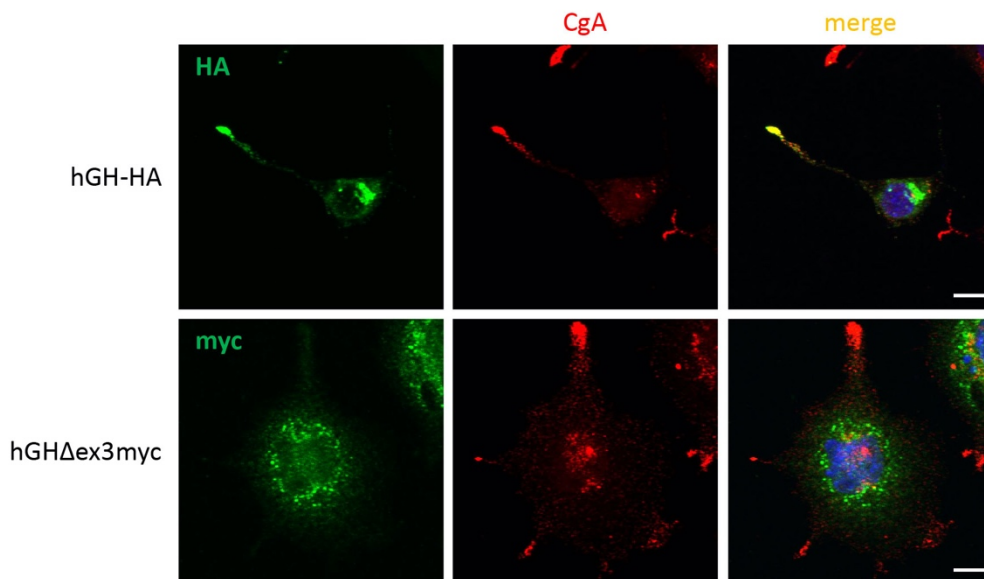
A**B****C**

Figure 23. Exon 3 deletion leads to aggregation of its mutant protein

Schematic representation of hGH-HA and hGH Δ ex3myc constructs with their mRNA exon structure (**A**). The hGH-HA protein is composed of the signal sequence and the mature GH chain fused to a C-terminal HA tag. hGH contains a CC loop at the C-terminus and a longer-range disulfide bond between cysteine 53 and 165. hGH Δ ex3myc lacks amino acid 32-71, caused by the exon 3 deletion, and is fused to a myc tag at its C-terminus. Neuro-2a cells were transiently transfected with hGH-HA and hGH Δ ex3myc and stained either with anti-HA or anti-myc antibodies, respectively (**B**), or co-stained with anti-CgA antibodies (**C**) and analyzed by immunofluorescence microscopy. Scale bars, 10 μ m

Similarly, the findings that mutant hGH Δ ex3myc accumulates and aggregates in the ER might suggest an interaction with the co-expressed wild-type hGH-HA to form mixed aggregates. By this, ER exit of the wild-type protein, granule sorting and regulated secretion might be reduced or prevented.

To investigate this proposal, we transiently co-transfected Neuro-2a cells with both constructs, hGH-HA and hGH Δ ex3myc, and studied their localization by immunofluorescence microscopy (Figure **24**). We observed a clear mis-localization of the wild-type when the mutant was present. Indeed, the mutant and wild-type were co-localized and co-aggregated with each other in the perinuclear area. Probably due to differences in expression levels upon transient transfection, the aggregates were either found loosely dispersed throughout the cell (top panels) or, most frequently, as very compact large perinuclear accumulation (bottom panels). Especially in the latter case, the cells were smaller than usual and thus probably sick. Consistent with this observation, we were so far unable to obtain stable Neuro-2a cell lines expressing hGH Δ ex3myc alone or together with hGH-HA, suggesting a toxic effect of the mutant.

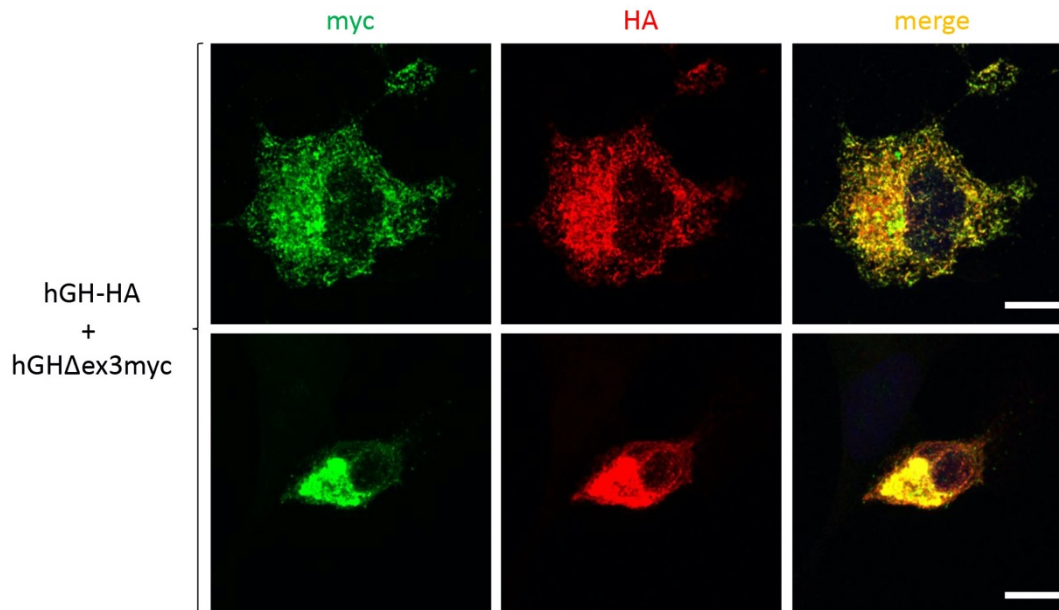


Figure 24. hGH-HA and hGHΔex3myc co-localized

Neuro-2a cell lines were transiently co-transfected with hGH-HA and hGHΔex3myc, stained with anti-HA or anti-myc antibodies respectively, and analyzed by immunofluorescence microscopy. Scale bars, 10 μ m.

To confirm a potential interaction between co-expressed wild-type and mutant proteins, we performed co-immunoprecipitation experiments (Figure 25). Neuro-2a cells were transiently transfected without DNA (–), with hGHΔex3myc or co-transfected with either hGH-HA and hGHmyc, or hGH-HA and hGHΔex3myc. Cells were lysed and immunoprecipitated either with anti-myc (Figure 25A) or anti-HA antibodies (Figure 25B). The samples were analyzed with anti-myc and anti-HA antibodies using either chemiluminescent (Figure 25A) or near-infrared fluorescence (Figure 25B) immunoblot analysis.

It turned out to be difficult to obtain consistent and balanced expression levels in double-transfections (input lanes 1–4). Upon immunoprecipitation with anti-myc antibodies, full-size and Δex3 GH were efficiently concentrated (Figure 25A, lanes 6–8). When hGHΔex3myc was co-expressed with hGH-HA, the wild-type hGH was efficiently co-isolated with the mutant protein (lane 8), indicating an interaction between mutant and wild-type protein. This result supports the notion that aggregating mutant hGH also draws in newly synthesized wild-type hGH. No co-immunoprecipitation could be detected between the two wild-type versions of hGH (lane 6), which is unfortunately not conclusive, since hGH-HA could not be detected in the lysate. The reverse co-immunoprecipitation experiment (Figure 25B) confirmed the

interaction between wild-type and mutant proteins, since hGH Δ ex3myc was co-isolated with immunoprecipitated hGH-HA (lane 8). Again, expression levels, were too low to positively interpret the absence of co-immunoprecipitation between the two wild-type proteins (lane 6).

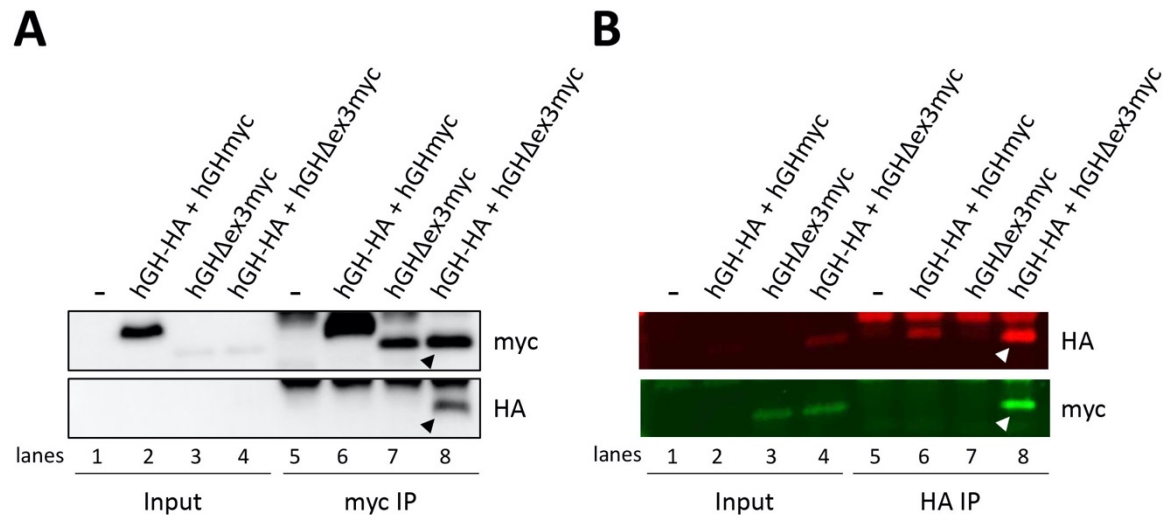


Figure 25. Wild-type and mutant hGH interact with each other

Neuro-2a cell lines were transiently transfected without DNA (–), with hGH Δ ex3myc or co-transfected with either hGH-HA and hGHmyc (hGH-HA + hGHmyc) or with hGH-HA and hGH Δ ex3myc (hGH-HA + hGH Δ ex3myc). The cells were lysed, 1/12th of the sample was used as the input and the remaining fraction of the sample was immunoprecipitated with either anti-myc (myc IP; **A**) or anti-HA (HA IP; **B**) antibodies. The input and the immunoprecipitated samples were subjected to chemiluminescent (**A**) or near-infrared (**B**) immunoblot analysis with anti-myc and anti-HA antibodies. Arrowheads point out the bands demonstrating the hGH-HA and hGH Δ ex3myc interaction.

We can conclude that the mutant is aggregating in the perinuclear region and, is inducing the aggregation of the co-expressed wild-type. Furthermore, both wild-type and mutant are interacting but, further experiments have to be performed in order to determine if the interaction is direct or indirect.

III. Discussion

The IGHDII is mainly caused by mutations leading to the skipping of the growth hormone exon 3. It results in a mutant version of hGH also causing reduced secretion levels of co-expressed wild-type and thus a dominant phenotype. Here, we began to study the mechanism by which the mutant achieves this dominant-negative effect on the secretion of the wild-type. For this purpose, we performed two different experiments, immunofluorescence microscopy and co-immunoprecipitations.

While it had previously been shown that the mutant is retained in the ER (Graves et al., 2001) and formed aggregates (McGuinness et al., 2003), we observed that it produced perinuclear aggregates. Co-expression of hGH-HA and hGH Δ ex3myc changed the localization of the wild-type from secretory granules to ER aggregates, completely co-localizing with the mutant suggesting a potential interaction. The aggregates were either loosely dispersed and clearly detectable or the signal was too strong to distinguish them. In the latter case, the cells looked smaller and probably very sick compared to the first aggregation state. This is likely due to different expression levels due to transient transfection and suggests that the ratio mutant/wild-type is leading to various severity, as proposed by McGuinness et al. (2003) and Hamid et al (2009).

Preliminary co-immunoprecipitation experiments confirmed that the wild-type and mutant hGH interact, most likely by co-aggregation. This probably leads to the failure of most wild-types to follow their route in the regulated secreted pathway causing a defect in the wild-type secretion.

Similarly to the growth hormone and IGHDII mutants, provasopressin and the dominant neurohypophyseal diabetes insipidus mutants interact which lead to the retention in the ER of co-expressed wild-type (Ito et al., 1999). Mutant hGH expression was shown to be toxic to transfected cells and induced apoptosis (Ariyasu et al., 2013). For this reason, stable cell lines with inducible promoters were used in some studies (Ariyasu et al., 2013; Lochmatter et al., 2010). Furthermore, transgenic hGH Δ ex3 mice and patients can exhibit a hypoplasia phenotype (Binder et al., 2002; Hess et al., 2007; Lee et al., 2000; McGuinness et al., 2003;

Mullis et al., 2005; Ryther et al., 2003). In contrast, provasopressin mutant expression did not lead to acute cell death in culture; only Ito et al. (1997) reported cell death over time. In transgenic mice, cell death was observed only upon stimulation of vasopressin neurons *via* frequent water deprivation (Hiroi et al., 2010) and was induced by autophagy-associated cell death rather than apoptosis (Hagiwara et al., 2014).

Finally, diabetes insipidus is caused by mutations producing ER aggregates by the CC loop in vasopressin (as well as by the glycopeptide; Beuret et al., 2017). Interestingly, growth hormone contains a C-terminal CC loop. It will be interesting to test whether the CC loop is implicated as an aggregating sequence. Another interesting aspect is that only deletion of exon3 – although caused by various mutations – lead to misfolded proteins known to cause IGHDII, whereas there are >70 different mutations causing diabetes insipidus. The latter suggests that any type of misfolding mutation has essentially the same effect: aggregation and co-aggregation of the wild-type products. It would be interesting to test, whether other folding-deficient mutants of hGH behave similarly to Δ exon3 and exciting to understand the specificity to the exon3.

Materials and methods

Plasmids and constructs

All constructs were cloned into the mammalian expression vector pcDNA3 (Invitrogen). The CCv-NPΔ and Pro1-NPΔ were described in Beuret et al. (2017) as 1-75 and 1-75Pro1, respectively. The other CCx-NPΔ constructs were produced as complementary synthetic oligonucleotides and inserted between the coding sequences of the signal peptide and neurophysin II. The same CC sequences were inserted between the signal peptide of prepro-enkephalin and the mature sequence of A1Pi variant M2 (Leitinger et al., 1994) with a C-terminal six-histidine (His₆) and myc epitope tag for CCx-A1Pimyc and additionally also between the C-terminus of A1Pi and the His₆ and myc epitope tag for 2xCCx-A1Pimyc. The cDNA of human PDI (from Dr. Julia Birk) was tagged at the N-terminus with a myc epitope by PCR. The cDNA of EBFP was cloned out from a multilabel plasmid from the Paul Scherrer Institute. The hGH cDNA (Origene, RC215644) was tagged at the C-terminus either with myc (hGHmyc) or HA (hGH-HA). The deletion of the exon 3 (hGHΔex3myc) was obtained by the cut and paste method using restriction sites. All the sequences are listed in suppl. Table S1. VHH_{mCherry} nanobodies, where VHH consists of the GFP-specific VHH domain, T7, HA and hexahistidine (His₆) tags, were provided by Dr. Buser (Addgene plasmid # 109421; <http://n2t.net/addgene:109421>; RRID: Addgene_109421).

List of antibodies

Primary antibodies: mouse monoclonal anti-myc antibodies 9E10 (precipitated from hybridoma cultures, RRID:CVCL_L708, 1:10 to 1:100 for immunofluorescence); rabbit monoclonal anti-myc antibodies (Genetex, GTX29106, Lot:821902572, RRID:AB_369669, 1:400 for immunofluorescence); mouse monoclonal anti-His₆ antibodies (HIS.H8, Millipore, MAI-21315, Lot: 2426469, RRID:AB_557403, 1:2000 for immunofluorescence), rabbit polyclonal anti-CgA antibodies (Novus Biologicals, NB120-15160, Lot:C-2, RRID:AB_789299, 1:200 for immunofluorescence and 1:5000 for western blot); monoclonal mouse actin antibodies (clone C4, Millipore, MAB1501, Lot:3282535, RRID:AB_2223041, used for immunoprecipitation); rabbit monoclonal anti-His₆ antibodies (Abcam, Ab213204, Lot:GR3199118-5, used for electron microscopy); rabbit monoclonal anti-POMC antibodies (Abcam, ab254257, GR3279295-2, 1:5000 for Western blot); self-made mouse monoclonal

anti-HA antibodies (precipitated from 12CA5 hybridoma cultures, 1:2000 for western blot); rabbit monoclonal anti-HA antibodies (Cell Signaling Technology, C29F4, Lot: 9, RRID:AB_1549585, 1:5000 for western blot)

Secondary antibodies: a non-cross-reacting A488-labeled donkey polyclonal anti-mouse immunoglobulin (Molecular Probes, A21202, Lot: 1975519, RRID: AB_141607, 1:300 for immunofluorescence), a A488-labeled donkey polyclonal anti-rabbit immunoglobulin (Molecular Probes, A21206, Lot: 1981155, RRID: AB_2535792, 1:300 for immunofluorescence). A HRP goat polyclonal anti-mouse (Fc specific, Sigma, A0168, Lot:024M4751. RRID: AB_257867, 1:20000 for Western Blot), a HRP goat polyclonal anti-rabbit (Sigma, A0545, Lot:022M4811, RRID: ab_257896, 1:20000 for Western Blot). An IRDye800CW donkey polyclonal anti-rabbit immunoglobulin (Li-Cor, 926-32213, Lot:C70405-07, RRID: AB_621848, 1:20000 for near-infrared Western Blot) and an IDy680RD donkey polyclonal anti-mouse immunoglobulin (Li-Cor, 926-68072, Lot:C80522-25, RRID: AB_10953628, 1:20000 for near-infrared Western Blot). A goat anti-rabbit immunoglobulin (BB International, EM GAR10, RRID: AB_1769128, used at 1:100 in electron microscopy).

Cell culture and transfection

Mouse neuroblastoma cells Neuro-2a (from Cornell university, USA), monkey kidney fibroblast-like cells COS-1 (Ph.D. Richard E. Mains, USA) and mouse pituitary corticotrope tumor cells AtT20 (from Pr.Dr Hans-Peter Hauri, Biozentrum) have been used to study aggregation in the ER (Neuro-2a and COS-1) and secretory granule formation (AtT20). They were grown in Dulbecco's modified Eagle's medium (DMEM, Sigma) containing 4500 mg/l glucose (Neuro-2a) or 1000 mg/l glucose (AtT20 and COS-1), supplemented with 10% fetal calf serum (FCS), 100 units/ml penicillin, 100 µg/ml streptomycin, and 2 mM L-glutamine at 37°C with 5% (Neuro-2a) or 7,5% CO₂ (AtT20 and COS-1). Cells were transfected using Fugene HD (Promega). Stably expressing AtT20 cells were selected using 100 µg/ml G418. Clonal cell lines were isolated by dilution into 96-well plates.

Immunofluorescence and quantitation

Cells were grown on glass coverslips until 50%-60% confluence, fixed with 3% paraformaldehyde for 30 min at room temperature, washed twice with phosphate-buffered

saline (PBS), quenched 5 min in 50 mM NH₄Cl in PBS, washed twice with PBS, permeabilized in 0.1% Triton X-100 (Applichem) in PBS for 10 min, washed twice with PBS, blocked with 1% bovine serum albumin (BSA, Roche) in PBS for 15 min, incubated at room temperature with primary antibodies for 1–2 h in BSA-PBS, washed twice with PBS, stained with fluorescent secondary antibodies in BSA/PBS for 30 min, and mounted in Fluoromount-G (Hoechst) with or without 0.5 µg/ml DAPI. The stainings were analyzed using a Zeiss Confocal LSM700 microscope.

Aggregation quantitation of control Pro1-NPΔ or CCx-NPΔ constructs in the ER of transfected Neuro-2a cells and COS-1 cells was quantified by counting the number of expressing cells containing punctate accumulations using a Zeiss Axioplan microscope. Between 120 and 150 expressing cells were counted for each construct and in three independent experiments.

For the granule quantification of A1Pimyc, CCx-A1Pimyc and 2xCCx-A1Pimyc in AtT20 cells, immunofluorescence experiments were performed using mouse anti-myc antibodies to detect the A1Pimyc constructs and rabbit anti-CgA antibodies to detect the secretory granules. The granules were quantified using Fiji program and a script made by Dr. Laurent Gerard (Biozentrum). The CgA was used to select the area where the secretory granules are located (corresponding to the tip of the cell) and the mean intensity of myc into this area was quantified by the script. Per Coverslip, around twenty pictures were taken (~ ten pictures for A1Pimyc+EBFP, and ten pictures for the construct co-seeded with it) with between 5-8 cells per picture which corresponds to 50-150 tips per constructs quantified. The mean intensity of anti-myc signal into the tips were normalized to the number of tips for each construct and for that in co-cultured A1Pimyc+EBFP cells. Three independent experiments were performed.

Electron microscopy

Transfected Neuro-2a cells were grown in 10-cm dishes, transiently transfected with the NPΔ constructs and grown until 80% confluence. Cells were fixed in 3% formaldehyde and 0.2% glutaraldehyde for 2 h at room temperature, then scraped, pelleted, resuspended and washed three times in PBS, incubated with 50 mM NH₄Cl in PBS for 30 min, washed three times in PBS, resuspended in 2% warm agarose, and left to solidify on ice. Agarose pieces were dehydrated and infiltrated with LR gold resin (London Resin, London, UK) and allowed

to polymerize for 1 day at -10°C . For immunogold labeling, sections of 60–70 nm were collected on carbon-coated Formvar Ni-grids, incubated with rabbit anti-His₆ antibodies in PBS, 2% BSA, 0.1% Tween-20 for 2 h, washed with PBS, and incubated with 10-nm colloidal gold conjugated goat anti-rabbit immunoglobulin antibodies in PBS, 2% BSA, and 0.1% Tween-20 for 90 min. Grids were washed five times for 5 min in PBS and then five times in H₂O, before staining for 10 min in 2% uranyl acetate. Sections were viewed with a Phillips CM100 electron microscope.

Radioactive labelling and determination of expression levels

AtT20 cells stably expressing A1Pi constructs were grown in 6-well plates until 80% confluence, incubated at 37°C for 30 min in 500 μl starvation medium (DMEM lacking methionine and cysteine) and another 30 min in 500 μl labeling medium containing 100 $\mu\text{Ci/ml}$ [³⁵S]methionine/cysteine (Hartmann Analytics, Braunschweig, Germany). The cells were washed twice with PBS and lysed in 500 μl lysis buffer (PBS with 1% Triton X-100, 0.5% deoxycholate, and 2 mM phenylmethylsulfonyl fluoride, pH 8) for 1 h at 4°C . The lysates were scraped and centrifuged for 20 min in a microfuge at 13000xg. 400 μl of supernatants were incubated overnight at 4°C with 20 μl of mouse monoclonal anti-myc antibodies (and 3 μl of anti-actin antibodies for some cases). Upon addition of 20 μl protein A Sepharose beads (Biovision) samples were incubated on a shaker for 1 h at 4°C , washed three times with lysis buffer, once with 100 mM Na-phosphate, pH 8, and once with 10 mM Na-phosphate, pH 8. Upon addition of 40 μl 2xSDS-sample buffer and 1/8 volume of 1M DTT, samples were heated at 95°C for 5 min and analyzed by SDS-polyacrylamide gel electrophoresis (10% acrylamide). Gels were fixed, dried, exposed to phosphorimager plates for 2-5 days, and analyzed by phosphorimager.

Stimulated secretion

AtT20 cells stably expressing A1Pi constructs were grown in 12-well plates until 80% confluence. Cells were washed with PBS, incubated for 30 min either with 150 μl of secretion medium (Earle's balanced salt solution without Ca^{2+} and Mg^{2+} , E6267, Sigma-Aldrich, supplemented with MEM amino acids, 2 mM L-glutamine, 97.65 mg/L MgSO_4 , containing 2 $\mu\text{g/ml}$ VHH_{mCherry} nanobodies for normalization) or with 150 μl of stimulation medium

(secretion medium supplemented with 2 mM barium chloride, BaCl₂). The secretion and stimulation media were collected, separated by SDS-gel electrophoresis, and subjected to quantitative near-infrared immunoblot analysis.

Lubrol solubility assay

AtT20 cell lines stably expressing A1Pi constructs were grown in 6-well plates to 80% confluence, washed 3 times with cold PBS, covered with 200 µl Lubrol solution composed of 5mM Na-phosphate, pH 7.4, containing 1,5% Lubrol, 0.3M sucrose, 2 mM PMSF, and protease inhibitor cocktail (5 mg/ml benzamidine, 1 mg/ml pepstatin A, 1 mg/ml leupeptin, 1 mg/ml antiparin, 1mg/ml chymostatin in 40% DMSO and 60% EtOH), scraped into a centrifuge tube, incubated 1 h at 4°C on a roller, and centrifuged for 5 min at 500xg at 4°C. 150 µl of the supernatant was centrifuged for 1 h at 50'000xg at 4°C. The supernatant was collected and supplemented with 37.5 µl 5xSDS-sample buffer, while the pellet was resuspended in 187.5 µl 1xSDS-sample buffer. Both fractions were heated for 3 min at 95°C. To analyze A1Pimyc constructs, 500 units endoglycosidase H (New-England Biolabs) was added to 40 µl aliquots of supernatant and pellet and incubated 1 h at 37°C. After addition of 1/8 volume of 1M DTT, samples were boiled 2 min at 95°C, separated on 7.5% or 10% SDS-gels for A1Pi constructs or for CgA, respectively, and analyzed by immunoblotting.

Mass spectrometry

Stable AtT20 cell lines expressing A1Pimyc, CCv-A1Pimyc, CCc-A1Pimyc, CCa-A1Pimyc, CCr-A1Pimyc or CCpN-A1Pimyc were grown in 10-cm dishes, washed twice with PBS, and incubated overnight with 4 ml medium without FCS. The medium was divided into two microfuge tubes and centrifuged for 1 min at 13000xg. The supernatants were incubated overnight with 40 µl of the mouse anti-myc antibodies and incubated with 25 µl protein A Sepharose beads (Biovision) for 1 h at 4°C on a shaker. The beads were washed 4 times with 100 mM and then 10 mM Na-phosphate, and the antigen was eluted with 40 µl of 0.2% glycine, pH 2.8. After neutralization with 80 µl ammonium bicarbonate, 20 µl digestion buffer (preparation for 4 ml: 2.3 g of guanidine-HCl, 400 µl of 1 M ammonium bicarbonate, 1 ml 0.75 M chloroacetamide) was added and samples were heated at 95°C for 10 min. 5 µl of tris(2-carboxyethyl)phosphine (TCEP), a reducing reagent, was added in only one sample out of two per construct, 5 µl of 0.4M iodoacetamide was added in all the samples and incubated 1 h at

room temperature, either 0.5 µg of trypsin (A1Pimyc, CCv-A1Pimyc, CCa-A1Pimyc, and Cc-A1Pimyc) or 0.5 µg of Lys-C (CCr-A1Pimyc and CCpN-A1Pimyc) was added to each sample and incubated on a shaker overnight at 37°C. 50 µl 2 M hydrochloric acid and 50 µl of 5% trifluoroacetic acid were added. In order to eluted, concentrated and dissolved the peptides, the BioPureSPN Mini C18 spin columns (Part #HUMS18V from The Nest Group) was used. The samples concentration was measured by the Nanodrop and collected into MS tubes. The samples were analyzed by an Orbitrap Elite Mass Spectrometer (Thermo Scientific).

Co-Immunoprecipitation

Neuro-2a cells were grown in a 10 cm dish until 80% confluence and transiently transfected with either no DNA (-) or hGhΔex3myc, or co-transfected either with hGhHA + hGhmyc or hGhHA +hGhΔex3myc. Cells were then incubated with 500 µl lysis buffer, detached, 40 µl of the sample were used as an input and the rest of the sample was incubated overnight either with mouse anti-myc or mouse anti-HA antibodies. The next day, the samples were incubated with protein A Sepharose beads (Biovision), washed two times with lysis buffer, two times with 100 mM Na-phosphate pH 8 and two times with 10 mM Na-phosphate pH 8. The beads a dissolved in sample buffer with 1/8 volume of 1M DTT and boiled at 95°C. The sample were split in two and subjected to near-infrared or chemiluminescent immunoblot analysis using rabbit anti-myc and rabbit anti-HA antibodies.

Supplementary Materials

Table S1: Amino acid sequences of the constructs used in the thesis

In grey: Enkephalin signal sequence

In red: CCx or Pro1

In blue: NPΔ

In green: His₆ tag

In orange: myc tag

In pink: HA tag

In violet: PDI

In black: restrictions sites

In black and highlighted in dark grey: A1Pi

In black and highlighted in light grey: hGH or hGHΔex3 with its signal sequence

*: stop codon

>CCc-NPΔ :

MAQFLRLCIWLLALGSCLLATVQARCGNLSTCMLGKRAMSDLELRQCLPCGPGGKGRFCGSPICCADEL
GCFVGTAEALRCQEENYLPSPCQSGQKACGSHHHHHH*

>CCr-NPΔ :

MAQFLRLCIWLLALGSCLLATVQASSKCSRLYTACVYHKRAMSDLELRQCLPCGPGGKGRFCGSPICCAD
ELGCFVGTAEALRCQEENYLPSPCQSGQKACGSHHHHHH*

>CCpN-NPΔ :

MAQFLRLCIWLLALGSCLLATVQALPICPGAARCVTKRAMSDLELRQCLPCGPGGKGRFCGSPICCA
DELGCFVGTAEALRCQEENYLPSPCQSGQKACGSHHHHHH*

>NPΔ-CCpC :

MAQFLRLCIWLLALGSCLLATVQAKRAMSDLELRQCLPCGPGGKGRFCGSPICCADEL
GCFVGTAEALRCQEENYLPSPCQSGQKACGSLKCRHHNNCHHHHHH*

>CCv-NPΔ :

MAQFLRLCIWLLALGSCLLATVQACYFQNCPRGGKRAMSDLELRQCLPCGPGGKGRFCGSPICCADEL
GCFVGTAEALRCQEENYLPSPCQSGQKACGSHHHHHH*

>Pro1-NPΔ :

MAQFLRLCIWLLALGSCLLATVQAGPPGPGPGPKRAMSDLELRQCLPCGPGGKGRFCGSPICCADEL
GCFVGTAEALRCQEENYLPSPCQSGQKACGSHHHHHH*

>CCa-NPΔ :

MAQFLRLCIWLLALGSCLLATVQAKCNTATCATQKRAMSDLELRQCLPCGPGGKGRFCGSPICCADEL
GCFVGTAEALRCQEENYLPSPCQSGQKACGSHHHHHH*

>Myc-PDI :

MAQFLRLCIWLLALGSCLLATVQA**EQKLISEEDL**LGSDAPEEEDHVLVLRKSNFAEALAAHKYLLVEFYAPW
CGHCKALAPEYAKAAGKKAEGSEIRLAKVDATEESDLAQQYGVRYPTIKFFRNGDTASPKEYTAGREA
DDIVNWLKRTGPAATTPDGA~~AAESL~~VESSEVAVIGFFKDVESDSAQFLQAAEAIDDIPFGITSNSDVF
SKYQLDKDGVVLFKKFDEGRN~~NFEGE~~VTKENLLDFIKHNQLPLVIEFTEQTAPKIFGGEIKTHILLFLPKSVS
DYDGKLSNFKTA~~AESFK~~GILFIFIDSDHTDNQRILEFFGLKKEECPAVRLITLEEEMTKYKPESEELTAERITE
FCHRFLGKIKPHLMSQELPEDWDKQPVKVLVGNFEDVAFDEKKNVFEFYAPWCGHCKQLAPIWDK
LGETYKDHENIVIAKMDSTANEVEAVKVHSFPTLKFFPASADRTVIDYNGERTLDGFKKFLESGGQDGAG
DDDDLELEEAE~~EPDMEED~~DDQKAVKDEL

>A1Pimyc :

MAQFLRLCIWLLALGSCLLATVQATG**EDPQGDAAQKTD**SHHDQDHPTFNKITPNLAEF~~AFSLYRQLAH~~
QSNSTNIFFSPVSIATAFAMLSLGTKADTHDEILEGLN~~FNLT~~IEPAQIHEGFQELLHTLNQPSQLQTTG
NGLFLSEGLKLV~~DKFLEDV~~KKLYHSEAFVNF~~GDTEEAKKQ~~INDYVEKGTQGKIVDLVKELDRDTVFALVN
YIFFKGKWERPFEVKDTE~~EEDFHVDQVTT~~VKVPMMKRLGMFNIQHCKKLSSWVLLMKYLG~~NATAIFFL~~
DEGKLQHLENELTHDIITK~~FLENEDRRSASLHLPKLSIT~~GT~~YDLKSILGQLG~~ITKVF~~SNGADLSGV~~T~~EEAPLKL~~
SKAVHKAVLTIDEK~~GTEAAGAMFLEAIPMSIPPEVKFNKPFVFLMIEQNTKSPLFMGKVVNPTQK~~GAPPL
INPPRHHHHHH**EQKLISEEDL***

>CCv-A1Pimyc :

MAQFLRLCIWLLALGSCLLATVQA**CYFQNCPRGGT**G**EDPQGDAAQKTD**SHHDQDHPTFNKITPNLAEF~~AFSLYRQLAH~~
QSNSTNIFFSPVSIATAFAMLSLGTKADTHDEILEGLN~~FNLT~~IEPAQIHEGFQELLHTLNQPSQLQTTG
NGLFLSEGLKLV~~DKFLEDV~~KKLYHSEAFVNF~~GDTEEAKKQ~~INDYVEKGTQGKIVDLVKELDRDTVFALVN
YIFFKGKWERPFEVKDTE~~EEDFHVDQVTT~~VKVPMMKRLGMFNIQHCKKLSSWVLLMKYLG~~NATAIFFL~~
PDEGKLQHLENELTHDIITK~~FLENEDRRSASLHLPKLSIT~~GT~~YDLKSILGQLG~~ITKVF~~SNGADLSGV~~T~~EEAPLKL~~
SKAVHKAVLTIDEK~~GTEAAGAMFLEAIPMSIPPEVKFNKPFVFLMIEQNTKSPLFMGKVVNPTQK~~GAPPLINPPRHHHHHH**EQKLISEEDL***

>CCa-A1Pimyc :

MAQFLRLCIWLLALGSCLLATVQA**KCNTATCATQT**G**EDPQGDAAQKTD**SHHDQDHPTFNKITPNLAEF~~AFSLYRQLAH~~
QSNSTNIFFSPVSIATAFAMLSLGTKADTHDEILEGLN~~FNLT~~IEPAQIHEGFQELLHTLNQPSQLQTTG
NGLFLSEGLKLV~~DKFLEDV~~KKLYHSEAFVNF~~GDTEEAKKQ~~INDYVEKGTQGKIVDLVKELDRDTVFALVN
YIFFKGKWERPFEVKDTE~~EEDFHVDQVTT~~VKVPMMKRLGMFNIQHCKKLSSWVLLMKYLG~~NATAIFFL~~
PDEGKLQHLENELTHDIITK~~FLENEDRRSASLHLPKLSIT~~GT~~YDLKSILGQLG~~ITKVF~~SNGADLSGV~~T~~EEAPLKL~~
SKAVHKAVLTIDEK~~GTEAAGAMFLEAIPMSIPPEVKFNKPFVFLMIEQNTKSPLFMGKVVNPTQK~~GAPPLINPPRHHHHHH**EQKLISEEDL***

>CCc-A1Pimyc :

MAQFLRLCIWLLALGSCLLATVQA**RCGNLSTCMLGTTG**G**EDPQGDAAQKTD**SHHDQDHPTFNKITPNLAEF~~AFSLYRQLAH~~
QSNSTNIFFSPVSIATAFAMLSLGTKADTHDEILEGLN~~FNLT~~IEPAQIHEGFQELLHTLNQPSQLQTTG
NGLFLSEGLKLV~~DKFLEDV~~KKLYHSEAFVNF~~GDTEEAKKQ~~INDYVEKGTQGKIVDLVKELDRDTVFALVN
YIFFKGKWERPFEVKDTE~~EEDFHVDQVTT~~VKVPMMKRLGMFNIQHCKKLSSWVLLMKYLG~~NATAIFFL~~
PDEGKLQHLENELTHDIITK~~FLENEDRRSASLHLPKLSIT~~GT~~YDLKSILGQLG~~ITKVF~~SNGADLSGV~~T~~EEAPLKL~~
SKAVHKAVLTIDEK~~GTEAAGAMFLEAIPMSIPPEVKFNKPFVFLMIEQNTKSPLFMGKVVNPTQK~~GAPPLINPPRHHHHHH**EQKLISEEDL***

>CCr-A1Pimyc :

MAQFLRLCIWLLALGSCLLATVQA**SSKCSRLYTACVYHK**TGEDPQGDAQAQKTDTSHHDDQDHPTFNKITPN
LAEFASFLYRQLAHQSNSTNIFFSPVSIATAFAMLSLGTKADTHDEILEGLNFNLTPEAQIHEGFQELLHTL
NQPDSQLQLTTGNGLFLSEGLKLVDFLEDVKKLYHSEFTVNFVGDTEEAKKQINDYVEKGTQGGKIVDLVK
ELDRDRTVFALVNYIFFKGGKWERPFVVDTEEEDFHVDQVTTVKVPMKRLGMFNIQHCKKLSSWVLLM
KYLGNATAIFFLPDEGKLQHLENELTHDIITKFLNEDRRSASLHLPKLSITGTDLKSILGQLGITKVFNSGAD
LSGVTEEAPLKLSKAVHKAVLTIDEKGTEAAGAMFLEAIPMSIPPEVKFNKPFVFLMIEQNTKSPLFMGKV
VNPTQK**GAPPLINPPRHHHHHHEQKLISEEDL***

>CCpN-A1Pimyc :

MAQFLRLCIWLLALGSCLLATVQA**LPICPGGAARCQVT**TGEDPQGDAQAQKTDTSHHDDQDHPTFNKITPN
NLAEFASFLYRQLAHQSNSTNIFFSPVSIATAFAMLSLGTKADTHDEILEGLNFNLTPEAQIHEGFQELLHTL
TLNQPDSQLQLTTGNGLFLSEGLKLVDFLEDVKKLYHSEFTVNFVGDTEEAKKQINDYVEKGTQGGKIVDLV
VKELDRDRTVFALVNYIFFKGGKWERPFVVDTEEEDFHVDQVTTVKVPMKRLGMFNIQHCKKLSSWVLL
LMKYLGNATAIFFLPDEGKLQHLENELTHDIITKFLNEDRRSASLHLPKLSITGTDLKSILGQLGITKVFNS
GADLSGVTEEAPLKLSKAVHKAVLTIDEKGTEAAGAMFLEAIPMSIPPEVKFNKPFVFLMIEQNTKSPLFM
GKVVNPTQK**GAPPLINPPRHHHHHHEQKLISEEDL***

>2xCCa-A1Pimyc :

MAQFLRLCIWLLALGSCLLATVQA**KCNTATCATQ**TGEDPQGDAQAQKTDTSHHDDQDHPTFNKITPNLAE
FAFSLYRQLAHQSNSTNIFFSPVSIATAFAMLSLGTKADTHDEILEGLNFNLTPEVQIHEGFQELLHTLNQ
PDSQLQLTTGNGLFLSEGLKLVDFLEDVKKLYHSEFTVNFVGDTEEAKKQINDYVEKGTQGGKIVDLVKEL
DRDRTVFALVNYIFFKGGKWERPFVVDTEEEDFHVDQVTTVKVPMKRLGMFNIQHCKKLSSWVLLMKY
LGNATAIFFLPDEGKLQHLENELTHDIITKFLNEDRRSASLHLPKLSITGTDLKSILGQLGITKVFNSGADL
SGVTEEAPLKLSKAVHKAVLTIDEKGTEAAGAMFLEAIPMSIPPEVKFNKPFVFLMIEQNTKSPLFMGKV
VNPTQK**PPQA KCNTATCATQPGAPPLINPPRHHHHHHEQKLISEEDL***

>2xCCr-A1Pimyc :

MAQFLRLCIWLLALGSCLLATVQA**SSKCSRLYTACVYH**TGEDPQGDAQAQKTDTSHHDDQDHPTFNKITPN
LAEFASFLYRQLAHQSNSTNIFFSPVSIATAFAMLSLGTKADTHDEILEGLNFNLTPEAQIHEGFQELLHTL
LNQPDSQLQLTTGNGLFLSEGLKLVDFLEDVKKLYHSEFTVNFVGDTEEAKKQINDYVEKGTQGGKIVDLV
KELDRDRTVFALVNYIFFKGGKWERPFVVDTEEEDFHVDQVTTVKVPMKRLGMFNIQHCKKLSSWVLL
MKYLGNATAIFFLPDEGKLQHLENELTHDIITKFLNEDRRSASLHLPKLSITGTDLKSILGQLGITKVFNSG
ADLSGVTEEAPLKLSKAVHKAVLTIDEKGTEAAGAMFLEAIPMSIPPEVKFNKPFVFLMIEQNTKSPLFMG
KVVNPTQK**PPSSKCSRLYTACVYHPGAPPLINPPRHHHHHHEQKLISEEDL***

>2xCCc-A1Pimyc :

MAQFLRLCIWLLALGSCLLATVQA**RCGNLSTCMLG**TGEDPQGDAQAQKTDTSHHDDQDHPTFNKITPNLA
EFASFLYRQLAHQSNSTNIFFSPVSIATAFAMLSLGTKADTHDEILEGLNFNLTPEAQIHEGFQELLHTLN
QPDSQLQLTTGNGLFLSEGLKLVDFLEDVKKLYHSEFTVNFVGDTEEAKKQINDYVEKGTQGGKIVDLVKE
LDRDRTVFALVNYIFFKGGKWERPFVVDTEEEDFHVDQVTTVKVPMKRLGMFNIQHCKKLSSWVLLMK
YLGATAIFFLPDEGKLQHLENELTHDIITKFLNEDRRSASLHLPKLSITGTDLKSILGQLGITKVFNSGAD
LSGVTEEAPLKLSKAVHKAVLTIDEKGTEAAGAMFLEAIPMSIPPEVKFNKPFVFLMIEQNTKSPLFMGKV
VNPTQK**PPVQARCGNLSTCMLGPGAPPLINPPRHHHHHHEQKLISEEDL***

>2xCCv-A1Pimyc :

MAQFLRLCIWLLALGSCLLATVQA**CYFQNCPRGG**TGEDPQGDAAQKTDTSHHDDQHPTFNKITPNLAE
FAFSLYRQLAHQSNSTNIFFSPVSIATAFAMLSLGTKADTHDEILEGLNFNLTEIPEAQIHEGFQELLHTLNQ
PDSQLQLTTGNGLFLSEGLKLVDFLEDVKKLYHSEAFVNFVGDTEEAKKQINDYVEKGTQGGKIVDLVKEL
DRDTVFALVNYIFFKGGWERPFVVKDTEEDFHVDQVTTVKVPMMKRLGMFNQHCCKLSSWVLLMKY
LGNATAIFFLPDEGKLQHLENELTHDIITKFLNEDRRSASLHLPKLSITGTDLKSLGQLGITKVFNSGADL
SGVTEEAPLKLKAVHKAVLTIDEKGTAAAGAMFLEAIPMSIPPEVKFNKPFVFLMIEQNTKSPLFMGKVV
NPTQKPP**CYFQNCPRGG**PGAPPLINPPR**HHHHHHEQKLISEEDL***

>2xCCpN-A1Pimyc :

MAQFLRLCIWLLALGSCLLATVQA**LPICPGGAARCQVT**TGEDPQGDAAQKTDTSHHDDQHPTFNKITP
NLAEFASLYRQLAHQSNSTNIFFSPVSIATAFAMLSLGTKADTHDEILEGLNFNLTEIPEAQIHEGFQELLH
TLNQPDSQLQLTTGNGLFLSEGLKLVDFLEDVKKLYHSEAFVNFVGDTEEAKKQINDYVEKGTQGGKIVDL
VKELDRDTVFALVNYIFFKGGWERPFVVKDTEEDFHVDQVTTVKVPMMKRLGMFNQHCCKLSSWVLL
LMKYLGNATAIFFLPDEGKLQHLENELTHDIITKFLNEDRRSASLHLPKLSITGTDLKSLGQLGITKVFNS
GADLSGVTEEAPLKLKAVHKAVLTIDEKGTAAAGAMFLEAIPMSIPPEVKFNKPFVFLMIEQNTKSPLFM
GKVVNPTQKPP**LPICPGGAARCQVT**PGAPPLINPPR**HHHHHHEQKLISEEDL***

>hGHmyc :

MATGSRTSLLAFGLLCPWLQEGSAFPTIPLSRLFDNAMLRAHRLHQLAFDITYQEFEEAYIPKEQKYSFL
QNPQTSLCFSESIPSPNREETQQKSNLELLRISLLLIQSWLEPVQFLRSVFANSLVYGASDSNVYDLLKDLE
EGIQTLMGRLEDGSPRTGQIFKQTYSKFDTNSHNDDALLKNYGLLYCFRKDMDKVETFLRIVQCRSVEGS
CGF**EQKLISEEDL***

>hGH-HA :

MATGSRTSLLAFGLLCPWLQEGSAFPTIPLSRLFDNAMLRAHRLHQLAFDITYQEFEEAYIPKEQKYSFL
QNPQTSLCFSESIPSPNREETQQKSNLELLRISLLLIQSWLEPVQFLRSVFANSLVYGASDSNVYDLLKDLE
EGIQTLMGRLEDGSPRTGQIFKQTYSKFDTNSHNDDALLKNYGLLYCFRKDMDKVETFLRIVQCRSVEGS
CGF**YPYDVPDYAYPYDVPDYAYPYDVPDYA***

>hGHΔex3myc :

MATGSRTSLLAFGLLCPWLQEGSAFPTIPLSRLFDNAMLRAHRLHQLAFDITYQEFNLELLRISLLLIQSW
LEPVQFLRSVFANSLVYGASDSNVYDLLKDLEEGIQTLMGRLEDGSPRTGQIFKQTYSKFDTNSHNDDALL
KNYGLLYCFRKDMDKVETFLRIVQCRSVEGSCGF**TRTEQKLISEEDLRPLEHA***

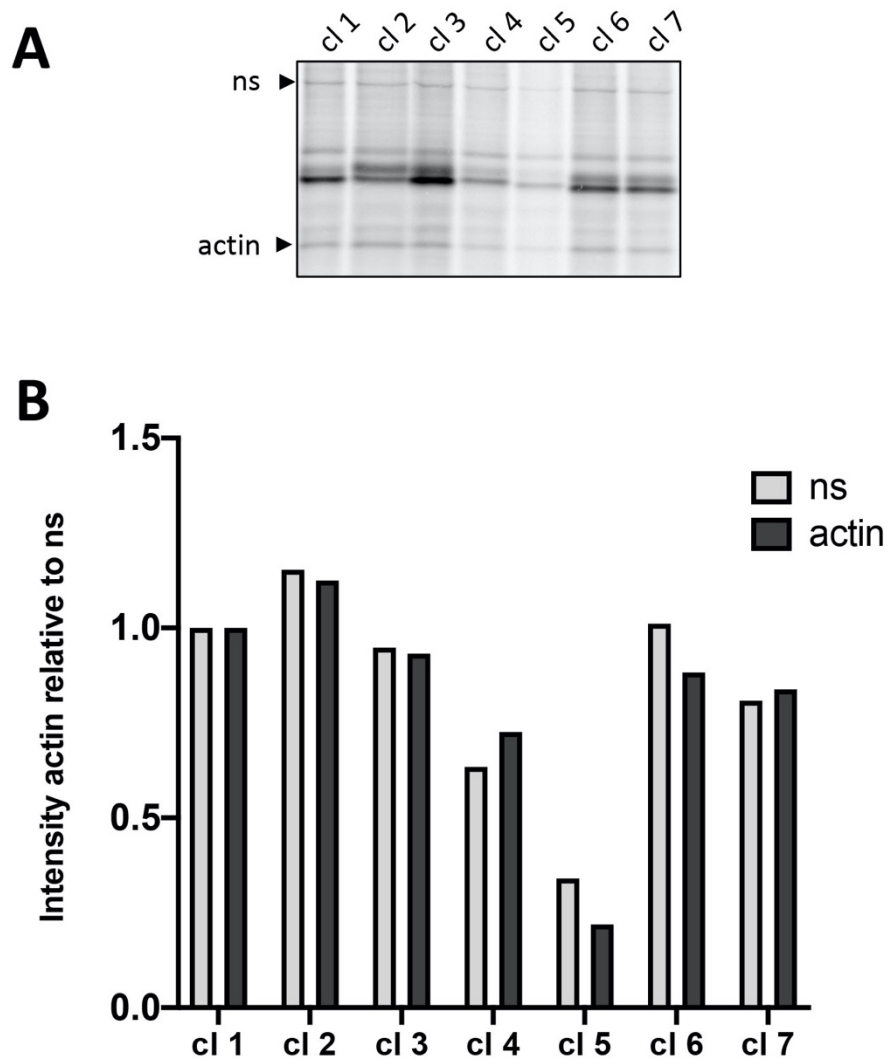


Figure S1. The non-specific band can be used as a loading control for radioactive labelling
(A) CCx-A1Pimyc stable clones were labeled for 30 min with [³⁵S]methionine and lysed. Both A1Pimyc constructs and actin were immunoprecipitated, separated by SDS-gel electrophoresis and autoradiographed. ns: non-specific band. **(B)** Both actin and the non-specific band were quantified and plotted relative to their intensity in clone 1. Intensities change very much in parallel, indicating that the non-specific band may be used as a measure of the amount of cells used.

References

Alatzoglou, K.S., Kular, D., and Dattani, M.T. (2015). Autosomal Dominant Growth Hormone Deficiency (Type II). *Pediatr Endocrinol Rev* 12, 347-355.

Anoop, A., Ranganathan, S., Das Dhaked, B., Jha, N.N., Pratihari, S., Ghosh, S., Sahay, S., Kumar, S., Das, S., Kombrabail, M., *et al.* (2014). Elucidating the role of disulfide bond on amyloid formation and fibril reversibility of somatostatin-14: relevance to its storage and secretion. *J Biol Chem* 289, 16884-16903.

Ariyasu, D., Yoshida, H., Yamada, M., and Hasegawa, Y. (2013). Endoplasmic reticulum stress and apoptosis contribute to the pathogenesis of dominantly inherited isolated GH deficiency due to GH1 gene splice site mutations. *Endocrinology* 154, 3228-3239.

Arnautova, I., Smith, A.M., Coates, L.C., Sharpe, J.C., Dhanvantari, S., Snell, C.R., Birch, N.P., and Loh, Y.P. (2003). The prohormone processing enzyme PC3 is a lipid raft-associated transmembrane protein. *Biochemistry* 42, 10445-10455.

Arvan, P., and Castle, D. (1998). Sorting and storage during secretory granule biogenesis: looking backward and looking forward. *Biochem J* 332 (Pt 3), 593-610.

Bartolomucci, A., Possenti, R., Mahata, S.K., Fischer-Colbrie, R., Loh, Y.P., and Salton, S.R. (2011). The extended granin family: structure, function, and biomedical implications. *Endocr Rev* 32, 755-797.

Baumann, G. (1991). Growth hormone heterogeneity: genes, isohormones, variants, and binding proteins. *Endocr Rev* 12, 424-449.

Baxter, J.D., and Funder, J.W. (1979). Hormone receptors. *N Engl J Med* 301, 1149-1161.

Beuret, N., Hasler, F., Prescianotto-Baschong, C., Birk, J., Rutishauser, J., and Spiess, M. (2017). Amyloid-like aggregation of provasopressin in diabetes insipidus and secretory granule sorting. *BMC Biol* 15, 5.

Beuret, N., Stettler, H., Renold, A., Rutishauser, J., and Spiess, M. (2004). Expression of regulated secretory proteins is sufficient to generate granule-like structures in constitutively secreting cells. *J Biol Chem* 279, 20242-20249.

Binder, G., Nagel, B.H., Ranke, M.B., and Mullis, P.E. (2002). Isolated GH deficiency (IGHD) type II: imaging of the pituitary gland by magnetic resonance reveals characteristic differences in comparison with severe IGHD of unknown origin. *Eur J Endocrinol* 147, 755-760.

Birk, J., Friberg, M.A., Prescianotto-Baschong, C., Spiess, M., and Rutishauser, J. (2009). Dominant pro-vasopressin mutants that cause diabetes insipidus form disulfide-linked fibrillar aggregates in the endoplasmic reticulum. *J Cell Sci* 122, 3994-4002.

Blazquez, M., Thiele, C., Huttner, W.B., Docherty, K., and Shennan, K.I. (2000). Involvement of the membrane lipid bilayer in sorting prohormone convertase 2 into the regulated secretory pathway. *Biochem J* 349 Pt 3, 843-852.

Borgonovo, B., Ouwendijk, J., and Solimena, M. (2006). Biogenesis of secretory granules. *Curr Opin Cell Biol* 18, 365-370.

Braulke, T., and Bonifacino, J.S. (2009). Sorting of lysosomal proteins. *Biochim Biophys Acta* 1793, 605-614.

Brechler, V., Chu, W.N., Baxter, J.D., Thibault, G., and Reudelhuber, T.L. (1996). A protease processing site is essential for prorenin sorting to the regulated secretory pathway. *J Biol Chem* 271, 20636-20640.

Bundgaard, J.R., Birkedal, H., and Rehfeld, J.F. (2004). Progastrin is directed to the regulated secretory pathway by synergistically acting basic and acidic motifs. *J Biol Chem* 279, 5488-5493.

Burgoyne, R.D., and Morgan, A. (2003). Secretory granule exocytosis. *Physiol Rev* 83, 581-632.

Chanat, E., Weiss, U., Huttner, W.B., and Tooze, S.A. (1993). Reduction of the disulfide bond of chromogranin B (secretogranin I) in the trans-Golgi network causes its missorting to the constitutive secretory pathways. *EMBO J* 12, 2159-2168.

Chen, L.Q., Rose, J.P., Breslow, E., Yang, D., Chang, W.R., Furey, W.F., Jr., Sax, M., and Wang, B.C. (1991). Crystal structure of a bovine neurophysin II dipeptide complex at 2.8 Å determined from the single-wavelength anomalous scattering signal of an incorporated iodine atom. *Proc Natl Acad Sci U S A* 88, 4240-4244.

Chen, X., Shen, J., and Prywes, R. (2002). The luminal domain of ATF6 senses endoplasmic reticulum (ER) stress and causes translocation of ATF6 from the ER to the Golgi. *J Biol Chem* 277, 13045-13052.

Chiti, F., and Dobson, C.M. (2017). Protein Misfolding, Amyloid Formation, and Human Disease: A Summary of Progress Over the Last Decade. *Annu Rev Biochem* 86, 27-68.

Cogan, J.D., Ramel, B., Lehto, M., Phillips, J., 3rd, Prince, M., Blizzard, R.M., de Ravel, T.J., Brammert, M., and Groop, L. (1995). A recurring dominant negative mutation causes autosomal dominant growth hormone deficiency--a clinical research center study. *J Clin Endocrinol Metab* 80, 3591-3595.

Cool, D.R., and Loh, Y.P. (1994). Identification of a sorting signal for the regulated secretory pathway at the N-terminus of pro-opiomelanocortin. *Biochimie* 76, 265-270.

Cool, D.R., and Loh, Y.P. (1998). Carboxypeptidase E is a sorting receptor for prohormones: binding and kinetic studies. *Mol Cell Endocrinol* 139, 7-13.

Courel, M., Soler-Jover, A., Rodriguez-Flores, J.L., Mahata, S.K., Elias, S., Montero-Hadjadje, M., Anouar, Y., Giuly, R.J., O'Connor, D.T., and Taupenot, L. (2010). Pro-hormone secretogranin II regulates dense core secretory granule biogenesis in catecholaminergic cells. *J Biol Chem* 285, 10030-10043.

Cunningham, B.C., Ultsch, M., De Vos, A.M., Mulkerrin, M.G., Clauser, K.R., and Wells, J.A. (1991). Dimerization of the extracellular domain of the human growth hormone receptor by a single hormone molecule. *Science* 254, 821-825.

de Vos, A.M., Ultsch, M., and Kossiakoff, A.A. (1992). Human growth hormone and extracellular domain of its receptor: crystal structure of the complex. *Science* 255, 306-312.

Delestre-Delacour, C., Carmon, O., Laguerre, F., Estay-Ahumada, C., Courel, M., Elias, S., Jeandel, L., Rayo, M.V., Peinado, J.R., Sengmanivong, L., *et al.* (2017). Myosin 1b and F-actin are involved in the control of secretory granule biogenesis. *Sci Rep* 7, 5172.

Dhanvantari, S., and Loh, Y.P. (2000). Lipid raft association of carboxypeptidase E is necessary for its function as a regulated secretory pathway sorting receptor. *J Biol Chem* 275, 29887-29893.

Dikeakos, J.D., Lacombe, M.J., Mercure, C., Mireuta, M., and Reudelhuber, T.L. (2007a). A hydrophobic patch in a charged alpha-helix is sufficient to target proteins to dense core secretory granules. *J Biol Chem* 282, 1136-1143.

Dikeakos, J.D., Mercure, C., Lacombe, M.J., Seidah, N.G., and Reudelhuber, T.L. (2007b). PC1/3, PC2 and PC5/6A are targeted to dense core secretory granules by a common mechanism. *FEBS J* 274, 4094-4102.

Dittie, A.S., Hajibagheri, N., and Tooze, S.A. (1996). The AP-1 adaptor complex binds to immature secretory granules from PC12 cells, and is regulated by ADP-ribosylation factor. *J Cell Biol* 132, 523-536.

Ellgaard, L., and Helenius, A. (2003). Quality control in the endoplasmic reticulum. *Nat Rev Mol Cell Biol* 4, 181-191.

Feliciangeli, S., Kitabgi, P., and Bidard, J.N. (2001). The role of dibasic residues in prohormone sorting to the regulated secretory pathway. A study with proneurotensin. *J Biol Chem* 276, 6140-6150.

Garcia, A.L., Han, S.K., Janssen, W.G., Khaing, Z.Z., Ito, T., Glucksman, M.J., Benson, D.L., and Salton, S.R. (2005). A prohormone convertase cleavage site within a predicted alpha-helix mediates sorting of the neuronal and endocrine polypeptide VGF into the regulated secretory pathway. *J Biol Chem* 280, 41595-41608.

Glombik, M.M., Kromer, A., Salm, T., Huttner, W.B., and Gerdes, H.H. (1999). The disulfide-bonded loop of chromogranin B mediates membrane binding and directs sorting from the trans-Golgi network to secretory granules. *EMBO J* 18, 1059-1070.

- Graves, T.K., Patel, S., Dannies, P.S., and Hinkle, P.M. (2001). Misfolded growth hormone causes fragmentation of the Golgi apparatus and disrupts endoplasmic reticulum-to-Golgi traffic. *J Cell Sci* 114, 3685-3694.
- Hagiwara, D., Arima, H., Morishita, Y., Wenjun, L., Azuma, Y., Ito, Y., Suga, H., Goto, M., Banno, R., Sugimura, Y., *et al.* (2014). Arginine vasopressin neuronal loss results from autophagy-associated cell death in a mouse model for familial neurohypophysial diabetes insipidus. *Cell Death Dis* 5, e1148.
- Hall, M., Howell, S.L., Schulster, D., and Wallis, M. (1982). A procedure for the purification of somatotrophs isolated from rat anterior pituitary glands using Percoll density gradients. *J Endocrinol* 94, 257-266.
- Hamid, R., Phillips, J.A., 3rd, Holladay, C., Cogan, J.D., Austin, E.D., Backeljauw, P.F., Travers, S.H., and Patton, J.G. (2009). A molecular basis for variation in clinical severity of isolated growth hormone deficiency type II. *J Clin Endocrinol Metab* 94, 4728-4734.
- Hayashi, Y., Yamamoto, M., Ohmori, S., Kamijo, T., Ogawa, M., and Seo, H. (1999). Inhibition of growth hormone (GH) secretion by a mutant GH-I gene product in neuroendocrine cells containing secretory granules: an implication for isolated GH deficiency inherited in an autosomal dominant manner. *J Clin Endocrinol Metab* 84, 2134-2139.
- Hebert, D.N., and Molinari, M. (2007). In and out of the ER: protein folding, quality control, degradation, and related human diseases. *Physiol Rev* 87, 1377-1408.
- Heinemann, C., von Ruden, L., Chow, R.H., and Neher, E. (1993). A two-step model of secretion control in neuroendocrine cells. *Pflugers Arch* 424, 105-112.
- Hess, O., Hujeirat, Y., Wajnrajch, M.P., Allon-Shalev, S., Zadik, Z., Lavi, I., and Tenenbaum-Rakover, Y. (2007). Variable phenotypes in familial isolated growth hormone deficiency caused by a G6664A mutation in the GH-1 gene. *J Clin Endocrinol Metab* 92, 4387-4393.
- Hetz, C., and Glimcher, L.H. (2009). Fine-tuning of the unfolded protein response: Assembling the IRE1alpha interactome. *Mol Cell* 35, 551-561.
- Hiller-Sturmhofel, S., and Bartke, A. (1998). The endocrine system: an overview. *Alcohol Health Res World* 22, 153-164.
- Hiroi, M., Morishita, Y., Hayashi, M., Ozaki, N., Sugimura, Y., Nagasaki, H., Shiota, A., Oiso, Y., and Arima, H. (2010). Activation of vasopressin neurons leads to phenotype progression in a mouse model for familial neurohypophysial diabetes insipidus. *Am J Physiol Regul Integr Comp Physiol* 298, R486-493.
- Hosaka, M., Suda, M., Sakai, Y., Izumi, T., Watanabe, T., and Takeuchi, T. (2004). Secretogranin III binds to cholesterol in the secretory granule membrane as an adapter for chromogranin A. *J Biol Chem* 279, 3627-3634.

- Hosaka, M., and Watanabe, T. (2010). Secretogranin III: a bridge between core hormone aggregates and the secretory granule membrane. *Endocr J* 57, 275-286.
- Hou, N., Mogami, H., Kubota-Murata, C., Sun, M., Takeuchi, T., and Torii, S. (2012). Preferential release of newly synthesized insulin assessed by a multi-label reporter system using pancreatic beta-cell line MIN6. *PLoS One* 7, e47921.
- Huh, Y.H., Jeon, S.H., and Yoo, S.H. (2003). Chromogranin B-induced secretory granule biogenesis: comparison with the similar role of chromogranin A. *J Biol Chem* 278, 40581-40589.
- Hummer, B.H., de Leeuw, N.F., Burns, C., Chen, L., Joens, M.S., Hosford, B., Fitzpatrick, J.A.J., and Asensio, C.S. (2017). HID-1 controls formation of large dense core vesicles by influencing cargo sorting and trans-Golgi network acidification. *Mol Biol Cell* 28, 3870-3880.
- Hutton, J.C. (1982). The internal pH and membrane potential of the insulin-secretory granule. *Biochem J* 204, 171-178.
- Ito, M., Jameson, J.L., and Ito, M. (1997). Molecular basis of autosomal dominant neurohypophyseal diabetes insipidus. Cellular toxicity caused by the accumulation of mutant vasopressin precursors within the endoplasmic reticulum. *J Clin Invest* 99, 1897-1905.
- Ito, M., Yu, R.N., and Jameson, J.L. (1999). Mutant vasopressin precursors that cause autosomal dominant neurohypophyseal diabetes insipidus retain dimerization and impair the secretion of wild-type proteins. *J Biol Chem* 274, 9029-9037.
- Jackson, M.P., and Hewitt, E.W. (2017). Why are Functional Amyloids Non-Toxic in Humans? *Biomolecules* 7.
- Kamijo, T., Phillips, J.A., 3rd, Ogawa, M., Yuan, L., Shi, Y., and Bao, X.L. (1991). Screening for growth hormone gene deletions in patients with isolated growth hormone deficiency. *J Pediatr* 118, 245-248.
- Kebache, S., Cardin, E., Nguyen, D.T., Chevet, E., and Larose, L. (2004). Nck-1 antagonizes the endoplasmic reticulum stress-induced inhibition of translation. *J Biol Chem* 279, 9662-9671.
- Keenan, R.J., Freymann, D.M., Stroud, R.M., and Walter, P. (2001). The signal recognition particle. *Annu Rev Biochem* 70, 755-775.
- Kim, T., Gondre-Lewis, M.C., Arnaoutova, I., and Loh, Y.P. (2006). Dense-core secretory granule biogenesis. *Physiology (Bethesda)* 21, 124-133.
- Kim, T., Tao-Cheng, J.H., Eiden, L.E., and Loh, Y.P. (2001). Chromogranin A, an "on/off" switch controlling dense-core secretory granule biogenesis. *Cell* 106, 499-509.

Kim, T., Zhang, C.F., Sun, Z., Wu, H., and Loh, Y.P. (2005). Chromogranin A deficiency in transgenic mice leads to aberrant chromaffin granule biogenesis. *J Neurosci* 25, 6958-6961.

Knowles, T.P., Vendruscolo, M., and Dobson, C.M. (2014). The amyloid state and its association with protein misfolding diseases. *Nat Rev Mol Cell Biol* 15, 384-396.

Kopchick, J.J., and Andry, J.M. (2000). Growth hormone (GH), GH receptor, and signal transduction. *Mol Genet Metab* 71, 293-314.

Kornfeld, S., and Mellman, I. (1989). The biogenesis of lysosomes. *Annu Rev Cell Biol* 5, 483-525.

Kromer, A., Glombik, M.M., Huttner, W.B., and Gerdes, H.H. (1998). Essential role of the disulfide-bonded loop of chromogranin B for sorting to secretory granules is revealed by expression of a deletion mutant in the absence of endogenous granin synthesis. *J Cell Biol* 140, 1331-1346.

Lee, A.S. (2005). The ER chaperone and signaling regulator GRP78/BiP as a monitor of endoplasmic reticulum stress. *Methods* 35, 373-381.

Lee, M.S., Wajnrajch, M.P., Kim, S.S., Plotnick, L.P., Wang, J., Gertner, J.M., Leibel, R.L., and Dannies, P.S. (2000). Autosomal dominant growth hormone (GH) deficiency type II: the Del32-71-GH deletion mutant suppresses secretion of wild-type GH. *Endocrinology* 141, 883-890.

Lee, M.S., Zhu, Y.L., Chang, J.E., and Dannies, P.S. (2001). Acquisition of Lubrol insolubility, a common step for growth hormone and prolactin in the secretory pathway of neuroendocrine cells. *J Biol Chem* 276, 715-721.

Leitinger, B., Brown, J.L., and Spiess, M. (1994). Tagging secretory and membrane proteins with a tyrosine sulfation site. Tyrosine sulfation precedes galactosylation and sialylation in COS-7 cells. *J Biol Chem* 269, 8115-8121.

Lindsay, R., Feldkamp, M., Harris, D., Robertson, J., and Rallison, M. (1994). Utah Growth Study: growth standards and the prevalence of growth hormone deficiency. *J Pediatr* 125, 29-35.

Lochmatter, D., Strom, M., Eble, A., Petkovic, V., Fluck, C.E., Bidlingmaier, M., Robinson, I.C., and Mullis, P.E. (2010). Isolated GH deficiency type II: knockdown of the harmful Delta3GH recovers wt-GH secretion in rat tumor pituitary cells. *Endocrinology* 151, 4400-4409.

Loh, Y.P., Kim, T., Rodriguez, Y.M., and Cawley, N.X. (2004). Secretory granule biogenesis and neuropeptide sorting to the regulated secretory pathway in neuroendocrine cells. *J Mol Neurosci* 22, 63-71.

Lou, H., Kim, S.K., Zaitsev, E., Snell, C.R., Lu, B., and Loh, Y.P. (2005). Sorting and activity-dependent secretion of BDNF require interaction of a specific motif with the sorting receptor carboxypeptidase e. *Neuron* 45, 245-255.

Lutcke, H. (1995). Signal recognition particle (SRP), a ubiquitous initiator of protein translocation. *Eur J Biochem* 228, 531-550.

Mahapatra, N.R., Taupenot, L., Courel, M., Mahata, S.K., and O'Connor, D.T. (2008). The trans-Golgi proteins SCLIP and SCG10 interact with chromogranin A to regulate neuroendocrine secretion. *Biochemistry* 47, 7167-7178.

Maji, S.K., Perrin, M.H., Sawaya, M.R., Jessberger, S., Vadodaria, K., Rissman, R.A., Singru, P.S., Nilsson, K.P., Simon, R., Schubert, D., *et al.* (2009). Functional amyloids as natural storage of peptide hormones in pituitary secretory granules. *Science* 325, 328-332.

McGuinness, L., Magoulas, C., Sesay, A.K., Mathers, K., Carmignac, D., Manneville, J.B., Christian, H., Phillips, J.A., 3rd, and Robinson, I.C. (2003). Autosomal dominant growth hormone deficiency disrupts secretory vesicles in vitro and in vivo in transgenic mice. *Endocrinology* 144, 720-731.

Meldolesi, J. (2002). Rapidly exchanging Ca(2+) stores: ubiquitous partners of surface channels in neurons. *News Physiol Sci* 17, 144-149.

Messenger, S.W., Falkowski, M.A., and Groblewski, G.E. (2014). Ca(2+)-regulated secretory granule exocytosis in pancreatic and parotid acinar cells. *Cell Calcium* 55, 369-375.

Miletta, M.C., Petkovic, V., Eble, A., Fluck, C.E., and Mullis, P.E. (2016). Rescue of Isolated GH Deficiency Type II (IGHD II) via Pharmacologic Modulation of GH-1 Splicing. *Endocrinology* 157, 3972-3982.

Missarelli, C., Herrera, L., Mericq, V., and Carvallo, P. (1997). Two different 5' splice site mutations in the growth hormone gene causing autosomal dominant growth hormone deficiency. *Hum Genet* 101, 113-117.

Mouchantaf, R., Kumar, U., Sulea, T., and Patel, Y.C. (2001). A conserved alpha-helix at the amino terminus of prosomatostatin serves as a sorting signal for the regulated secretory pathway. *J Biol Chem* 276, 26308-26316.

Mullis, P.E., Akinci, A., Kanaka, C., Eble, A., and Brook, C.G. (1992). Prevalence of human growth hormone-1 gene deletions among patients with isolated growth hormone deficiency from different populations. *Pediatr Res* 31, 532-534.

Mullis, P.E., Deladoey, J., and Dannies, P.S. (2002). Molecular and cellular basis of isolated dominant-negative growth hormone deficiency, IGHD type II: insights on the secretory pathway of peptide hormones. *Horm Res* 58, 53-66.

Mullis, P.E., Robinson, I.C., Salemi, S., Eble, A., Besson, A., Vuissoz, J.M., Deladoey, J., Simon, D., Czernichow, P., and Binder, G. (2005). Isolated autosomal dominant growth hormone deficiency: an evolving pituitary deficit? A multicenter follow-up study. *J Clin Endocrinol Metab* *90*, 2089-2096.

Nakatsukasa, K., and Brodsky, J.L. (2008). The recognition and retrotranslocation of misfolded proteins from the endoplasmic reticulum. *Traffic* *9*, 861-870.

Okada, S., and Kopchick, J.J. (2001). Biological effects of growth hormone and its antagonist. *Trends Mol Med* *7*, 126-132.

Orci, L., Ravazzola, M., Amherdt, M., Madsen, O., Perrelet, A., Vassalli, J.D., and Anderson, R.G. (1986). Conversion of proinsulin to insulin occurs coordinately with acidification of maturing secretory vesicles. *J Cell Biol* *103*, 2273-2281.

Pakdel, M., and von Blume, J. (2018). Exploring new routes for secretory protein export from the trans-Golgi network. *Mol Biol Cell* *29*, 235-240.

Park, E., and Rapoport, T.A. (2012). Mechanisms of Sec61/SecY-mediated protein translocation across membranes. *Annu Rev Biophys* *41*, 21-40.

Perez-Castro, C., Renner, U., Haedo, M.R., Stalla, G.K., and Arzt, E. (2012). Cellular and molecular specificity of pituitary gland physiology. *Physiol Rev* *92*, 1-38.

Puertollano, R., Aguilar, R.C., Gorshkova, I., Crouch, R.J., and Bonifacino, J.S. (2001). Sorting of mannose 6-phosphate receptors mediated by the GGAs. *Science* *292*, 1712-1716.

Raven, J.F., Baltzis, D., Wang, S., Mounir, Z., Papadakis, A.I., Gao, H.Q., and Koromilas, A.E. (2008). PKR and PKR-like endoplasmic reticulum kinase induce the proteasome-dependent degradation of cyclin D1 via a mechanism requiring eukaryotic initiation factor 2alpha phosphorylation. *J Biol Chem* *283*, 3097-3108.

Rona, R.J., and Tanner, J.M. (1977). Aetiology of idiopathic growth hormone deficiency in England and Wales. *Arch Dis Child* *52*, 197-208.

Rutishauser, J., and Spiess, M. (2002). Endoplasmic reticulum storage diseases. *Swiss Med Wkly* *132*, 211-222.

Ryther, R.C., McGuinness, L.M., Phillips, J.A., 3rd, Moseley, C.T., Magoulas, C.B., Robinson, I.C., and Patton, J.G. (2003). Disruption of exon definition produces a dominant-negative growth hormone isoform that causes somatotroph death and IGHD II. *Hum Genet* *113*, 140-148.

Seidah, N.G., Mayer, G., Zaid, A., Rousselet, E., Nassoury, N., Poirier, S., Essalmani, R., and Prat, A. (2008). The activation and physiological functions of the proprotein convertases. *Int J Biochem Cell Biol* *40*, 1111-1125.

Shen, J., Chen, X., Hendershot, L., and Prywes, R. (2002). ER stress regulation of ATF6 localization by dissociation of BiP/GRP78 binding and unmasking of Golgi localization signals. *Dev Cell* 3, 99-111.

Shi, G., Somlo, D.R.M., Kim, G.H., Prescianotto-Baschong, C., Sun, S., Beuret, N., Long, Q., Rutishauser, J., Arvan, P., Spiess, M., *et al.* (2017). ER-associated degradation is required for vasopressin prohormone processing and systemic water homeostasis. *J Clin Invest* 127, 3897-3912.

Spiess, M., Friberg, M., Beuret, N., Prescianotto-Baschong, C., and Rutishauser, J. (2020). Role of protein aggregation and degradation in autosomal dominant neurohypophyseal diabetes insipidus. *Mol Cell Endocrinol* 501, 110653.

Steiner, D.F., Smeekens, S.P., Ohagi, S., and Chan, S.J. (1992). The new enzymology of precursor processing endoproteases. *J Biol Chem* 267, 23435-23438.

Stettler, H., Beuret, N., Prescianotto-Baschong, C., Fayard, B., Taupenot, L., and Spiess, M. (2009). Determinants for chromogranin A sorting into the regulated secretory pathway are also sufficient to generate granule-like structures in non-endocrine cells. *Biochem J* 418, 81-91.

Tam, W.W., Andreasson, K.I., and Loh, Y.P. (1993). The amino-terminal sequence of pro-opiomelanocortin directs intracellular targeting to the regulated secretory pathway. *Eur J Cell Biol* 62, 294-306.

Tanaka, S., Yora, T., Nakayama, K., Inoue, K., and Kurosumi, K. (1997). Proteolytic processing of pro-opiomelanocortin occurs in acidifying secretory granules of AtT-20 cells. *J Histochem Cytochem* 45, 425-436.

Taupenot, L., Harper, K.L., Mahapatra, N.R., Parmer, R.J., Mahata, S.K., and O'Connor, D.T. (2002). Identification of a novel sorting determinant for the regulated pathway in the secretory protein chromogranin A. *J Cell Sci* 115, 4827-4841.

Taupenot, L., Harper, K.L., and O'Connor, D.T. (2005). Role of H⁺-ATPase-mediated acidification in sorting and release of the regulated secretory protein chromogranin A: evidence for a vesiculogenic function. *J Biol Chem* 280, 3885-3897.

Tirasophon, W., Welihinda, A.A., and Kaufman, R.J. (1998). A stress response pathway from the endoplasmic reticulum to the nucleus requires a novel bifunctional protein kinase/endoribonuclease (Ire1p) in mammalian cells. *Genes Dev* 12, 1812-1824.

Urbe, S., Dittie, A.S., and Tooze, S.A. (1997). pH-dependent processing of secretogranin II by the endopeptidase PC2 in isolated immature secretory granules. *Biochem J* 321 (Pt 1), 65-74.

Walter, P., and Ron, D. (2011). The unfolded protein response: from stress pathway to homeostatic regulation. *Science* 334, 1081-1086.

Wang, Y., Thiele, C., and Huttner, W.B. (2000). Cholesterol is required for the formation of regulated and constitutive secretory vesicles from the trans-Golgi network. *Traffic* *1*, 952-962.

Wells, J.A., and de Vos, A.M. (1993). Structure and function of human growth hormone: implications for the hematopoietins. *Annu Rev Biophys Biomol Struct* *22*, 329-351.

Wendler, F., Page, L., Urbe, S., and Tooze, S.A. (2001). Homotypic fusion of immature secretory granules during maturation requires syntaxin 6. *Mol Biol Cell* *12*, 1699-1709.

Westermarck, P. (2005). Aspects on human amyloid forms and their fibril polypeptides. *FEBS J* *272*, 5942-5949.

Wu, C.K., Hu, B., Rose, J.P., Liu, Z.J., Nguyen, T.L., Zheng, C., Breslow, E., and Wang, B.C. (2001). Structures of an unliganded neurophysin and its vasopressin complex: implications for binding and allosteric mechanisms. *Protein Sci* *10*, 1869-1880.

Yang, Y., Zhou, Q., Gao, A., Chen, L., and Li, L. (2020). Endoplasmic reticulum stress and focused drug discovery in cardiovascular disease. *Clin Chim Acta* *504*, 125-137.

Yoo, S.H. (2010). Secretory granules in inositol 1,4,5-trisphosphate-dependent Ca²⁺ signaling in the cytoplasm of neuroendocrine cells. *FASEB J* *24*, 653-664.

Yoshida, H., Matsui, T., Yamamoto, A., Okada, T., and Mori, K. (2001). XBP1 mRNA is induced by ATF6 and spliced by IRE1 in response to ER stress to produce a highly active transcription factor. *Cell* *107*, 881-891.

Zhu, T., Goh, E.L., Graichen, R., Ling, L., and Lobie, P.E. (2001). Signal transduction via the growth hormone receptor. *Cell Signal* *13*, 599-616.

Zhu, Y.L., Conway-Campbell, B., Waters, M.J., and Dannies, P.S. (2002). Prolonged retention after aggregation into secretory granules of human R183H-growth hormone (GH), a mutant that causes autosomal dominant GH deficiency type II. *Endocrinology* *143*, 4243-4248.

Curriculum Vitae

**Jennifer
RECK**

**PhD
in Biochemistry**



Personal infos

04.05.1992

jennifer.reck@laposte.net

68460 Lutterbach
France

Languages

French : native

English : written, spoken,
read

German : basics

Reference

Prof. Dr Martin Spiess

Biozentrum,
University of Basel,

martin.spiess@unibas.ch

Education

2021 – PhD in Biochemistry; Biozentrum; University of Basel, Switzerland

2016 – Master in Biochemistry : Molecular and Cellular Biology; University of Strasbourg, France

2014 – Bachelor in Biology: cellular biology and physiology; University of Strasbourg, France

Work experiences

Since June 2021 – Post doctoral researcher; in the team « Biogenesis and transport of membrane proteins » of Prof. Martin Spiess, Biozentrum, University of Basel, Switzerland

2016-2021 – PhD student in Biochemistry; in the team « Biogenesis and transport of membrane proteins » of Prof. Martin Spiess, Biozentrum, University of Basel, Switzerland

Project title: Small disulfide loops in peptide hormones mediate self-aggregation in secretory granule biogenesis

2014-2016 – Master student in Biochemistry; in the team « Membrane trafficking and lipid signaling » of Dr. Sylvie Friant, UMR7156 GMGM, University of Strasbourg, France

Project title: Intracellular trafficking of the human GASP1 (G protein coupled-receptor associated sorting protein) protein in the yeast *Saccharomyces cerevisiae*

Laboratory skills

– Cloning techniques, primer design, mutagenesis, DNA extraction, plasmid purification

– Mammalian cell culture : transfection and stable expression of genes

– Various biochemical assays : western blot, co-immunoprecipitation, stimulated secretion, radioactive labelling

– Confocal and epi-fluorescence microscopy, preparation of the sample for analysis, staining for immunofluorescence and data analysis

Teaching experience

November 2016, 2017, 2018, 2019, 2020 – Assistant of the Biochemistry Block Course week “Nucleic Acids” for Bachelor students at the University of Basel

2019 – 5 months supervision of a Master Student in Medicine, University of Basel. Responsible for project management, teaching and laboratory training

2018 – 2 months supervision of a Medecine student from the “Biozentrum Research Summer ” program. Responsible for project management, teaching and laboratory training

Computer skills

Software MS Office (Word, Excel, PowerPoint), ApE plasmid editor, Illustrator, Photoshop, Endnote, ImageJ (microscopy picture treatment), GraphPad Prism

Hobbies

Dance (African dance, contemporary, modern jazz); Football; Running; Fitness; Travelling; Hiking; Nature